# Calorimetric Measurements of a Yang-Koldamasov Device

by

Jennifer Novosad

Submitted to the Department of Electrical Engineering and Computer Science
in partial fulfillment of the requirements for the degree of

Master of Engineering in Computer Science and Engineering

at the

MASSACHUSETTS INSTITUTE OF TECHNOLOGY

February 2007



Author .....
Department of Electrical Engineering and Computer Science
February 1, 2007

Certified by .....
Peter Hagelstein
Associate Professor
Thesis Supervisor

Accepted by .....
Arthur C. Smith
Chairman, Department Committee on Graduate Students

**Calorimetric Measurements of a Yang-Koldamasov Device**

by

Jennifer Novosad

Submitted to the Department of Electrical Engineering and Computer Science
on February 1, 2007, in partial fulfillment of the
requirements for the degree of
Master of Engineering in Computer Science and Engineering

## Abstract

Due to the finite supply of oil, energy availability and price are issues facing the world. Among the possible approaches to this problem is research of new physical effects which may produce energy in novel ways.

The Yang-Koldamasov device was reported to produce excess heat by iESi by pumping oil through a thin nozzle; however, the theoretical mechanism for this effect is at the present unknown. The subject of this thesis is an attempt at independent confirmation of the effect at MIT and FRC.

To perform calorimetry on this device, there are several issues involved, such as thermocouple offset errors, RF noise, and erroneous readings due to fluid flow conditions. Methods for handling these issues are discussed in application to two independent measurements of energy gain in the system, differential calorimetry over the cell, and flow calorimetry via a heat exchanger. The differential calorimetry has been improved compared to what was earlier available on Yang-Koldamasov devices, and the flow calorimetry is new to the device.

Data was collected on several tests After analysis, the data was found consistent with a null result. However, over the course of the runs the behavior of the device was very different than the behavior at earlier demonstrations where excess heat was observed. For example, earlier demonstrations exibited electrical arcing perpendicular to the flow of oil, while the current device shows only arcing in the direction of oil flow. Future work is being conducted by FRC to identify the reasons that the current apparatus behaves differently.

Thesis Supervisor: Peter Hagelstein
Title: Associate Professor

# Acknowledgments

I would like to thank my mother and father, Laura and Richard Novosad, my advisor, Peter Hagelstein, Epsilon Theta Fraternity, my family, and my friends for giving me the emotional and intellectual support I needed to get through these 5.5 years at MIT. I would also like to thank Dexter for the emotional support he gave me (and editing assistance) during the time that I was working on this project.

Jim Gimlett's help on this project has been invaluable. He has helped me to understand the complex experimental issues involved in this work, reviewed my analysis for common errors and helped me with the presentation of it, and provided suggestions for experiments.

I also thank Fusion Research Corp (FRC) for the wonderful opportunity to work on this experiment and financial support in my last year, and the Canadian government for allowing me across the border to observe work at FRC. I would not have been able to complete this project without the people I met there: Chris, Dave, Sean, Stephen, Mike, Christine, Carston, Denis, and Chansoo. These people contributed greatly to the design, operation, and analysis of this experiment. In particular, Chris helped with organization and communications with Korea. Dave, Mike and Sean helped with design and manufacture of many of the parts I needed, even for experiments that I wanted to try but did not pertain to the main focus of the company. Stephen created the setup for getting data from the instrumentation to the DAQ, and set up the vast majority of the instrumentation. Christine and Carston enabled me to go to FRC, and helped me to deal with customs and my financial situation. Mike and Chansoo taught me how to run the machine. Denis provided me with many resources as to the work which had already been done in the area. This was invaluable, since very little work has been published in this area. He also kept my spirits up with his optimistic attitude combined with an experimentalists viewpoint.

Thank you to the individuals who responded to my requests for advice and help in areas what I wasn't well equipped to handle, such as Fran Tanzella, who recommended parts and methodology related to calorimetry.

Lastly, David Griswold provided the funding necessary for me to complete this project. Thank you very much for enabling me to complete my Master's degree.

# Contents

# List of Figures

# List of Tables

# Chapter 1

# Introduction

Due to the finite supply of crude oil, world faces problems in energy price, quantity, and quality (see Chapter 2). There are many potential approaches to address the problem, for instance, coal, nuclear power, or solar energy. Cold Fusion is an emerging field which is looking at a new mechanisms for energy production.

Dr. Hyunik Yang and collaborators believe that they have discovered a new technology that produces energy; however, the physical mechanism for the energy production is at present unknown. One implementation of this technology is displayed in Fig. 1-1. The device operates by pumping oil through a thin nozzle, resulting in electrical discharges (Fig. 1-2). One of the reasons that this device is interesting is that if it works, it would be almost immediately practical.

In light of other successful Cold Fusion experiments, and demonstrations of the machine at iESi [1], an attempt at a confirmation of the effect was made at MIT. This work was later continued at FRC [2]. These demonstrations and other successful work in the Cold Fusion field are further discussed in Chapter 3.

To perform a confirmation, a machine, operational instructions, and calorimetry instrumentation were needed. Our group collaborated with FRC, who provided the machine, procedures and instrumentation (see Chapters 6 and 7).

[1] Innovative Energy Solutions Inc. The abbreviation potentially refers to two groups, iESi, the parent company based in Las Vegas and the subsidiary iESiUSA based in Edmonton, Canada. References to iESi in this work are to iESiUSA.

[2] Fusion Research Corporation

Figure 1-1: Photography of an oil-based Yang-Koldamasov device taken by S. B. Krivit, ©New Energy Times. Fair use permitted for non-commercial educational use.

Initially, the machine had a simple differential calorimetry set up. Our tasks included improving the differential calorimetry so that it would provide meaningful and reliable measurements, and adding flow calorimetry with a heat exchanger.

These are two independent measurements of the energy balance in the system. The differential calorimetry measurement estimates the thermal power over the nozzle from a measurement of the temperature differences across the nozzle. This value is compared to the mechanical power over the cell to create a heat gain.

$$P_{heat} = C_{oil}\Delta T\rho\frac{dV}{dt}$$
$$P_{mechanical} = \Delta P\frac{dV}{dt}$$
$$gain = \frac{P_{heat}}{P_{mechanical}} = \frac{C_{oil}\rho\Delta T}{\Delta P}$$

The flow calorimetry measurement compared the electrical power put into the motor to the power taken out of the cooling water in the form of heat. The comparison was

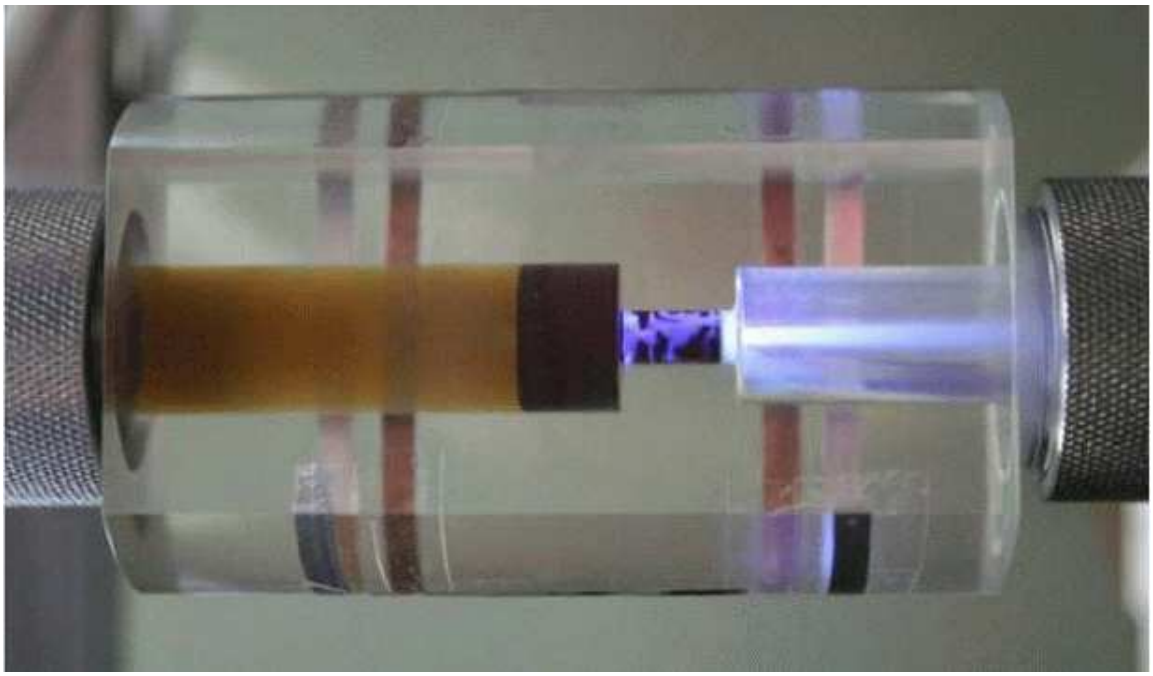

Figure 1-2: Photography of a Russian cell with electrical discharge taken by S. B. Krivit, ©New Energy Times. Fair use permitted for non-commercial educational use.

done in two ways, the difference and the ratio.

$$P_{water} = C_w \rho_w \Delta T_w \frac{dV_w}{dt}$$
$$gain = \frac{P_{water}}{P_{electric}}$$
$$difference = P_{water} - P_{electric}$$

Several measurements were taken of the behavior of the device. These included

- scanning over pressure and temperature
- varying nozzle configurations
- injecting gases such as $HD$, $D_2$, $Xe$, and $He$

The results are expected to fall into one of two categories, based on earlier work done on this machine:

- In February 2005, iESi conducted demonstrations for several scientific observers including Prof. Hagelstein. An integral temperature measurement of the reservoir temperature before and after the 15 minutes run was used to calculated

power gain. Electrical discharges perpendicular to the flow of oil and high voltages outside the cell (with the machine frame defined as ground) were also observed. Excess thermal energy in the oil was more than 300% of the input electric power when running around 800W. The total thermal power, including heating of the frame of the machine and losses to air, was probably greater than 500%.

- At later visits in June and July 2005, the machine behaved qualitatively differently. Electrical arcing was only in the direction of oil flow, and integral calorimetry was no longer used. An audit performed in July indicated that there was no excess power.

- At the reproduction attempts performed at MIT and later FRC in 2006, electrical arcing was only in the direction of oil flow. Measurements of power indicated that there was no excess power.

Despite our efforts, the data collected in the experiments in this thesis was from a device behaving much like the device in June and July 2005. Visual behavior such as electrical arcing was very similar, as was the lack of anomalous heat. The analysis of this data is presented in Chapter 10 and discussed in Chapter 11.

Given that the current machine is behaving differently than the February 2005 demonstration device, work has gone into theorizing how the original device may have worked, so that the current device can be made to operate in the anomalous regime. Conventional explanations are presented in Chapter 4 and nuclear explanations are presented in Chapter 5.

## 1.1 Focus of this Thesis

The focus of this work is the experimental data collected, its analysis, and interpretation. To better understand the experiment in this thesis, several supplemental materials are provided which are not directly the conducted research, but taken from outside sources. Chapter 2 covers the motivation for conducting this work, Hubbert's

Peak and the coming energy crisis due to the decreasing supply of oil. Chapter 3 describes the background of the field and the previous work with the Yang-Koldamasov effect. Nuclear explanations are presented in Chapter 5. Explanations for this effect which are not nuclear in nature are given in Chapter 4, such as combustion and measurement error. The measurement error discussions are primarily derived from outside sources who observed the original demonstrations at iESi. The combustion calculation was done in collaboration by the author, P. Hagelstein and J. Gimlett.

# Chapter 2

# Motivation

Our world faces serious problems of energy supply in the coming years, which has motivated many scientists to pursue research into areas which might provide solutions. Energy problems have been one of my main motivations. In this chapter I provide some discussion from recent sources concerning the aspects of this problem that I am interested in.

Dr. M. King Hubbert's oil supply theory predicts drastic changes in the way we live. The currently available solutions cannot support the world's current energy consumption without oil. Because researching new solutions requires a great deal of energy, if research into solutions is to be done, it needs to happen while energy is still plentiful rather than after the energy crunch has occurred.

In addition to putting research efforts into conventional methods like solar, wind, and water power, some effort should be put into double checking some promising cold fusion experiments. While these experiments may have a low probability of success based on current physical theory, if they do produce energy they would be incredibly helpful in keeping the cost of energy low.

This chapter covers the theory of Hubbert's Peak, other viewpoints, roughly when the end of cheap energy will occur, and the current available solutions.

## 2.1 Hubbert's Peak and the Coming Energy Crisis

In 1949, Dr. Hubbert predicted that use of fossil fuels would be short lived, not due to their utility, but their supply [19]. The prediction is based on the fact that since oil is being used at a rate much faster than it is created, one can consider the total amount of oil on Earth to be a constant. With a few additional assumptions, Hubbert computed an estimate of when the price of oil would begin to drastically rise, as a result of reduced supply. This computation is summarized below, from [6].

First, define $Q(t)$ to be the total quantity of discovered oil at time $t$ (this quantity is known up until $t$ is right now), $Q_f$ to be the total that will be discovered. Consequentially, $Q(t) - Q_f$ is the amount undiscovered at time t.

So far, $Q(t)$ has roughly followed unconstrained exponential growth, $dQ/dt = rQ$ where r is some rate. Since the quantity of oil is finite, exponential growth is not sustainable. One assumption that can be made is the rate $r$ is actually a function of the remaining amount of oil. As the amount of oil left in the world decreases, the ability to find oil becomes more difficult. One guess for the amount of remaining oil is $r = A(Q_f - Q)/Q_f$. $A$ relates to the ability of people to locate oil and find ways of accessing it. While A might vary with time as technologies improve, for simplicity this analysis will treat $A$ as a constant. Since $Q_f$ is a constant and $A$ is unknown, we could also absorb the $Q_f$ in the denominator into $A$ and have the same equation.

The equation is now

$$\frac{dQ/dt}{Q} = A(Q_f - Q)/Q_f$$

This equation is the form of logistic population growth. $dQ(t)/dt$ resembles a bell curve, though it is not a Gaussian. This equation can be rearranged to form Hubbert's equation 27 from his 1982 paper in Oil and Gas Supply Modeling, from the National Bureau of Standards Special Publication [6].

$$\frac{dQ/dt}{Q} = A - (AQ)/Q_f$$

Dr. Hubbert's estimates of the total amount of oil may have ignored that as price increases, harder to access oil becomes more economical to obtain. US oil production

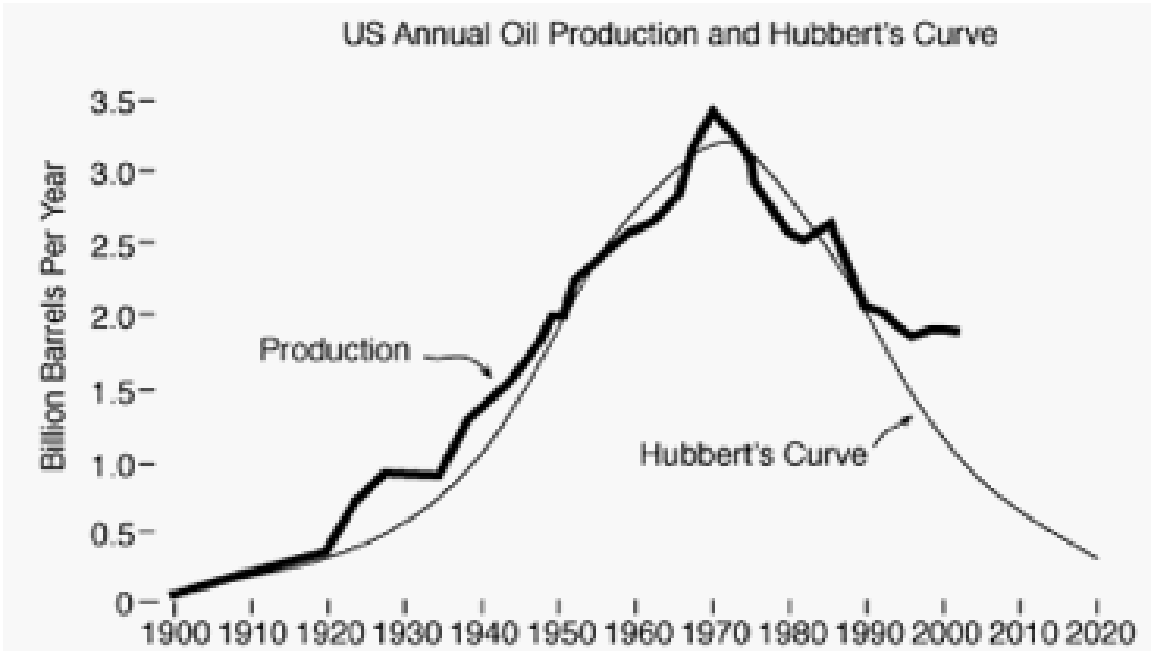


Figure 2-1: Hubbert logistic graph predicting US oil production [17]

after 1990 is higher than Hubbert's original estimate, perhaps due to the cost of oil becoming high enough that investing in technologies to retrieve oil became more affordable.

## 2.2 How Oil is Formed: Why One Can't Just 'Find More'

This section summarizes the viewpoints given by K. S. Deffeyes in [6] on oil formation via saporels, the signs that this formation leaves for companies drilling for oil, and how productive future searching for oil is likely to be.

Saporels are deposits rich in organic material. These saporels can only form when the nutrients aren't being consumed by bacteria or being swept away by ocean currents. In deeper water, the lack of light and oxygen will discourage the growth of bacteria which would consume organic oils. Saporels can occur in bowl shaped sections of water near land. If the deeper water is coming in, and the surface water leaving, then nutrients will be carried in and deposited. These water patterns might

occur if the surface water is less salty, due to a fresh water river or a lot of rain. However, if the surface water is saltier, perhaps due to evaporation from sunlight, then the surface water will sink, pushing the nutrients out of the saproel and into the sea. Because saporel formation is very weather sensitive, saporels occur sporadically over time, leaving black bands of organic rich source rock. The source rock bands are seen in drilling sites which eventually lead to oil.

Plate tectonics move the source rock deeper into the earth, exposing them to warmer temperatures. If the temperatures are not hot enough, then the organic structures won't change significantly. However, hot enough temperatures will 'crack', or rearrange the molecules, resulting in crude oil. Additionally, if the source rock goes too deep for too long a time period, the organic material will become the simplest of hydrocarbons: methane (natural gas). Based on fossil and pollen samples found in drilling holes, the cracking process is believed to take millions of years. Because of the time that it takes to naturally create crude oil, we can consider the amount available to us over the next 100 years to be essentially a finite supply.

When searching for new oil, there are several constraints which help guide the search. For instance, it is very unlikely that oil will be found where temperatures are too hot (instead one may find natural gas). Since temperatures rise as depth increases, searching below a certain depth for oil is unlikely to result in oil discoveries. Additionally, oil won't be present without source rocks. Lastly, crude oil can't form without enough heat. Unless the rocks show evidence of having at some point been deep enough for long enough, source rocks can't develop into crude oil.

According to [6], most areas of the earth, except the South China Sea, have been searched for oil . Oil estimates are reasonably well known, except for the amount that may be found in the South China Sea and the amount in the middle east (which is a national secret of the countries involved). Searching more thoroughly everywhere else is unlikely to produce much more crude oil, since it has already been determined that the region lacks source rocks or rocks that have passed through proper temperatures. Drilling deeper may yield natural gas (particularly in areas where crude oil has already been found), but it is unlikely to produce crude oil [6]. With this information and

knowledge of current oil reserves, estimates of the amount of crude oil available can be created.

## 2.3 Arguments for and against Hubbert's Peak

Note that the arguments given above by [6] are not universally agreed upon, and that there are other models for oil development. The idea that oil is of essentially finite supply is not under dispute. There are disagreements on the amount of oil left, which are inn general agreement with the concept of Hubbert's Peak that oil will run out soon, and energy availability will peak and then prices will drastically rise. Arguments on the amount of oil left only change the peak date a few years in one direction or the other; the peak is still expected to occur. Some of this debate is reviewed briefly in the next section.

Three other arguments on energy consumption do not look at energy supply for a variety of reasons, and are briefly presented here. These arguments can be summarized as the environmentalist, economist, and politician arguments. The discussion given here is a summary of the interpretation of these arguments given by R. Heinberg in [16].

The environmentalist viewpoint doesn't focus on the limited supply of oil because its main priority is preserving some portion of the earth's natural state. While the goal isn't to reduce the current standard of living, living quality is measured in terms other than consumption, such as the quality of weather and ones surroundings (i.e. acid rain is not characteristic of a high quality of life). While this viewpoint advocates the use of alternative energies, it is for cleanliness rather than necessity.

The economist viewpoint is that market forces will correct the over or underpricing of crude oil naturally, as would occur with any other commodity. Higher prices caused by reduced supply will naturally result in increased exploration, both with new oil drilling and new energy sources, as well as lowered demand [16] [9]. Political viewpoints frequently agree with this, perhaps because it is a positive outlook that helps garners more votes. Energy crunches are blamed on either greedy corpo-

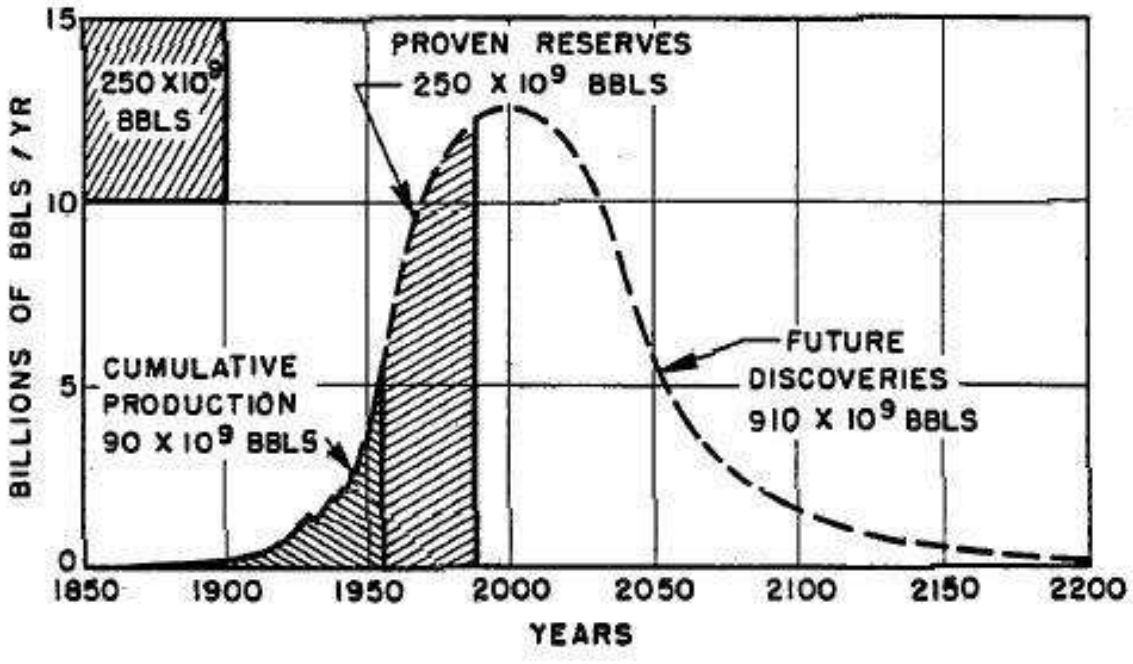


Figure 2-2: Hubbert logistic graph predicting world oil production [20]

rations reserving supply to artificially raise the price of energy, or on environmental regulations which restrict the drilling of new wells or processing oil [16].

Petroleum geologists in agreement with the Hubbert's Peak predictions find several problems with the above arguments. In the case of the environmentalists, alternative energies are a good idea to use, but in their current state they can't replace oil, because of energy density and quantity. The political viewpoint incorrectly assigns blame, and is fundamentally flawed.

The economist viewpoint ignores the differences between oil and other commodities. Foremost, oil is a finite resource, and more cannot be found at will. If it was possible to do this, more US oil would have been located in the 1980's, when demand drastically out paced supply, causing prices to rise [6]. Secondly, oil interacts with other commodities differently, forcing all prices higher because it is required for transport and some raw materials such as plastics. During extreme energy crunches, an estimated 90% of the cost in producing corn was from the cost of oil [6]. While higher oil prices do encourage the development of alternative energies, if energy prices are

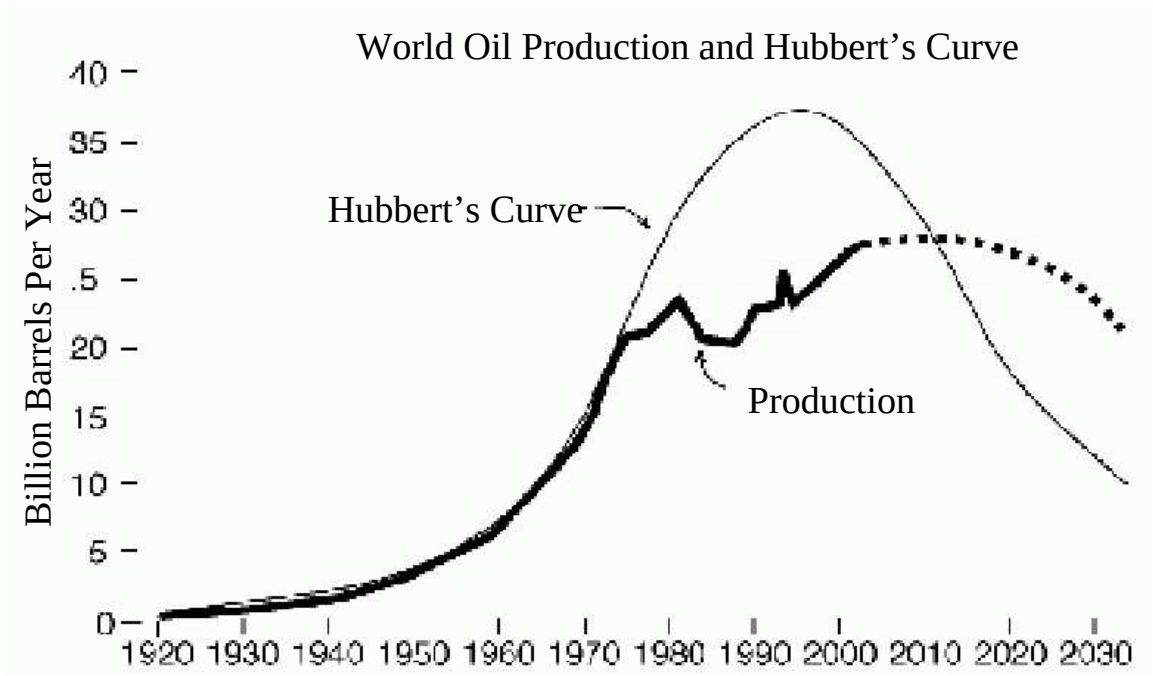


Figure 2-3: Comparing Hubbert's prediction to actual world oil production [17]

too high, there will not be enough energy available for the necessary research and development into them. Regardless of how high prices soar, the amount of energy available will become greatly restricted, which will have serious repercussions on the rest of the economy.

## 2.4 When Will it Peak?

The discussions in this section come primarily from [6] and [42]. As a geologist for Shell, Dr. Hubbert had privileged knowledge on how much more oil would be found within the US. He predicted two estimates of US oil production peaks based on a conservative and optimistic guess of the amount of undiscovered oil: 1965 and 1972 [6]. The actual peak occurred around 1970. The clearest sign of this peak was in the spring of 1971, when the Texas Railroad Commission "announced a 100 percent allowable" [6]. The regulatory body which controlled the production of oil allowed all oil wells in the US to produce as much oil as possible. The US could no longer meet its oil demand. Despite demand increasing, there was not the supply. As predicted,

production began to drop off after that point, and the US became dependent on oil imports.

Hubbert in 1974 claimed that if current trends continued, peak oil for the world would occur in 1995 [21].This does not seem to have been the case, as is illustrated in by comparing his predicted production curve to world oil production (Fig. 2-2 and Fig. 2-3). Possible reasons include the recession in the 80's from reduced oil consumption and may have contributed to a delayed peak; poor estimates of the total world supply of oil due to the lack of information available from the Middle East may also be involved [35]. Another way to look at oil supply is to envision the amount of oil in the ground which can be extracted at a certain price. As prices have risen, harder to access oil has become profitable to drill and new technologies have been developed for this purpose which were not available when Hubbert made his estimates. Based on new reserve findings, and the chance of finding new technologies which will allow us to access previously unprofitable oil deposits, new estimates have been made for when the actual peak will occur.

In a 2004 study based on numerical data from the Energy Information Administration, John Wood, Gary Long, and David Morehouse estimate several peak oil scenarios by extrapolating current trends and guessing the amount of oil available. They find that if a 2% growth rate continues, assuming a total oil volume of 3003 Billion Barrels, oil will most likely peak in 2037 [42]. They also calculated the effect on the date of the peak of different economic growth rates and total oil estimates. This estimate is considered by some by some to be overly optimistic. Their results are redisplayed in Fig. 2-4. Because growth rate is likely to be exponential, finding more oil does not move the peak forward much. Reductions in growth rate have a larger effect.

Other individuals expect that peak oil will occur much sooner, based on how quickly oil discoveries occur. Even if larger oil reserves exist, the process of drilling exploratory holes and developing the technology to access the oil takes around ten years [6]. Consumption already drastically overcomes finds; in 1998, on a global scale about 5.5 billion barrels were found per year, and about 26 billion used [44]. Deffeyes

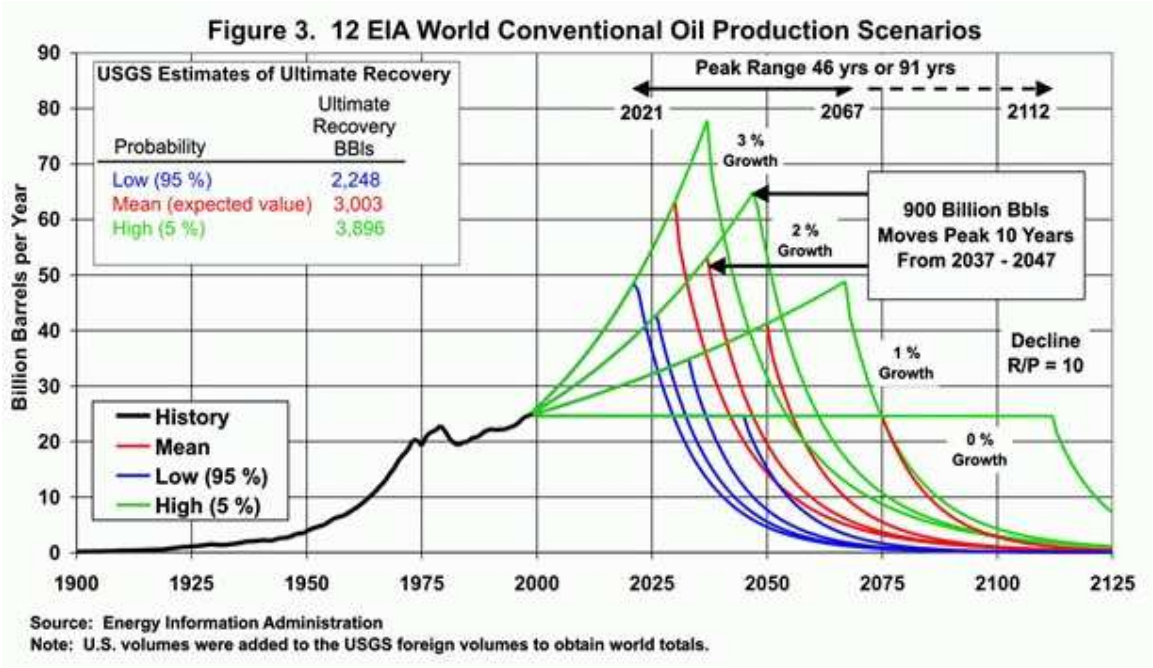


Figure 2-4: World oil production scenarios, based on variable growth rates and total oil estimates [42]

of [6] expected peak oil to occur around 2004, though commented that other scientists had estimated as late as 2008.

## 2.5 Consequences

The discussion in this section summarizes the arguments given by K. S. Deffeyes in [6], P. Roberts in [35], and R. Heinberg in [16]. The most obvious uses of oil are for the transportation of people, goods, and armies. Oil is also used for electricity, fertilizers, and plastics. Regardless of what happens in the future, the way in which these things are done will have to change. The way in which lifestyle will change is still under debate.

It is possible, though fairly unlikely, that developing technology will find a way to produce enough power, and save enough energy, that the way in which we live will not change noticeably. Others have suggested that the global political structure as we know them will fall apart, governments will fight bitterly for resources, and large

populations will have to starve to survive on the land available.

A third outcome is one of cooperation between people. The population would need to be smaller, and the economy would need to change from one of unbounded growth to a stable model. Quality living standards are possible with sustainable resources; however, societies would need to undergo a great deal of changes [35], [16].

To avoid a violent possibility, working towards political and technological solutions should begin right now, while energy resources are still plentiful.

## 2.6 Replacing oil

This section draws heavily upon the arguments made by K. S. Deffeyes in [6], P. Roberts in [35], and R. Heinberg in [16]. In developing technologies to replace oil there are at least seven considerations: return, quantity, density, quality, storage, environmental impact, and safety. Energy output should be greater than energy input, or the return should be greater than 1. The return needs to be improved across the entire line of manufacture, since the amount of energy available is a global quantity. For example, a car which requires less energy is not a valuable technology if it requires additional energy manufacture over previous cars, and does not manage to save this amount of energy over the course of its use. Energy quantity will need to be great enough to meet the basic needs of people available. Problems of quantity can be approached both by finding new energies and by reducing total consumption. Energy density is the amount of energy per unit size (either volume, mass, or surface area). Cars and planes require particularly high energy densities to run, and oil has an incredibly high energy density. Energy quality relates to how easily one energy can be transformed into another and how useful each form is. Electricity is of high quality – it can be used for many things, and is difficult to make. Heat is of low quality – it is the by product of other processes doing work and is difficult to use. Petroleum is a wonderful chemical storage mechanism, whereas electricity is very difficult to store well. Environmental impact and safety relate to the risks for the ecosystems and consumers.

There are many renewable energies currently under consideration: solar, wind, tide, wood, dams, geothermal, plant oil, hydrogen, and alcohol. Coal, natural gas, and nuclear energy will be valuable as transition energies, though they are finite like oil. As an example, below is a discussion of some of the problems and strengths of one energy type, solar power.

Unlike some of the other renewable resources, quantity is not much of a problem with solar energy – the industrialized nations could be powered on the sunlight falling on 1% of the Earth's surface [35]. However, energy density, quality, storage, and return prevent solar energy from solving the current energy problem.

Capturing 1 percent of the sunlight falling on the earth's surface actually requires a great deal of surface area, due to its low energy density of about 22 watts per square foot, averaged over day and night [16]. The surface area of the planet is around 510 million $km^2$, while the surface area of the US is around 9.6 million $km^2$, or 2%. So, half of the surface area of the US would need to be completely covered in 100% efficient soar cells to power the world.

Solar cells however are not efficient, due to the losses in capturing sunlight and transforming it into a high quality energy like electricity. The theoretical maximum efficiency for photovoltaic (solar to electricity) cells is 72% with 36 junctions (layers of materials), and manufacturing difficulties currently prevent the creation of photovoltaic cells better than 30% efficient [39]. Technologies currently in development due to a new effect found in Indium gallium nitrides look like they could produce photovoltaic cells up to 50% efficient [39]. So, the surface area estimate above needs to be multiplied by a factor of at least 2, if not a little over 3.

Solar energy is also available only when time of day and weather permits. At other times it must be stored. When converting solar energy into electricity, the most cost efficient storage method currently available is to send it into the power grid during the day to reduce the amount of fossil fuels being used at that moment and take from the grid at night from the fuels not burned during the day. Solar power alone can't handle all the energy needs because it simply isn't available at night.

Photovoltaic cells are made primarily out of forms of silicon, which are fairly

energy expensive to create. The energy return on energy invested (EROEI) on solar energy was estimated at 1.9 for solar space heaters, and 1.7 to 10.0 for photovoltaics in 1984 by Cleveland, Costanza, Hall, and Kaufman[16]. The EROEI of photovoltaic cells, however, was estimated at .41 by Odum in 1996. Odum also estimated solar water heaters to have an EROEI of .18 [16]. Based on these numbers, it is hard to determine if solar energy is actually worth the energy invested into creating the cells. Of course, as manufacturing technology on these improves, the EROEI will improve because the cost of creating a cell will drop.

Currently, the market for solar energy is growing rapidly (about 30% a year) despite a negative view of it from the 1980s, when the technology was not developed to a feasible level [35]. As more solar cells are sold, manufacturing techniques will improve, and eventually solar cells will become a commercially attractive option. They are about three to four times as costly as fossil fuels at the moment though.

Most photovoltaic cells are silicon based in nature, so their manufacture results in the same environmental and safety hazards as computer equipment . Health and environmental risks such as spontaneous combustion and toxicity are primarily manufacture concerns, and described in [36].

For the most part, there are similar issues which prevent the other renewable energies from providing enough energy to meet the current energy consumption. For example, wind is similar to solar power in energy density, hydrogen will always consume more energy to create than it will yield (though it is very good for storing energy), and geothermal is only available in very specific, limited locations. No one solution will be enough, in fact it is unlikely that all the solutions combined will be enough. Changes in lifestyle, reorganization of the economy, and population reduction may all be necessary.

The concerns with the transition energies (coal, natural gas, and nuclear power) are from very different metrics. While energy density and quantity are enough for at least a limited period of time, there are concerns of cleanliness and safety.

We have not yet solved the energy problem, and we do not know how much time we have left to try. In addition to putting resources into improving these conventional

methods, it is important to take a risk and put some resources into examining the many cold fusion experiments to see if any of these can contribute to the solution. If any of these experiments were to work, it would lead to the discovery of a new physical mechanism which could provide energy in a cheap, clean way. This would help soften the blow of the energy crunch.

# Chapter 3

# Background

This chapter covers the previous work done on the Yang-Koldamasov effect. To give context to this work, there is also a discussion of the state of the Cold Fusion field and the reasons for it.

Hot fusion is very unlikely to occur at low temperatures due to the large Coulomb barrier. While electron screening of the nuclear charges increases the probability of fusion reaction in metals, fusion at normal temperatures is still very unlikely. These processes are discussed briefly in the first two sections of this chapter.

Because of these temperature constraints, the announcement of Fleischmann and Pons in 1989 of an excess energy effect seen at room temperature and thought to be nuclear in origin was very disruptive. The effect of the announcement on the field is discussed in section 3.3.

Since the 1989 announcement, work in the field has continued and many experiments have been conducted. In 2004, the Department of Energy agreed to conduct a review of the field based on this new information. The amount of work conducted and the results of this review are summarized in sections 3.4 and 3.5.

The development and research which has already gone into the Yang-Koldamasov effect is presented in section 3.6.

## 3.1 Hot Fusion

Fusion is the process by which two nuclei come together to form a single heavier nucleus. For small nuclei, this process releases energy, while for large nuclei it requires energy. The energy released for a few fusion reactions is given in table 3.1, along with the temperatures at which the energy produced by the reaction exceeds the amount lost due to bremsstrahlung radiation.

| Reaction | | Temperature [37] | |
|---|---|---|---|
| Fuel | Products | Millions C | keV |
| D+D | $\rightarrow{}^3$He(0.8 MeV)+n(2.45 MeV) | 45 | 4 |
| D+D | $\rightarrow$T(1.0 Mev)+p(3.02 MeV) | 350 | 30 |
| D+T | $\rightarrow{}^4$He(3.5 MeV)+n(14.1 MeV) | 400 | 35 |
| D+$^3$He | $\rightarrow{}^4$He(3.6 MeV)+p(14.7 MeV) | 400 | 35 |

Table 3.1: Energies of fusion for a few deuterium reactions

Two main forces are involved in fusion, the strong nuclear force and the Coulombic force. Since both nuclei in the reaction are positively charged, the Coulombic force pushes the nuclei away from each other. The strong force is attractive, but only powerful at very short distances. Above the distance $r_n = 1.44 \times 10^{-15}(A_1^{1/3} + A_2^{1/3})$m, where $A_1$ and $A_2$ are the atomic weight of the two nuclei, the dominant forces are Coulombic, and therefore repulsive [4]. The nuclei must be closer together than $r_n$ in order for fusion to occur.

One can approximate the energy needed to overcome the Coulombic forces by calculating the Coulomb energy at this distance,

$$V_{coulomb}(r_n) = q_1 q_2 / r = Z_1 Z_2 / (A_1^{1/3} + A_2^{1/3}) \text{ MeV}$$

For example, two deuterium atoms require $1/(2 * 2^{1/3}) \approx 0.4$ MeV to undergo fusion. This energy corresponds to temperatures around $3.09 \times 10^9$ C, using the relation $E = 3/2 k_B T$.

This simple classical viewpoint does not take into account quantum tunneling, or the possibility that a particle can pass through an energy barrier to reach a potential well. A useful quantity when thinking about tunneling is the probability of reaction

per unit time at a certain center of mass energy, $E$. This quantity is called the cross section, $\sigma(E)$.

$$\sigma \approx \lambda_b^2 \times \tau \times R$$

where $\lambda_b^2$ is the square of the de Broglie wavelength, and roughly $1/E$, $\tau$ is the barrier transparency, and $R$ is the probability that the nuclei will fuse.

$\tau \approx e^{-\sqrt{E_G/E}}$ as long as $E \ll E_G$. $E_G$ is the Gamow factor,

$$E_G = (\pi\alpha_f Z_1 Z_2)^2 2c^2 m_1 m_2/(m_1+m_2) = 986.1 Z_1^2 Z_2^2 m_1 m_2/m_p(m_1+m_2).$$

$R$ is specific to the particular reaction; however, its effect is small in most reactions [4]. It is a weak function of $E$, and sometimes written as $S(E)$, the astrophysical S factor.

The effect of tunneling then is

$$\sigma(E) = \frac{S(E)}{E} e^{-\sqrt{E_G/E}}$$

A plot of the fusion cross sections for D-D and D-T reactions are given in Fig. 3-1. The probability of reaction is very small unless temperatures are fairly large.

If we approximate the center of mass energy to be $3/2k_BT$, then near room temperature $E \approx .0353eV$ and $\sigma_{dd} \approx 3.6 \times 10^{-2298}$ barn. At room temperature, this probability is nearly zero (thought not quite, as in the classical case). This is a simplification and other physics is involved. In molecular $D_2$, there is tunneling due to zero-point fluctuations and screening which results in $D_2$ having a theoretical half-life of about $10^{64}$ sec [26].

## 3.2 Electron Screening

The calculations above assume 'bare' nuclei, or protons and neutrons without electrons. Nuclei usually travel with electrons, which reduces the apparent charge of the atom from a distance. This effect is called electron screening. The required energy for

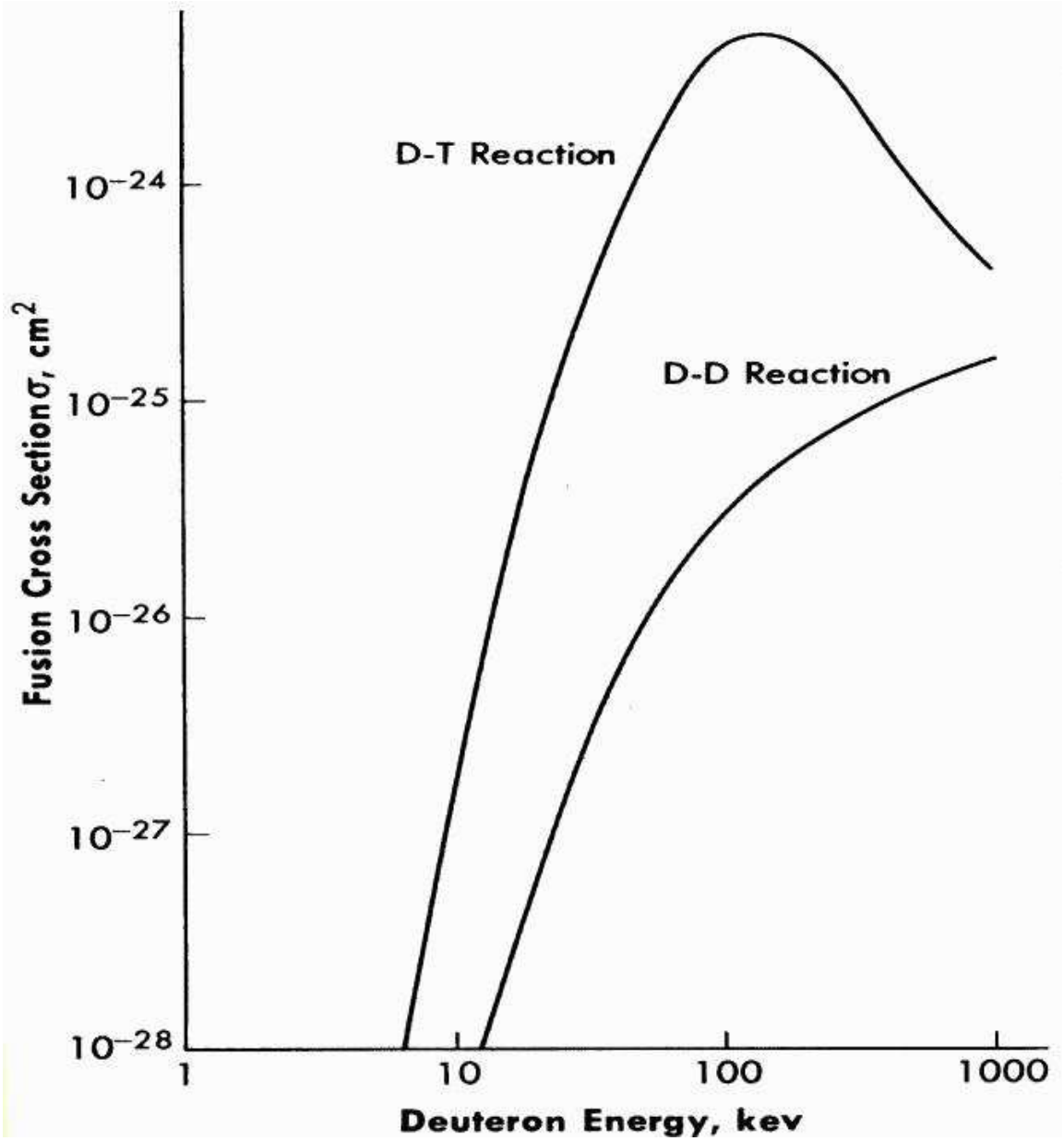


Figure 3-1: Fusion cross sections as a function of deuteron energy [37]

| Material | $U_e$ (eV) | Material | $U_e$ (eV) |
|---|---|---|---|
| metals | | semiconductors | |
| Sn | $130 \pm 20$ | C | $\leq 60$ |
| Al | $520 \pm 50$ | Si | $\leq 60$ |
| Fe | $460 \pm 60$ | Ge | $\leq 80$ |
| Ag | $330 \pm 40$ | insulators | |
| Cu | $470 \pm 50$ | BeO | $\leq 30$ |
| Pd | $800 \pm 90$ | B | $\leq 30$ |
| | | Al2O3 | $\leq 30$ |
| | | CaO2 | $\leq 50$ |

Table 3.2: Screening power for several materials at 20 C

nuclear fusion is lower because the two atoms "see" a lower charge as they approach each other.

Of interest to experimentalists is the ratio of the cross section with screening versus the cross section with bare nuclei. This quantity is call the enhancement factor, $f_{lab} = \sigma_s(E)/\sigma_b(E)$ [3]. Using a simple screening model which fits the data well, the enhancement factor is

$$f_{lab} = \sigma_s(E)/\sigma_b(E) = \frac{ES(E+U_e)}{E+U_eS(E)} e^{\sqrt{(E_G/(E+U_e))}-\sqrt{(E_G/E)}}$$

Here, $U_e$ is the effect of the shielding on the energy barrier, and is roughly a constant [5]. For deuterium reactions in insulators, $U_e$ is measured to be less than 30 eV. In metals, $U_e$ for deuterium reactions is much larger, in excess of 100 eV.

The screening energy $U_e$ can be found for different materials by comparing $\sigma_b$ to $\sigma_s$, which can be measured by shooting a beam of particles at a material composed of the target particles [33]. Several examples are shown in Table 3.2, a subset of the table presented in [34]. In this table, the target and beam particles were both deuterium. This effect was also tested with a $^3He$ beam fired at deuterated Pt, and it was found that the effect was not beam dependent [34]. Interestingly, the values differ greatly between metals and other situations like insulators, semiconductors, and gases.

In metals, $U_e$ varies with the free electron concentration and the temperature [32]. The results are empirically found to follow a classical Debye model scaling. As temperature increases, the effect of screening decreases. Variations between metals seem

to relate to the number of free electrons [34]. However, metals have structure different than plasmas. Initial work on screening models more appropriate for metals show more significant effects than those found in experiment [5]. The current mechanism for screening of the powers seen in experiment is unclear.

## 3.3 Fleischmann and Pons

The following discussion of the Fleischmann and Pons 1989 announcement and its repercussions is based on an input from Dr. P. Hagelstein [13].

On March 23, 1989, Fleischmann and Pons at the University of Utah announced an incredible result: that running a voltage through electrolysis heavy water using palladium cathodes resulted in excess heat so great that it could not be explained by chemical means. Fleischmann conjectured that the effect was due to deuterons somehow reacting to form $^4$He, and hence the energy of the order of nuclear reactions. It seemed that the only two possibilities were: they may have stumbled across something amazing, or they made serious experimental errors. This announcement produced two primary responses, one from the physics community and one from the chemistry community.

The physics community had a background of about 70 years of research into nuclear physics and hence fusion, which led to the identification of possible problems with the interpretation of the experiment.

1. Energy is carried away from fusion reactions by energetic particles.

   The experiment suggested that energy was not put directly into energetic particles, but provided no information on the specific reaction mechanism.

2. The primary D+D reaction pathways (p+t and n+$^3$He) were already known, which produce energetic particles and happen about as fast as the laws of physics allow.

   These known pathways happened so quickly, that once the deuterons were close enough together it would be impossible for any new mechanism to happen

fast enough to compete, as seemed to be implied by the experiments. The experiment implications would be inconsistent with relativity.

3. The reaction rates of nuclear D+D fusion can be calculated at room temperature. These rates are so small that it was thought that screening could not improve them enough for reactions to occur sufficiently fast to be consistent with the observations.

Some in the chemistry community had a very different response. A new physical process was on the table, so the absence of a corresponding theoretical picture was not an impediment. Additionally, Fleischmann was a well-regarded electrochemist. A 30% to 50% excess heat effect had been measured, when 0.1-1% accuracy was common for calorimetry in the field.

Efforts to reproduce the experiment, mostly negative, followed. On May $1^{st}$, American Physics Society (APS) included in their regular meeting a session on cold fusion results of experiments, most of which were very negative. The viewpoint was put forth that the original announcement was an error at best, and a hoax at worst. This viewpoint was solidified by this meeting, many talks at conferences, books, and the DoE review of the work in 1989, done by the Energy Research Advisory Board (ERAB).

The experiment had originally been presented as a simple (sophomore-level) electrochemistry experiment, and early reproduction attempts appeared to treat it as such. There was little information on the operation requirements for the original experiment available at this time. In less than forty days of time, there was not enough information to determine the necessary conditions for operation. Finding the necessary conditions took other groups years; within two years time successful reproductions had occurred at SRI and other labs.

In addition to the correctness of the experiment, there were two other large considerations: the funding and reputation of all other science fields. At the time of the announcement, cold fusion was a topic very much in the public eye. It was appearing in magazines, newspapers, and television. Since science is funded by the good will

of the public, who are generally content with continuing funding. However, a large failure receiving funding and in the public eye had the potential to diminish funding for all (other) scientific fields. Likewise, the reputation of science as an honorable, competent discipline would be tarnished. Since there was little guarantee that the effect existed, or was of a nuclear nature, it could have been very risky for scientists to allow attention on cold fusion for very long.

Even at the present time, there are still very strong feelings on both sides of the debate. On one hand, people perusing experiments in the lab continue to see abnormalities. On the other hand, most physicists are convinced that there can be no new effects, and view the work with skepticism. Mainstream reproduction attempts have not been conducted in recent times, even though the experiment is now much better understood. Due to the absence of funding, it is difficult to perform rigorous scientific experiments.

## 3.4 Experiments after Fleischmann and Pons

Since 1989, many experiments have been performed in the field of low energy nuclear reactions. An archive of many of these papers can currently be found at http://lenr-canr.org, with around 250 authors and 900 papers as of 2007. Additionally, twelve international conferences on cold fusion (ICCF) have been held across the world, each with around 100 papers submitted. For instance, the proceedings from the tenth conference (ICCF10) has 1013 pages devoted to 90 papers on experiments, related experimental topics like electron screening and calorimetry practices,and discussions of social topics like website maintenance and teacher debates [15]. The experiments in the field have varying experimental set-ups and detect nuclear effects in a variety of ways: excess heat, protons, neutrons, tritium, and helium. It is worth noting that the observation of particles is generally anti-correlated with the observation of excess heat. Early experiments have a large variance in repeatability, though in recent times this has improved greatly.

## 3.5 The 2004 DoE review

In 2003 P. Hagelstein (MIT), M. McKubre (SRI), D. Nagel (George Washington University), T. Chubb (NRL and Research Systems Inc.), and R. Hekman (Hekman Industries) asked the DoE to do a second review of cold fusion [31]. In recent years, Cold Fusion had been identified with ESP and UFOs. Their aim was for the DoE to publicly recognize the research in this field as science rather than as not science. They approached the DoE because of strong experimental evidence.

There were a total of eighteen reviewers from fields related to cold fusion such as materials science, chemistry, nuclear physics and atomic physics. Written work was available to all reviewers, and nine attended oral presentations. The content of the work was selected by the cold fusion scientists who requested the review; however, unlike the initial DoE ERAB report which allowed for unlimited material, this review was restricted to fifteen pages and seven presentations that occurred in one morning and one afternoon. The eighteen reviewers were charged with three tasks, quoted from the mailed review charge letter below [7]:

1. "Evaluate the experimental evidence presented for the occurrences of nuclear reactions in condensed matter at low energies (less than a few electron volts)."

2. "Determine whether the evidence is sufficiently conclusive to demonstrate that such nuclear reactions occur."

3. "Determine whether there is a scientific case for continued efforts in these studies, and, if so, to identify the most promising areas to be pursued."

These charges were developed while the fifteen page review material was being prepared. Note that while the review material focused on excess power measurements, by asking specifically for evidence of nuclear reactions the first review charge implies a need for energetic reaction products to be present as evidence. These particles are not present quantitatively in excess heat experiments. The second question has the same issue, and in light of the first question, can only be answered negatively. The

DoE did not include a charge on excess power or energy measurements, which were known in advance to be the focus of the review material.

The reviewers' general response to the body of work was that reproducibility, documentation, credibility, and high level direction were all problems [2]. However, many reviewers found the body of work convincing that some interesting new effect was occurring, and that individual well written proposals should be funded.

While a small few were impressed that reproducibility had been improving in the field over time, most were concerned that even within the same lab, the ability to reproduce an experiment was spotty, and the parameters which led to the effect were not well known. Many reviewers felt that this was attributable to a lack of consistent documentation of the trials done and characterization of the experimental apparatus. These viewpoints are somewhat surprising, since the reviewer charges never brought up the issues of reproducibility, the review document gave instances of multiple labs repeating the same experiment, (implying good reproducibility), and questions about reproducibility were directly answered at the oral presentations with the assurance that several labs were reporting 100% reproducibility of excess heat in addition to other effects.

The reviewers were divided on the likelihood that fusion was the cause of the anomalous signals seen in the experiments presented [2]. Two individuals thought that the evidence presented was conclusively nuclear reactions, though one of these individuals was still skeptical. Three reviewers did not find the current body of work sufficiently different from the original experiment, or the credibility of the field high enough, for this body of work to merit close review. The rest of the reviewers had intermediate opinions. Five thought it was possible that the evidence could be fusion related. Four agreed that the results were anomalous, but felt that it was more likely that a new undiscovered process was behind the results than fusion reactions. Four did not think that the experimenters had properly considered and ruled out all of the possible experimental errors (such as a chemical reaction between deuterium and oxygen creating the heat), which would explain the results with already understood theories. Overall, the majority of reviewer comments recognized that some abnormal

effect was occurring, whether or not it was related to fusion. This result is very positive and significant, given how easy it would have been to ignore the entire body of work due to social stigma and preconceived opinions [15]. Additionally, many reviewers made positive comments on the excess power measurements.

The reviewers were much less divided in their recommendations for future funding of this work by the DoE [2]. One felt that the DoE should specifically fund research in this area. Eleven agreed with varying levels of enthusiasm that individual, careful proposals should be considered if they met certain conditions. While these conditions varied from reviewer to reviewer, they often included a clear proposal as to the purpose of the experiment, a clear description of how this experiment differed from previous ones, or what knowledge would be obtained by the results of this experiment. One reviewer recommended that such proposals should be small, while another suggested a specific proposal to reproduce the work of S. Jones in another lab. One reviewer felt no funding should be given. One did not reply to the question directly and had a fairly negative view of the work, while four did not comment on whether or not the DoE should fund, but did say that work should be continued in the field.

The benefit of this review is that despite the initial very difficult challenges laid out by the DoE, the final summary report showed mixed opinions on the possibility of cold fusion. Many took notice that the review was requested of the DoE by the field. Such a request would not have been made without great confidence in the body of evidence produced. The evidence in the review document was compelling enough for many reviewers to rethink their opinion of the field. As a result, attitudes are changing elsewhere; papers are being considered for mainstream journals, some papers are in print, and several commercial ventures have been founded [15]. Lenr-canr.org is also reporting record downloads, comparable to the amount of downloads for the Physical Review journal website.

## 3.6 Previous Work on the Yang-Koldamasov Effect

Work began on this effect in the mid 1990s in Russia. Koldamasov developed a cell, with heavy water filled pores, which released excess heat when irradiated with ultrasound [29]. However, the energy could not easily be extracted in a high quality form, and so development began on a hydroelectric machine, which eventually became the current device under test [29].

During this time period, Dr. Hyunik Yang met Dr. Koldamasov, and together they published "Explosive Generation of Isotopes/Nucleosynthesis". They created a patent together for the current device which divided up commercial rights across the globe [29].

The patent application details a machine as follows [1]:

- an operating fluid appropriate for generating ionization and nuclear fusion reactions

  the fluid can be either

  - light water with resistivity larger than $10^6 \Omega m$
  - light/heavy water mixture between 100:1 to 100:30, again with resistivity higher than $10^6 \Omega m$
  - mineral oil of viscosity ranging from 5 to 30

  If water is used, a purifying unit will be necessary.

- an output pump designed to make the operating fluid at a predetermined pressure

  The pump can be a gear, piston, or vane pump. In addition, a pulse generator is needed to supply pulses at a frequency determined by the resonance of the fluid and metallic and dielectric inserts.

- a reservoir of operating fluid

- a dielectric body with an inlet and outlet to allow for the passage of fluid, perhaps multiple holes with different diameters.

  In this paper, this body will be called the cell. The different diameters are used to hold the insert described below using pressure from the pump, and to allow cavitation formation just after the insert by reducing the pressure. An image of the cell used in the experiment discussed here is shown in Fig. 6-1

- at least one metallic insert with a through hole for the dielectric, which allows for the passage of fluid

  The metallic insert can be copper, aluminum, gold, silver, palladium, or any alloy which will facilitate the ionization of the operating fluid by emitting electrons.

- a dielectric insert with at least one through hole for the passage of fluid, to be inserted in the dielectric body, promoting nuclear reactions through cavitation emission

  The material of this insert can be industrial plastic, Pyrex, crystal, ceramic, ruby, or silicon carbide. It must retain the electrons emitted by the nuclear fusion reactions due to cavitation emission.

  In this paper, this insert will be called the tip. An image of it is available in Fig. 6-2.

- at least one pair of metal members to control the polarity of the ionized operating fluid or collect electricity

The patent application also provides a procedure for running the device [1].

In the early 2000s, Dr. Yang worked with Baranov in developing a water unit which could be spiked with heavy water to produce the effect [29]. At the Keldish Institute in Moscow, Director Andre Desyatov, Prof. Vladimir Vysotskii of Kiev Shevchencko University and Prof. Alla Kornilova of Moscow University worked on a unit similar to the original unit, with additional sensors, a vacuum pump, and better RF shielding [27] [29].

As of 2005, two Russian groups were working on the project in addition to work being performed in Korea and Canada. The second Russian group was composed of Evgeny Pavlovich Velikhov, Gerasimovich Gnedenko, and Vital'evich Goryachev of the Kurchatov Research Institute also worked on the device [27]. The latter two are patent holders of the device under Russian patent RU2232210 [27]. The Korean group includes Dr. Hyunik Yang, and Dr. Nahm Choe, mechanical engineering professors at Hanyang University in Korea [27].

The various units in existence have a fair amount of variation between them. The Keldish units have a gear pump, sharp angles, and are fairly compact, while the Korean built units generally have longer pipes, smoother angles, and frequently have vane pumps [29]. Pipe diameter and reservoir size also vary. Sometimes the connecting tubing is all metal, other times there are plastic components.

In 2004, the company iESi was founded in Edmonton, Canada [29]. This company did several live presentations for various scientists and investors, including one around Feb 13, 2005 for scientists and one June 6, 2005 for investors[25] [27]. Scientists who attended the presentations in February include P. Hagelstein and D. McConnell. Attendees in June and July include M. Fleischmann, M. McKubre, and D. McConnell [25] [27] [29].

In February, visitors were shown large arcing and discharges through the tip, oil, and inch thick acrylic cell in addition to at least 3300 watts of heat production (associated only with heating the oil, and not the frame and room) at an operating power of 800 watts based on temperature measurements of the reservoir before and after the run [25] [29]. However, little to no scientific data was presented. While observers had high confidence that the machine was working, there was no way to be certain that the effect was not being faked in some way [25] [27]. iESi made two claims to P. Hagelstein during his February visit, though these were not necessarily observed [25]:

1. At maximum operation, the machine produces a factor of 5 gain at temperatures around but less than 100 C.

2. The effect is nearly 100% reproducible. In support of this claim, the machine was operated three times during the February visit with apparent discharge and excess heat.

P. Hagelstein recommended an independent observation of the effect to increase credibility [25].

The later visits in June and July looked visually different. In both visits, the arcing through the oil was primarily in the direction of oil flow, unlike the earlier visit where arcing was perpendicular to it. The June visit was primarily a demonstration for investors, and the effect was not verified with instrumentation, so it is not clear that the machine was producing excess heat at this time. An attempt was made to confirm the effect in July which produced a null result. Between the February demonstration and the two later demonstrations the behavior of the machine was both visually and measurably different.

At ICCF12 there were two presentations on the Yang-Koldamasov, one done by Steven Krivit of New Energy Times, and one by its current operators on their findings and investigations with $^{11}B$ in the device [27] [23]. Journalist S. Krivit presented both the amazing claims of the device and the state of the current research. While the designers claimed high reproducibility, control in operating and turning off the device, and power of commercial magnitude [27], there was little to no scientific data collected, little to no published work, and no independent reproductions [28]. While iESi claimed that independent audits had been conducted, the content of these audits was not publicly released because they were the private property of those who paid for them [27].

For the rest of this thesis, the working fluid will be taken to be oil, since this was the working fluid in the experiment that Dr. Yang and FRC requested confirmation of.

Figure 3-2: M. Fleischmann observing a damaged cell, provided by S. B. Krivit, ©New Energy Times, use permitted for non-commercial educational purposes

# Chapter 4

# Non-Nuclear Explanations: Combustion or Measurement Error

This chapter discusses two of the possible explanations for the Yang-Koldamasov effect which are not nuclear in nature: the possibility of measurement error, and combustion. I do not have access to the original devices that the effect was seen on, so any discussion of measurement error is only conjecture. Discussions of combustion reflect simplified models that have been proposed in our collaboration at MIT.

## 4.1 Measurement Error

A single measurement error does not appear to account for the excess power seen at iESi during their early demonstrations. It is the opinion of an observer of some of the iESi demonstrations (Denis McConnell) that the heat power out was greater than the maximum motor output, so power measurement error alone is not the cause of the large power gain.

There have been two independent visits to iESi by P. Hagelstein, which each measured the power or energy out in very different ways. The possibility of measurement error needs to be considered separately for each of these independent measurements.

At the first visit in February, the measurement of energy out was one integrated over time. The reservoir temperature was taken before the run began and after it

was completed. The temperature of the reservoir was independently verified by the observer Denis McConnel, who used his own thermocouple to check for spatial variations in the tank by measuring at multiple points. Since the temperature difference is so different from start to finish over the 15 minute run, a small thermocouple error of around 2 C would make a small percentage change over the range of about 50 C. For this calculation, four measurements were used: oil specific heat, tank volume, temperature difference, and electrical energy in. While a combination of measurement errors could have lead to an apparent effect, it is unlikely that a single measurement error could have resulted in the 300% to 500% gain observed.

On a later visit in July, the measurement of power was achieved using differential calorimetry over the cell. P. Hagelstein observed that the thermocouples had an offset error, which caused the total heat power to seem to grow with increased flow rate [12]. Because the temperature difference over the cell is only a few degrees, a thermocouple offset of the order of 1 to 2 C results in a large percentage change in the results of the calculation.

## 4.2 Combustion

To determine if combustion was a likely cause of the effect observed at iESi, an order of magnitude complete combustion calculation can be compared to the iESi observations of a power gain of roughly a factor of three to five when running around 800 W over 15 min with about 30 kg of oil, corresponding to a temperature rise of about 50 C.

There are three requirements necessary for combustion: fuel, oxygen, and sufficient energy to begin the reaction. Assuming that the oil provided will have sufficient volatiles for combustion, and that the arcing and palladium catalysts will allow combustion, the limiting factor for combustion will be oxygen. This scenario is called fuel-rich.

The amount of oxygen in the system can be computed by Henry's law:

$$C = x_2 \times p$$

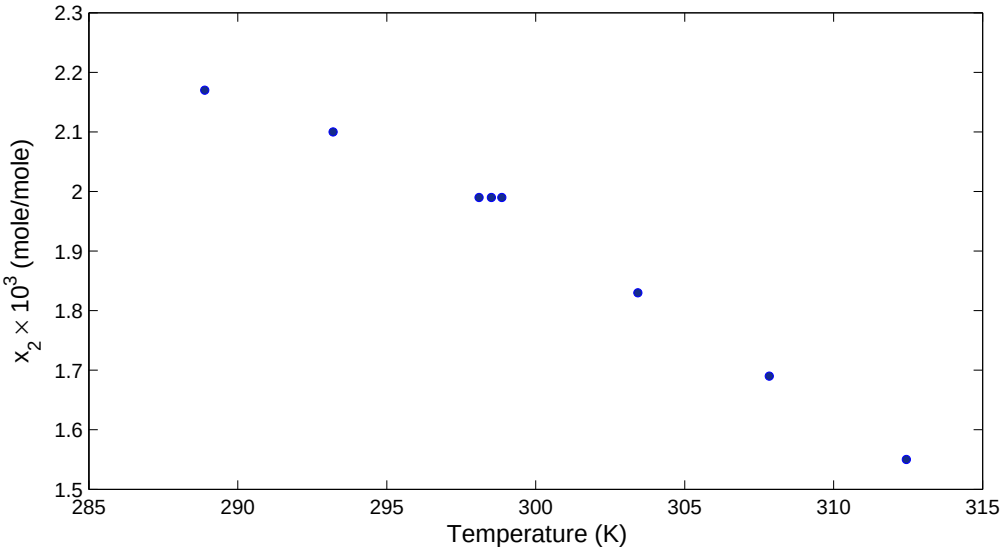


Figure 4-1: Solubility of $O_2$ in hexane as a function of temperature [8]

where $C$ is the concentration, $x_2$ is the solubility of oxygen in the oil, and $p$ is the partial pressure of oxygen above the oil. The partial pressure of oxygen in air at standard pressure is about .2095 atm. An upper limit on the solubility of oxygen in the oil used at iESi can be obtained by considering the solubility in a pure n-alkane, such as nonane. The solubility of oxygen in nonane at 25 C is .00212 moles $O_2$ per mole nonane [38]. This solubility value is larger than the oxygen solubility of the oil used in the experiment in this thesis, based on the Herguth lab measurements. Since the exact oil used at iESi is unknown, for this calculation $x_2 = 0.00212$ will be used.

The partial pressure of oxygen in air at room pressure is about 0.2095. Based on the solubility estimate of a normal alkane solvent, oxygen partial, and Henry's law, the oxygen concentration in oil at 25 C is less than 0.000444 moles $O_2$ per mole solvent. If the oil on average has a molecular weight similar to nonane of 128 g/mol, then 30 kg of oil would contain 234 moles of solvent, implying around 0.104 moles $O_2$.

The estimate above does not take into account that solubility is a function of temperature. As an example of how oxygen solubility might change with temperature in an n-alkane, Fig. 4-1 shows how oxygen solubility changes in hexane, based on data

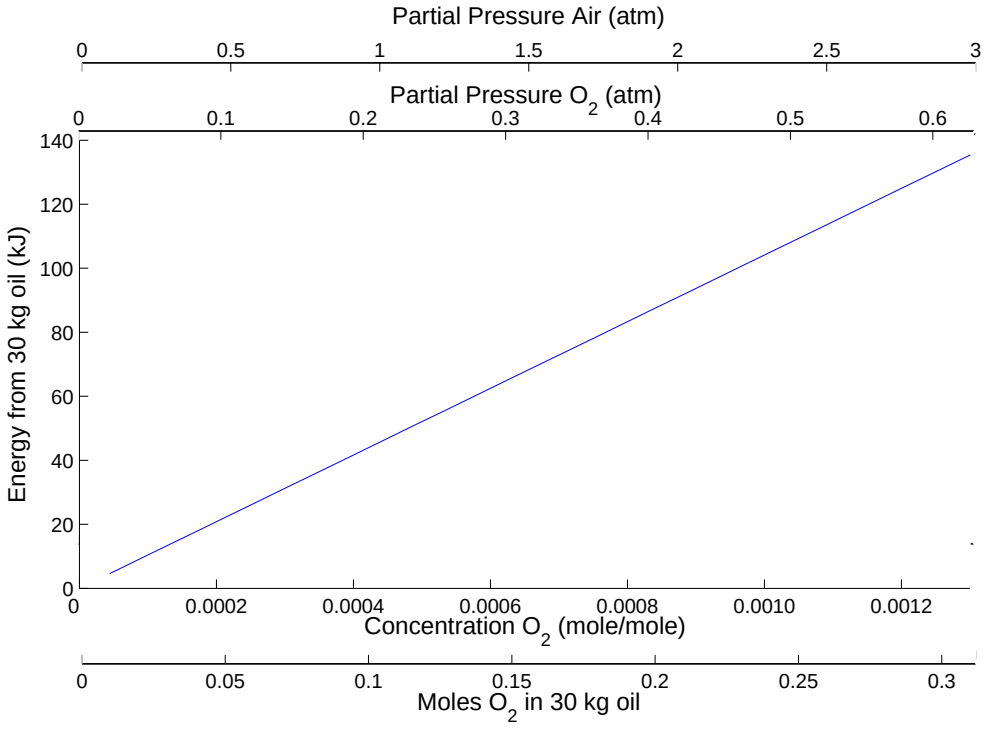


Figure 4-2: Combustion energy dependence on oxygen quantity

from [8]. Again assuming that the oil behaves roughly like a normal alkane solvent, the solubility estimates used here at 25 C will be larger than the solubility when the machine is running, and between 25 and 70 C.

With this estimate of oxygen the energy produced can be calculated. The amount of energy from combustion per mole of oxygen is shown in table 4.1. Assuming the complete combustion of a volatile such as methane, ethane, or propane, the energy per mole of oxygen is about 445 kJ/mole. The estimate of 0.104 moles of $O_2$ implies 46.2 kJ of energy . The effect of varying the oxygen level is shown in Fig. 4-2. This value is likely to be an overestimate, since complete incomplete combustion is more likely in this situation.

The demonstrations at iESi lasted about 15 min. At the energy output given above, assuming constant power there would be 51 watts produced over the course of the experiment (see Fig. 4-3). A factor of three gain from 800 watts input would be

| Fuel | Reaction | E (kJ/mole) |
|---|---|---|
| | Complete Combustion of Volatiles | |
| Methane | $CH_4+2O_2 \rightarrow CO_2+2H_2O$ | 445.2 |
| Ethane | $C_2H_6+3.5O_2 \rightarrow 2CO_2+3H_2O$ | 445.7 |
| Propane | $C_3H_8 + 5O_2 \rightarrow 3CO_2+4\ H_2O$ | 444.0 |
| | Other Fuels | |
| Hydrogen | $H_2+.5O_2 \rightarrow H_2O$ (g) | 484.0 |
| Aluminum | $2Al+1.5O_2 \rightarrow Al_2O_3$ | 1117.1 |

Table 4.1: Energy per mole $O_2$ for several combustion reactions

2400 watts, much larger than the estimate of the amount combustion could produce.

$$\Delta T = \frac{E}{mC_{oil}}$$

is the equation for computing the temperature rise of the oil associated with this effect, where $C_{oil}$ is the specific heat of the oil. Assuming that the specific heat of the oil at iESi was similar to 1.933 J/gC, the specific heat of the oil used in the experiments in this thesis, the temperature rise of 30 kg of oil would be 0.8 C. Fig. 4-4 shows the dependence of temperature rise on the amount of oxygen. Overall, the increase in temperature would not have been much larger than the amount due to pump power at the expected level of oxygen in the system.

A lack of oxygen severely limits the ability of this system to burn volatiles. If the amount of oxygen was increased sufficiently, then enough energy could be produced from burning.

Oxygen might be replenished from air via reabsorption as the oil cycled through the machine. Assuming that the oxygen dissolved instantaneously, the amount of oxygen in the system could be replenished once per cycle, as the oil fell into the reservoir and was exposed to air. However, with only about three to five cycles over fifteen minutes, the amount of oxygen would only increase by about a factor of five. Hence, 250 watts of power (a temperature rise of 4 C) is an order of magnitude smaller than the smallest reported effect.

Depending on the specific set up of the machine, air bubbles might be introduced to the oil stream before entering the pump, and dissolve due to the pressure increase

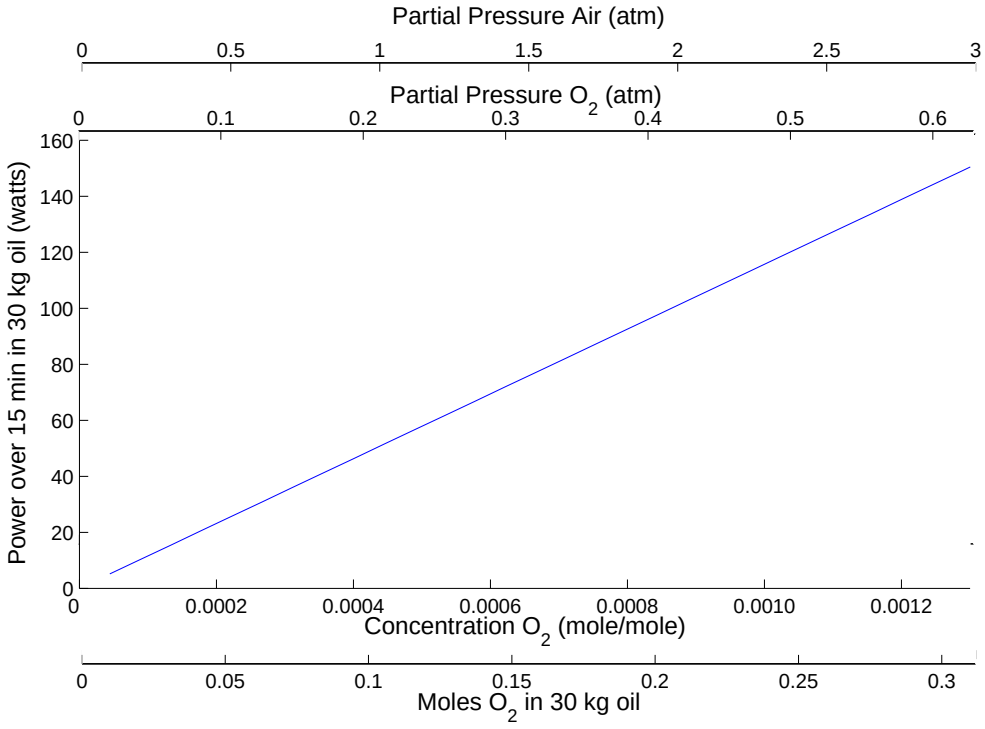


Figure 4-3: Combustion power dependence on oxygen quantity

on the downstream side. To produce 2400 watts of power from combustion, 4.8 moles of oxygen would be needed over the 15 minute time period. At one atmosphere and 25 C, this amount of oxygen is present in 567 L of air. To absorb this much air into the oil, 0.63 L/s of air bubbles would need to be introduced. More air than oil would need to be traveling through the pump.

Because oxygen is a limiting factor on combustion, and not enough oxygen can be absorbed into the machine, it is unlikely that combustion was the cause of the effect seen at iESi unless there was either a way to store oxygen in the system (perhaps chemically), or a fuel better than the volatiles.

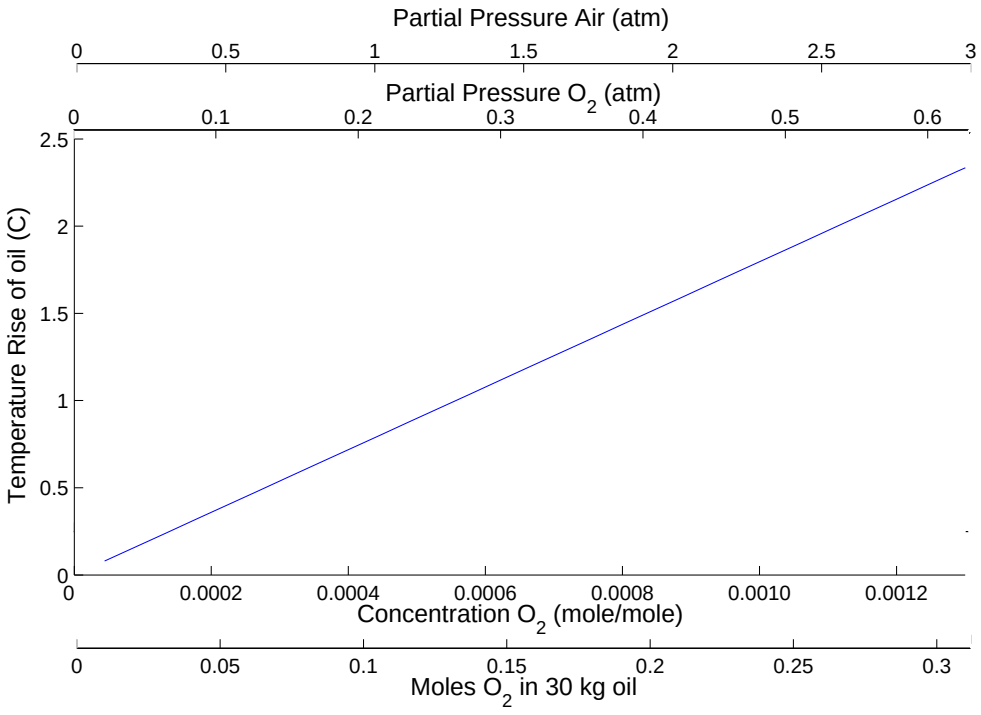


Figure 4-4: Temperature rise of the oil as a function of oxygen quantity

# Chapter 5

# Nuclear Explanations

Theoretical work is not the focus of the research in this thesis. Ideally, experiments can be influenced by theory and vice versa, each one refining the other. Theory is valuable to experiment in that in points out the areas of exploration which may be more interesting.

## 5.1 Theories Proposed In Designer's Papers

The theoretical basis for the operation of the machine that is presented by its operators and designers has varied slightly between the documents that they have created. Below are the theoretical explanations given in two of the documents they have produced.

### 5.1.1 Theory Presented in the Patent Application

The following is my best attempt at presenting the theory described in [1]. After the fluid leaves the channel of the dielectric insert (the tip), it enters a much larger chamber. The resulting pressure drop causes a fine vapor of bubbles to form. Meanwhile, repeated passage of the oil through the metallic insert preceding the tip results in the buildup of static charge which causes the oil and cavitation bubbles to become ionized.

In normal operation, the cavitation bubbles implode as pressure rises downstream of the tip. These implosions cause large pressure pulses (10,000 psi) and thermal energy pulses. The released energy propagates back to the holes in the tip. The increased temperature results in increased ionization due to friction. "... [T]herefore, the hydrogen separated by cavitation emission at the inner surface of the ...[tip] and the ionized operating fluid carries a positive charge" [1]. The electrons generate Vavilov-Cherenkov radiation into the operating fluid.

Because electrons are rapidly emitted, the operating fluid develops an excess of positive charge. The positive ions are larger, and so cannot disperse as quickly. The properties of the dielectric allow for very high voltages to accrue without generating discharge. These high voltages, in the range of several million volts, force the positive ions towards the center axis of the hole of the tip. Here, the coulomb barrier is over come by electrical pulses accelerating the hydrogen or deuterium atoms.

The expected reactions are

$$\mathrm{H+H \rightarrow D+e^{+}+neutrino+0.93\ MeV}$$
$$\mathrm{D+H \rightarrow {}^{3}He+\gamma+5.49\ MeV}$$
$$\mathrm{D+D \rightarrow {}^{3}He+n+3.26\ MeV}$$
$$\mathrm{D+{}^{3}He \rightarrow {}^{4}He+p+18.3\ MeV}$$

The author of this patent application, whose name I do not know, notes that the $\gamma$ rays, neutrons, and Cherenkov radiation can all be verified by experiment.

The information in this patent application influenced our experimental design. Experiments with a variety of tip designs over a range of pressures and temperatures were conducted with the hope of reaching the resonance condition described above.

### 5.1.2 Theory Presented at ICCF12

The materials presented at ICCF12 by Dr. Yang et al rely on the use of cavitation to enhance the probability of reaction [24]. As such, they experimentally try to create the following reaction by doping the working fluid with $^{11}$B, because this reaction lacks dangerous nuclear byproducts:

$$p+^{11}B \rightarrow 3^4He$$

Two models are mentioned in the conference paper: a "coherent non-stationary interference model", in which barrier-free fusion occurs in a self-compressing micro-cavity, and direct models which involve high temperatures from bubble collapse. Barrier free fusion models are not generally accepted. The authors mention that bubble collapse will probably not produce high enough temperatures in this system; however, they claim that the coherent self-compressing model can result in any fusion reaction that would release energy [24].

## 5.2 Phonon Exchange with a Two-State System

The theory in this section is summarized from [14]. The basic model of the theory is built on two sets of 2-state systems which are each coupled to a harmonic oscillator (Fig. 5-1).

### 5.2.1 Physical Model

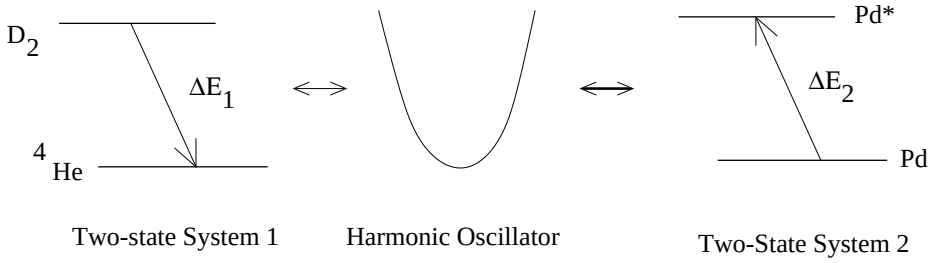


Figure 5-1: A graphical schematic of two two-state systems coupled to a low energy harmonic oscillator

The first two-state system is the 'donor'; members of this two-state system set are predominately in the excited state initially and might transfer energy to the oscillator. A donor example might be the excited state $D_2$ and the ground state $^4$He. Another example could be the excited state HD and the and $^3$He in the ground state. For this two-state system, the energy difference between the two-states is $\Delta E_1$

Transitions in these example two-state systems do not preserve nuclear spin; however, this is not a problem since nuclear potentials can convert between spin and angular momentum.

| Isotope | Atomic Spin of the Ground State |
|---|---|
| $^4$He | +0 |
| $^3$He | +1/2 |
| D | +1 |
| $D_2$ | 0, +1, +2 |
| H | 1/2 |
| HD | +1/2, +3/2 |

Table 5.1: Nuclear spin of the ground state of several nuclear isotopes [10]

The second two-state system is the 'receiver' side. Members of this two-state system set are predominately in the ground state, and might receive energy from the oscillator. An example of a receiver side could be Pd in the ground state, and Pd in a stable nuclear excited state. A similar configuration with Ni could also be a receiver side. These two metals are candidates for two reasons: they have good loading factors of a hydrogen isotope (deuterium in the case of $Pd$ and hydrogen in the case of Ni), and they have large screening factors. For the receiver side, the energy difference between the two energy levels is $\Delta E_2$.

The oscillator is a phonon field, such as those produced by vibrations of a metal lattice. The energy quanta of this oscillator are $\hbar\omega_0$, and much smaller than $\Delta E_1$ or $\Delta E_2$.

The coupling between the donor two-state system and the oscillator is mediated by force constant changes similar to Frank-Condon factors. The $D_2$ molecule is much larger than the $^4$He atom. The size change allows the lattice to couple to the transition.

Coupling between the receiver side and the oscillator is not common in nature. A possible way that this mechanism could occur would be the existence of an intermediate nuclear state which had a center of mass different from the center of charge. For example, the $^4$He$\rightarrow$D$_2$(compact state) receiver could be accomplished if the $^4$He state temporarily became a compact n+$^3$He state. States such as this have been shown to

improve computer models of nuclei experiments, and probably exist. If this compact state existed, then putting it into a harmonic potential would result in a center of mass different than the center of charge, and the particle would develop some angular momentum. Calculations of the $^4$He receiver side in a superposition of nuclear states suggest that the coupling would be non-zero. In this way the receiver side could couple to the oscillator.

### 5.2.2 Hamiltonian

The above model can be expressed as a Hamiltonian (an operator that measures the energy of the system):

$$\hat{H} = \Delta E_1 \frac{\hat{S}_z^{(1)}}{\hbar} + \Delta E_2 \frac{\hat{S}_z^{(2)}}{\hbar} + \hbar\omega_0 \hat{a}^\dagger \hat{a} + V_1 e^{-G\frac{2\hat{S}_x^{(1)}}{\hbar}}(\hat{a} + \hat{a}^\dagger) + V_2 \frac{2\hat{S}_x^{(2)}}{\hbar}(\hat{a} + \hat{a}^\dagger)$$

Here the $\hat{S}_z^{(i)}$ is an operator that measures how many of the two-state systems of type $i$ are excited, and $\hat{S}_x^{(i)}$ is an operator that describes transitions between the excited and ground state of two-state systems of type $i$. The oscillator and couplings are assumed to be linear for simplicity.

Each term contributes to the Hamiltonian as follows:

- $\Delta E_1 \hat{S}_z^{(1)}/\hbar$

  This term measures the number of excited states of the $D_2$ to $^4He$ two-state system, and contributes their energy to the Hamiltonian.

- $\Delta E_2 \hat{S}_z^{(2)}/\hbar$

  This term is much like the previous, except that it measures the energy contributed by the $Pd$ atoms in the excited state.

- $\hbar\omega_0 \hat{a}\hat{a}^\dagger$

  This term measures the energy contributed by the oscillator. $\hbar\omega_0$ is the energy difference between modes of the oscillator, and $\hat{a}\hat{a}^\dagger$ measures the mode that the oscillator is in.

- $V_1 e^{-G} 2\hat{S}_x^{(1)}(\hat{a}+\hat{a}^\dagger)$

  This term describes the coupling between the oscillator and the $D_2$ to $^4He$ two-state system, through the coupling strength $V_1 e^{-G}$. The Gamow factor $e^{-G}$ represents that the transition from $D_2$ to $^4He$ is very difficult because of the coulomb barrier.

- $V_2 2\hat{S}_x^{(2)}(\hat{a}+\hat{a}^\dagger)$

  This term describes the coupling between the oscillator and the $Pd$ two-state system, through the coupling strength $V_2$.

Numerical methods can be applied to this Hamiltonian to show that when the energy exchange is on resonance, energy is exchanged from the donor two-state system to the receiver two-state system via the oscillator. However, this energy is exchange is on a very slow time scale. A specific example is given in [14], with 14 two-state donor systems exchanging energy to 14 receiver systems on time scales of about $10^5 \Delta E t/\hbar$.

A rotation operator can be applied to the Hamiltonian so that the coupling between the donor and receiver two-state systems is explicit. This rotation is equivalent to changing the axis of a problem; the fundamental math equations are unchanged, but new information is apparent. The coupling term that mediates energy exchange between the donor and receiver side is

$$\hbar\omega_0 \frac{\left[\frac{V_2}{\Delta E_2}\right]^2}{\left[1+\frac{4V_2^2(\hat{a}+\hat{a}^\dagger)^2}{\Delta E_2^2}\right]^2}\left(\frac{2\hat{S}_y^{(2)}}{\hbar}\right)^2$$

The term that mediates the excitation exchange between the two sets of two-level systems is

$$\hbar\omega_0 \frac{\left[\frac{V_1 e^{-G}}{\Delta E_1}\right]}{\left[1+\frac{4V_1^2 e^{-2G}(\hat{a}+\hat{a}^\dagger)^2}{\Delta E_1^2}\right]} \frac{\left[\frac{V_2}{\Delta E_2}\right]}{\left[1+\frac{4V_2^2(\hat{a}+\hat{a}^\dagger)^2}{\Delta E_2^2}\right]} \left(\frac{2\hat{S}_y^{(1)}}{\hbar}\right)\left(\frac{2\hat{S}_y^{(2)}}{\hbar}\right)$$

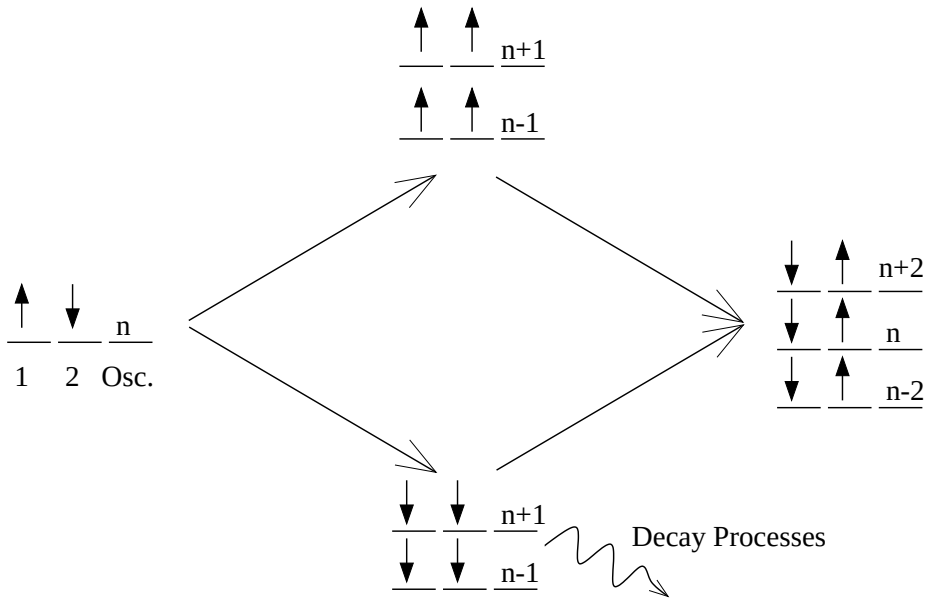


Figure 5-2: Paths by which $D_2$ can transfer energy to Pd

The full rotated Hamiltonian is given in [14]. A direct excitation transfer exists between the two 2-state systems; however, it is fairly weak, second order effect and requires resonance to occur.

### 5.2.3 Inclusion of Loss

This section describes some of the possible mechanisms for loss, the effect of loss on the Hamiltonian, and the effect of that new Hamiltonian on energy exchange between the two-state systems.

There are two pathways by which energy can be transfered from the donor to the receiver two-state system (see Fig. 5-2). Fig. 5-2 uses a form of spin notation: an arrow pointing up denotes that the two-state system is excited; an arrow pointing down denotes that the two-state system is in the ground state. Because the oscillator has more than just two-states, the number of phonons is given rather than the spin notation. The $\uparrow\uparrow$ and $\downarrow\downarrow$ states are virtual states; the first requires more energy than is available, and the second has an excess of energy available. Because of the excess of energy, the $\downarrow\downarrow$ state has the potential to decay.

In particular, we will not discuss the decay of a single state (such as the excited Pd

or $D_2$ state), but in the decay of a coupled state. Decay of a single state is interesting because if it was occurring quickly, then the energy exchange model above would not have been possible. However, single state decay has not yet been incorporated into the theory. Coupled state decay mechanisms might include particle emission or k-shell electron recoil.

One interesting result is that the greater the loss term, the lower the probability that the path with loss is taken. In the general case this problem can be explored by solving

$$\hat{E}\begin{pmatrix} c_1 \\ c_2 \end{pmatrix} = \begin{bmatrix} H_1 & V \\ V & H_2 - i\frac{\hbar}{2}\gamma \end{bmatrix}\begin{pmatrix} c_1 \\ c_2 \end{pmatrix}$$

for $c_1$ and $c_2$, where $-i\hbar\gamma/2$ is a loss term, $c_1$ is a state which does not rapidly decay and $c_2$ is a state which does rapidly decay. The solution is

$$c_1 = \frac{V}{E - H_2 + i\frac{\hbar}{2}\gamma}c_2$$

From this, energy eigenstates can be found. In general, there are two energy eigenstate solutions, one which is high loss and one which is low loss. The high loss system behaves much like intuition would suggest; higher loss terms result in greater amounts of loss. The low loss solution can be thought of as avoiding the high loss region: $c_2 \propto c_1/\gamma$ and $E - H \propto 1/\gamma$. Larger loss terms $\gamma$ result in a smaller probability amplitude $c_2$ that is decayed.

Therefore, a large loss term has the potential to remove one of the two pathways that causes destructive interference. To solve for the effects of loss, a loss term is added to the original Hamiltonian to create a new Hamiltonian $H_L$

$$\hat{H}_L = \hat{H} - \tfrac{i\hbar}{2}\hat{\Gamma}(E)$$

The loss term $\hat{\Gamma}(E)$ is a function of the amount of energy in the oscillator, and is of the form $i\Im\{\hat{V}[E - \hat{H}_0]^{-1}\hat{V}\}$. Now that a Hamiltonian for the model with loss is

calculated, the effect of coupling strength on excitation and energy transfer can be explored.

### Weak Coupling Limit

The coupling between the donor and receiver two-state system derived in 5.2.2 can also be augmented to include loss. Keeping only the terms on resonance, the coupling with loss is

$$\hat{V}_{12} = V_1 V_2 e^{-G} \frac{\hat{S}_+^{(1)}}{\hbar} \frac{\hat{S}_-^{(2)}}{\hbar} \left( \frac{\hat{a}^\dagger \hat{a}}{\Delta E_1 + \hbar\omega_0 + i\hbar\Gamma/2} + \frac{\hat{a}\hat{a}^\dagger}{\Delta E_1 - \hbar\omega_0 + i\hbar\Gamma/2} - \frac{\hat{a}^\dagger \hat{a}}{\Delta E_2 - \hbar\omega_0} - \frac{\hat{a}\hat{a}^\dagger}{\Delta E_2 + \hbar\omega_0} \right)$$

$$+ V_1 V_2 e^{-G} \frac{\hat{S}_-^{(1)}}{\hbar} \frac{\hat{S}_+^{(2)}}{\hbar} \left( \frac{\hat{a}^\dagger \hat{a}}{\Delta E_1 + \hbar\omega_0 + i\hbar\Gamma/2} + \frac{\hat{a}\hat{a}^\dagger}{\Delta E_1 - \hbar\omega_0 + i\hbar\Gamma/2} - \frac{\hat{a}^\dagger \hat{a}}{\Delta E_2 - \hbar\omega_0} - \frac{\hat{a}\hat{a}^\dagger}{\Delta E_2 + \hbar\omega_0} \right)$$

As expected, setting the loss terms to zero gives a result in agreement with the original Hamiltonian without loss. Using perturbation theory, one finds in the limit that the loss becomes very large,

$$\hat{V}_{12} \rightarrow -\frac{2V_1 V_2 e^{-G}}{\Delta E} (\hat{a}^\dagger \hat{a} + \hat{a}\hat{a}^\dagger) \left[ \frac{\hat{S}_+^{(1)}}{\hbar} \frac{\hat{S}_-^{(2)}}{\hbar} + \frac{\hat{S}_-^{(1)}}{\hbar} \frac{\hat{S}_+^{(2)}}{\hbar} \right]$$

The coupling between the two 2-state systems is dramatically increased; unlike before, this term is proportional to twice the number of phonons, $(\hat{a}^\dagger \hat{a} + \hat{a}\hat{a}^\dagger)$, which is quite large.

This term is on the order of

$$V_{12} \sim \frac{2V_1 V_2 e^{-G}}{\Delta E} (2n) \sqrt{S^2 - M^2}$$

where $n$ is the number of phonons, $S$ is the total spin, and $M$ is the spin in the z-direction. Initially, $M$ and $S$ are roughly the same, though slightly different. As time progresses, $M$ tends towards zero and the term in under the square root becomes large.

**Strong Coupling Limit**

Applying similar simplifications to the strong coupling limit as the weak coupling limit, one finds that

$$V_{12} \sim V_1 e^{-G} \sqrt{n}$$

when

$$\frac{V_2 \sqrt{n} \sqrt{S^2 - M^2}}{\Delta E} \gg 1 \text{ and } \Gamma \approx V_{12} \sqrt{S_1^2 - M_1^2}/\hbar.$$

In this case, coupling on the receiver side is quite strong, and the coupling on the donor side is the limiting factor.

All three terms in $V_{12}$ need to be large for energy transfer to occur. The tunneling factor $e^{-G}$ is too small for excitation transfer to occur unless large electron screening factors are present, such as those found in metals in table 3.2.

### 5.2.4 Application to this Experiment

Sources for the appropriate metals and hydrogen isotopes both exist. Hydrogen and naturally occurring deuterium could be stripped off of hydrocarbon chains to form hydrogen gas. There are two possible ways that metal could be introduced into the system: either via the walls of the metal pipes, or through metal particulate in the oil stripped off tips. The hydrogen isotopes would need to be introduced into the metal, and the metal would need a lot of defects for the strong coupling theory to predict excess heat.

It is possible that the pump and structure of the machine could lead to a phonon field in the fluid. If this was the case, then phonon mediated energy exchange between two 2-state systems might be possible, leading to excess heat.

The weak coupling aspect of this theory effected our experimental design with the inclusion of tests that added several gases. The HD gas tests were done with the hopes that $^{13}$C naturally occurring in the oil would act as a receiver and HD $\rightarrow$ $^3$He would be the donor. The $D_2$, $^4$He, and Xe tests were done to see if Xe or Pd would

act as receiver side atoms, and $D_2 \rightarrow {}^4He$ would behave as the donor side. The strong coupling model was developed after experiments were conducted, and did not effect the experimental design.

# Chapter 6

# Experimental Setup

Fusion Research Corporation designed and provided access to the experimental apparatus. They own the machine and its copyright.

## 6.1 Simplified Oil Loop

The basic experiment consists of a pump, which moves oil through the tip in the cell, into a reservoir, through a heat exchanger, and then back to the pump. More information on the specific parts used for the motor, pump, heat exchanger, and reservoir is in Section 6.6.1.

The cell is an acrylic structure which houses the device under test, called the tip. A diagram of the cell can be seen in Figure 6-1. During runs, cavitation often forms in the downstream chamber of the cell. Sometimes the exit diameter is reduced with an orifice plate, which resembles a thick washer.

A diagram of the tip can be seen in 6-2. There are many variations on the basic tip design. These include varying the number of holes, and their diameter, changing the length of the shaft (the thinner portion), and adding chamfers. Additionally, the tip can be preceded by a number of metal and acrylic disks with varying number of holes, hole diameters, and thicknesses. Of these disks, there are two with special designations: swirlers and spacers.

A swirler is a disk with multiple holes in a ring pattern. The holes taper inward

so that the entrance ring pattern has a larger diameter than the exit, forming the outline of a cone. The holes are also rotated about the axis of the cone, which gives the exiting fluid some angular momentum. A swirler is described by its thickness, number of holes, and two angles (one angle for how much the holes come towards the axis, and one angle for how much the holes turn around it). The most common swirler has six holes, and both angles are at 35°.

A spacer is a disk where the inside diameter is almost as large as the outside diameter. These are used between plates with different numbers of holes, or different hole formations. For instance, they are often found after spacers, which have hole configurations and angles very different than the other components.

## 6.2 The Oil

The working fluid in the system was PetroCanada TurboFlo 10 R & O. New and used samples were sent to Herguth Laboratories Inc, and tested for dissolved gases, specific heat, resistivity, and a few other properties. These are given in table 6.1. $\rho$ is the density and $\mu$ is the viscosity. Dissolved gas measurements are in parts per million volume, where the gas volume is at standard pressure and temperature, and the liquid volume is at the pressure and temperature of measurement.

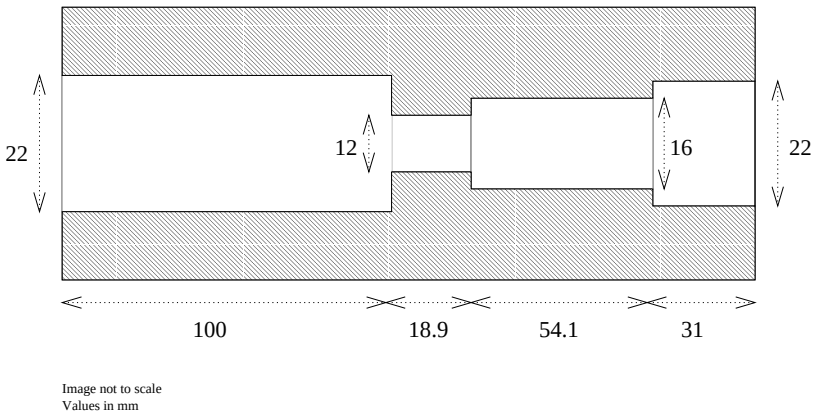


Figure 6-1: A cross section of the cell, based on [1]

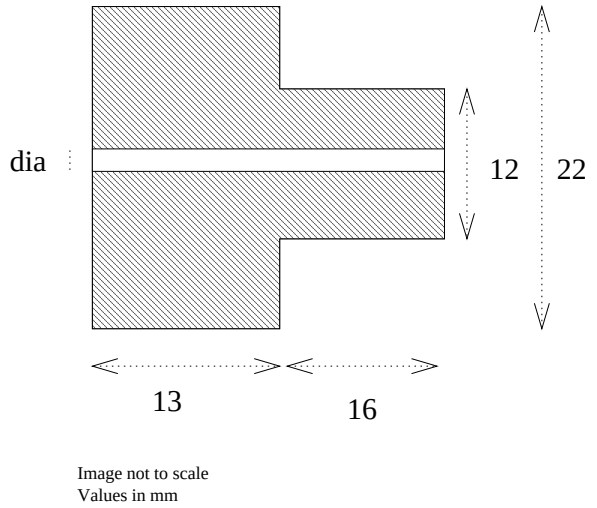


Figure 6-2: A cross section of the tip, based on [1]

## 6.3 Oil Loop Embellishments

In addition to the main test loop and instrumentation on the oil loop (discussed in the instrumentation section), the system had some additional setup to allow the purging of air from the reservoir, injecting of gases, and changing of the cell while minimizing oil spills and air introduction. A diagram of this is given in Fig. 6 .

### 6.3.1 Downstream Pressure Control

To control the downstream pressure, the top of the reservoir was connected to a tank of $N_2$, and to vacuum. In addition to allowing more experimental control, this helped to prevent the pump from cavitating when the downstream pressure was too low.

| Test | New | Used | Test | New | Used |
|---|---|---|---|---|---|
| $\rho$ 15C (kg/L) | .8300 | .8295 | Water (ppm) | 21 | 44 |
| Resistivity ($\Omega/cm$) | 2.56E-13 | 3.08E-13 | $\mu$ at 40C | 10.46 | 10.50 |
| Hydrogen (ppm) | $< 1$ | $< 1$ | Oxygen (ppm) | 23656 | 21523 |
| Nitrogen (ppm) | 45434 | 42702 | Volatiles (ppm) | 1453 | 1 |
| Dielectric Breakdown | | | | | |
| $1^{st}(kV)$ | 43 | 38 | $2^{nd}(kV)$ | 47 | 35 |

Table 6.1: Some properties of new and used PetroCanada TurboFlo 10 [18]

### 6.3.2 Cell Removal

When removing the cell, precautions were taken to avoid excessive oil leaks, or oxygen introduction into the system. The two ball valves on either side of the cell close off the rest the system when the cell needed to be changed, reducing the amount of oil lost, or potential air getting into the system.

To avoid the remaining volume of oil between these two valves from contaminating the rest of the lab space, oil was removed from a valve on the downstream side before cell removal. In addition, a drip pan was made to rest on the frame just below the cell.

To avoid getting air into the rest of the system from the cavity in the cell, the ball valves were kept closed while vacuum was pulled on the cell through a valve on the downstream side. After vacuum was pulled and the gases were removed, the ball valves were opened so that oil could move freely.

### 6.3.3 Gas Injection and Removal

Gas injection was performed in two ways: into the top of the reservoir, or via a 24.5 cc gas chamber at the bottom of the reservoir. Gases could be partially removed by applying vacuum to the system from the top of the reservoir.

### 6.3.4 Safety

To reduce the danger of running this machine, it was placed in a well ventilated trailer. The ventilation in the trailer was located directly above the motor. The electronics and control were outside the trailer so that an operator could run the machine from outside the trailer. This feature was particularly important when hydrogen gas was added. To allow the operator to observe the run, and to record the visual display, a security camera was placed in the trailer.

Additionally, there was an e-stop on the motor, and a pressure relief valve set below the breaking point of the other machine components.

## 6.4 Water Loop

The purpose of the water loop was to assist in maintaining steady state temperature conditions in the oil loop. It consisted of water coming from the wall, then through a pressure regulator, an electronic flow control valve, two flow meters, the heat exchanger, two manual valves, and then down the drain. The thermocouples on either side of the heat exchanger and the water flow meter are discussed in the instrumentation section, along with the water flow meters. The water loop intersects with the oil loop at the heat exchanger. A diagram of the water loop can be found in Fig. 6-4

### 6.4.1 Flow Control Valve

To automate getting into steady state, a FloCon flow control valve was hooked up to a simple AI and thermocouple sensor $T_2$. However, due to RF noise and the occasional noise spike, the AI would over compensate. Later, the FloCon was connected to a potentiometer instead, and the operator used this to manually control the water flow.

### 6.4.2 Manual Valves

When the FloCon was out of service, the operator used two valves, a needle valve and a gate valve, to control the water flow. The needle valve was used for fine tuning, and the gate valve for large changes.

### 6.4.3 Pressure Regulator

Because the city water pressure varies over the course of the day depending on nearby usage, a valve isn't enough to keep a consistent water flow rate. To alleviate this problem, we had a pressure regulator set at 27 lbs on the intake of the water line.

## 6.5 Instrumentation

### 6.5.1 Temperature

We used 9 $\frac{1}{8}$ inch omega J type thermocouples to take temperature measurements. These were located

- in the oil
  - two before the cell
  - two after the cell
  - one at the bottom of the reservoir, just before the heat exchanger
  - one after the heat exchanger
- in the water
  - one before the heat exchanger
  - one after the heat exchanger
- and one measuring ambient room temperature

To calibrate the thermocouples, we used an omega 17 L bath.

Despite the Omega's assurance that the bath temperature reading was accurate to .1 C, we found that because the bath's measuring device was so close to the heating coil, the bath gave a reading higher than the actual temperature near the thermocouples. In response, we used 2 thermistors to measure the value of the temperature right next to the thermocouples. These two thermistors were in agreement to .014 C, and calibrated by Insturlab Inc.

### 6.5.2 Pressure

The upstream pressure measurement was conducted with a model IS-20-S pressure transducer from WIKA Alexander Wiegand Gmbh & Co. It was calibrated at the factory to .25 % of the span or better.

The downstream pressure was measured with a Winters LF series quality pressure gauge (model number Q820). This pressure gauge can measure -1.5 bar to 1.8 bar relative to 1 atm, and was selected because the downstream pressure is likely to be close to atmosphere (either slightly above or below, depending on vacuum or gas over pressure).

### 6.5.3 Other Instruments

There were three other instruments, a Micromotion flow meter, a Yokogawa flow meter, and a Siemens VFD. The micromotion flow meter measured oil flow, and was located at the bottom of the machine after the pump. There were a few feet of straight tubing before and after the flow meter, to ensure smooth flow. The Yokogawa flow meter measured the flow of coolant water through the heat exchanger. It was located upstream of the heat exchanger. The Siemens VFD measured electrical power and current into the system. The electrical power input was calibrated to the input power to the motor (as opposed to the input power to the pump) using a fluke meter.

### 6.5.4 Data Acquisition

Data acquisition was done by a Keithley 2700 DAQ. Thermocouples were connected directly to the DAQ with Omega shielded thermocouple wire. Other instruments gave current outputs. Because the DAQ has most voltage channels, these current loops were connected in parallel with a $248.5 \pm .1\Omega$ resistor to the DAQ. The resistor connections were made in a shielded, grounded metal box just before the DAQ.

Three signals, the $P_1$ pressure transducer, the motor power and the motor current, were electronically displayed for safety reasons. To display them, the DAQ was put in series with an Omega DPI 32 process transmitter for each of these three signals.

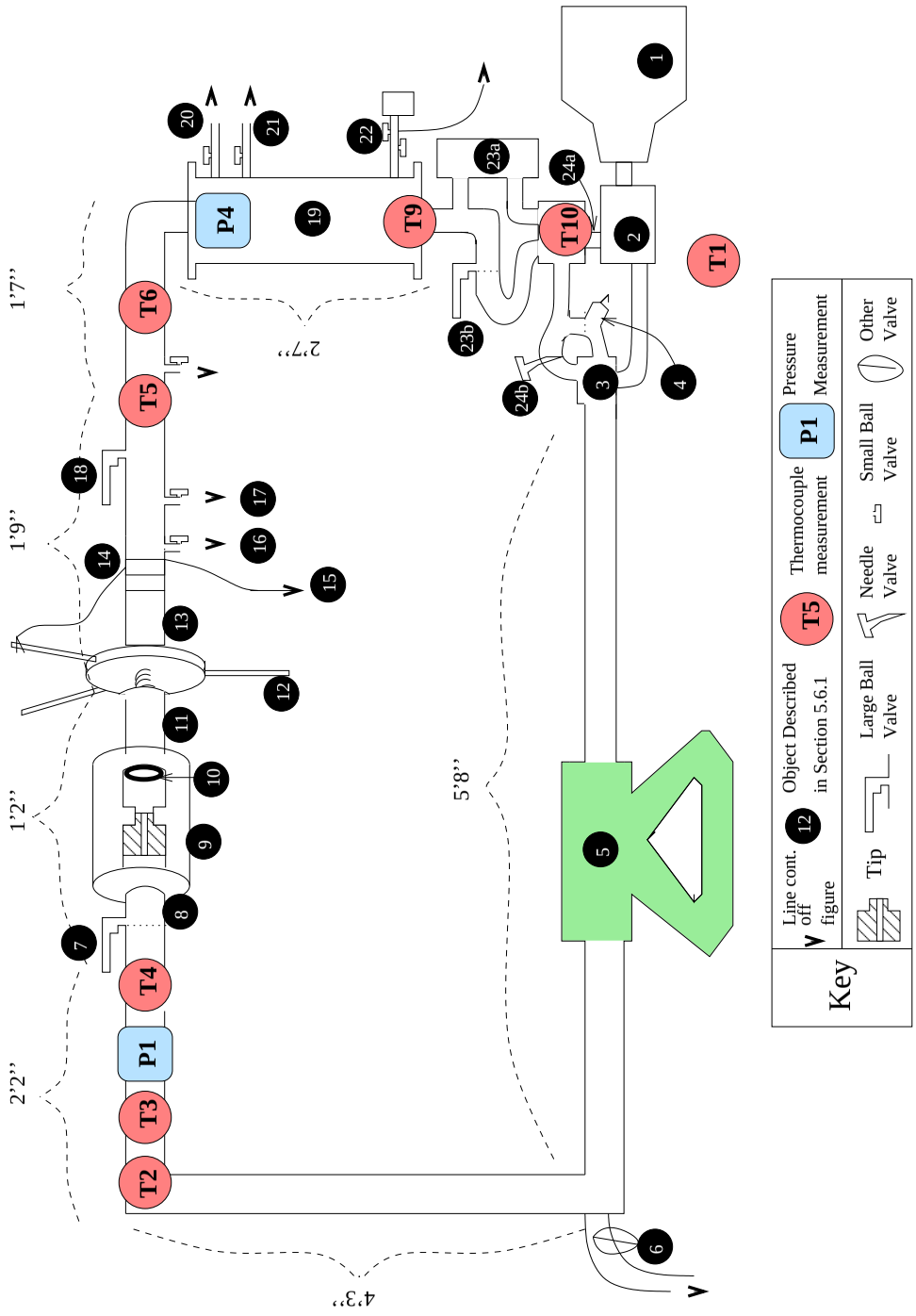


Figure 6-3: Schematic of experimental setup

## 6.6 Complete Loop Lists

### 6.6.1 Complete Oil Loop

Fig. 6-3 shows the complete oil loop, not to scale. The numbered shapes are described in the following itemized list. Starting from the motor, the complete oil loop contains,

1. Motor, Siemens 10 horse power with variable speed display
2. Vane Pump, Vickers Eaton Hydraulics, model V20-1P8P-1C11, 40 L/min
3. A junction. For earlier runs, this was connected to an accumulator set at 600 lb.

T1. $T_1$, a thermocouple measuring ambient air temperature

4. Pressure relief valve, at 1500 psi
5. Flow meter, Micromotion
6. A valve for emptying the oil

T2. $T_2$, a thermocouple for the FlowControl valve

T3. $T_3$, a thermocouple for an upstream temperature measurement

P1. $P_1$, a pressure transducer for an upstream pressure measurement

T4. $T_4$, a thermocouple for an upstream temperature measurement

7. Valve, Swagelok high pressure full port ball valve, 6-20 internal diameter (ID).
8. Cell end connector, with 2 O rings to seal the connection.
9. The cell, containing the tip
10. The orifice plate, a flat metal ring that reduces the exit diameter.
11. Cell end connector, with 2 O rings to seal the connection.

12. Mechanism for removing the cell

13. about 2 inches of plastic pipe

14. Cross shaped insert inside pipe to break up the possibly jet streamed oil flow.

15. Grounding wire, from mechanism to remove the cell to frame, to ground.

16. Small ball valve to vacuum

17. Small ball valve to remove oil from cell cleanly

18. Valve, Swagelok high pressure full port ball valve, 6-20 internal diameter (ID).

T5. $T_5$, a thermocouple for a downstream temperature measurement

T6. $T_6$, a thermocouple for a downstream temperature measurement

19. Reservoir, Acrylic .25 inch wall thickness, 3.5 inch ID, 4 inch OD, 2' 7" tall

P4. $P_4$, a Winters pressure gauge for downstream pressure measurement

20. Small ball valve to vacuum

21. Small ball valves to gas tanks

T9. $T_9$, a thermocouple for a reservoir temperature measurement, and before the heat exchanger measurement

22. Small ball valve to a 24.5 cc holding chamber for gases, connected to a small ball valve to the gas tanks

At this point the flow splits into two options:

23a. The Heat Exchanger, parallel plate, with oil exiting at T10

23b. a bypass valve, through hydraulic rubber line to T10

T10. An oil chamber, containing $T_{10}$, a thermocouple for a heat exchanger exit measurement

At this point the flow splits again:

24a. Return to the pump

24b. Return to the junction via a Swagelok needle valve.

In this list, when a valve connects to vacuum, there is a urethane 3/8 inch ID tube which connects from that valve to a junction, which then connects to a standard refrigeration vacuum pump. The vacuum pump was a oil filled vane pump that could pull 29.5 inches of Hg.

The connecting pipe in general was stainless steel 3/4 inch DOM Swagelok tubing. The exception is from the heat exchanger bypass valve to the chamber, which had hydraulic rubber line. Connections were via Swagelok compression fittings (ferrules). Thermocouple connections were with Swagelok compression fittings and Teflon tape. The gas chamber was sealed with Teflon tape and pipe dope.

The metal piping and heat exchanger were both insulated, the metal piping with 1/4 inch foam pipe insulation and the heat exchanger with Styrofoam.

### 6.6.2 Complete Water Loop

The water loop intersects with the oil loop at the heat exchanger. Its set up is described in Fig. 6-4.

1. Supply from the city

2. ball valve to shut off supply at night

3. pressure regulator set at 27 lb

4. Yokogawa magnetic flow meter

T8 $T_8$, a thermocouple for a water measurement before the heat exchanger

5. Parallel Plate Heat Exchanger

T7 $T_7$, a thermocouple for a water measurement after the heat exchanger

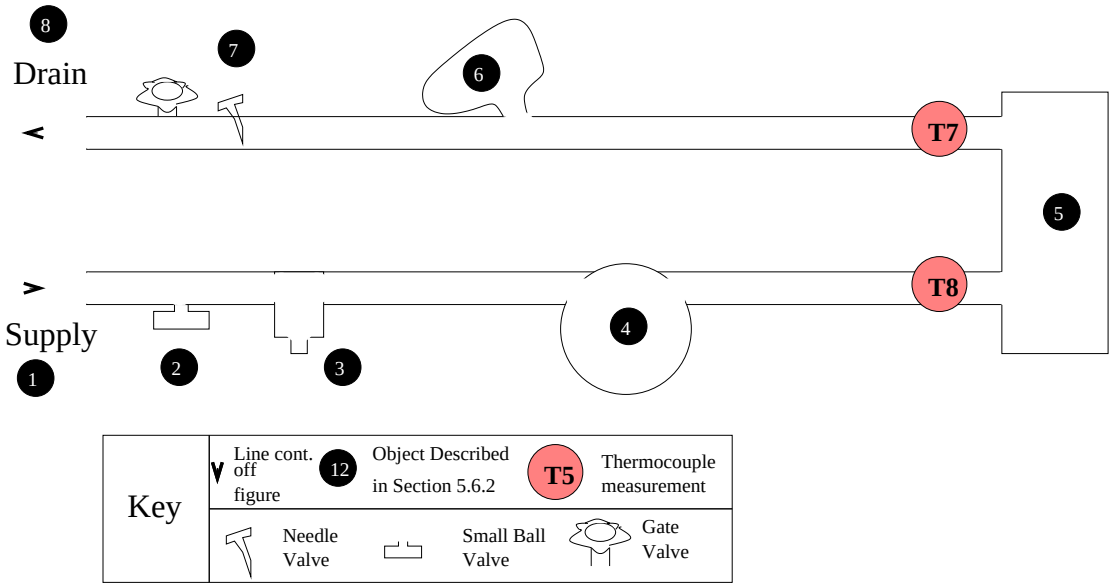


Figure 6-4: Schematic of water loop

6. A mini FloCon flow control valve

7. A needle valve and a gate valve for getting into steady state manually

8. Drain

# Chapter 7

# Procedures

## 7.1 Changing a Tip

1. Turn off the machine.

2. Close valves before and after the cell.

3. Remove cell (placing a drip pan below the cell is recommended).

4. Remove the old tip (a rubber tipped tool may be required).

5. Put the new tip into the cell, then put the cell back on the machine.

6. Open valve between the cell and the vacuum pump. Pull vacuum on the cell to remove air.

7. Close valve to the vacuum pump and open the valves on the oil pipe before and after the cell.

8. Wipe excess oil off the machine and empty the drip pan,

9. Clean oil off exposed skin.

## 7.2 Changing the Oil

1. Close to the bottom of the machine, connect a hose to a valve. Place the other end of the hose is a bucket.

2. Make sure the system is not over pressured. If it is, relieve the pressure by letting out the gas from the top.

2. Drain the old oil.

3. Add a liter of new oil.

4. Close the system and gently cycle the oil.

5. Drain this oil. If it is full of particulate, repeat steps 3 and 4.

6. Close the system and run the vacuum pump while gently cycling the oil to remove air. Continue until the oil is no longer frothy.

## 7.3 Injecting Gas

1. Make sure that the cell is in, has the correct tip for the run, and that data acquisition is on.

2a. If adding $N_2$ or $He$, open the valve between the reservoir and the gas tank.

2b. If adding $D_2$ or $HD$, fill the 24.5 cc chamber first. Then open the valve between that chamber and the reservoir.

3. Cycle the oil so that the gas mixes.

## 7.4 Heuristics for Light Emission

Light emission heuristics will depend very closely on the particular oil, machine design, and tip being used. For this reason, some trial and error will be necessary, and often a safe tip (one that does not cause electrical arcing through the acrylic tip or cell, as in

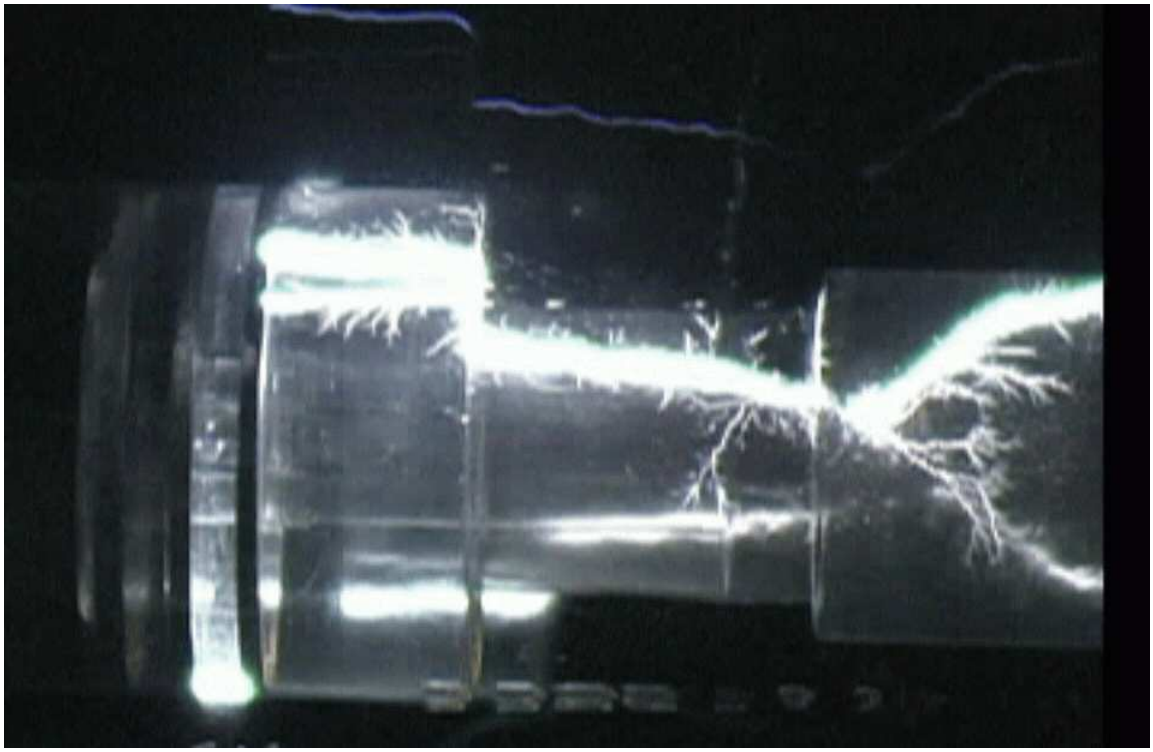

Figure 7-1: Photography of discharge through the tip, provided by S. B. Krivit, ©New Energy Times, use permitted for non-commercial educational purposes

Fig. 7-1) which still produced a great deal of electrical activity and light generation would be chosen based a series of runs over many slight tip modifications. This particular tip would then be used in a separate run with steady state points, and perhaps the addition of gases.

As a general rule, a higher viscosity oil seems to generate more electrical sparking, because there is more friction between the working fluid and the acrylic. Cavitation appears to reduce the resistivity in the channel, and encourages electrical discharge to go through the oil rather than through the acrylic. Once an arc has traveled through the acrylic, a track is made in the acrylic, and future arcs will preferentially for travel along that track.

When the machine first turns on, the oil is cold (around 25 C) and the pressure is low. Because the oil is cold, the viscosity is higher than normal run conditions (around 30 to 50 C). Because the pressure is low, there is less cavitation in the channels than during normal run conditions. As a result, some tips (in our situation, those with

metal plates), produce a great deal of arcing early on, and this arcing tends to prefer the acrylic over the oil for its path. While often sudden changes result in even more arcing, in this situation we found quickly ramping up the pressure to create cavitation as soon as possible to be the best choice of action to prevent damage to the tips and the cell.

As an alternative to quickly ramping up the pressure, the oil can be heated very slowly by running the machine at flow rates low enough that there is not enough friction to produce arcing. The oil can also be heated with a different tip, and then the machine turned off and the tips changed. This practice works in most cases, unless the temperature that you need to reach makes it difficult to take off the cell, either because the acrylic has swollen from the temperature rise, or because it is too hot to comfortably handle.

## 7.5 An Example Run

1. write down the purpose of the run, the tip design, oil condition, and any modifications to the machine.

2. start data acquisition to warm up the DAQ.

3. Verify that the valves around the cell are open, and the by pass valves are positioned correctly.

4. Turn on the ventilation fans, water, make sure that the flow meters are on.

5. Start the motor. Visually verify that oil is flowing. If not, stop. Something is wrong.

6. Get light emission (see section 7.4). Be sure to record a written description of the light and electrical discharge.

7. Get a steady state data point by controlling water flow to maintain temperature. If possible, maintain temperature for 1,000 sec, at a slope smaller than .1 C over 3 min.

8. Loop over steps 6 and 7, varying the temperature and pressure of the data point, as appropriate. Do not exceed 75 C (the acrylic begins to soften at higher temperatures). Do not exceed 105 Bar (the pressure rating of the machine cannot handle much more).

9. Ramp the machine down slowly over about 3 minutes. Turn off oil flow. Turn off data acquisition. Copy into data file the visuals from the run, and anything odd which occurred.

# Chapter 8

# Data

The data was taken on one of four machine versions. The data from version zero was not used in the final analysis for several reasons; however, the runs on that machine helped us to diagnose some problems that can lead to misleading results:

- System not in steady state

  There are two reasons to maintain steady state conditions. First, if energy into the system is not going into changing the system (for example, heating it up, or being stored in some other way), then the energy going in should come back out (for example, through heat loss to the surrounding air and the water in the heat exchanger). So, if the system is in steady state, one can compare the inputs to the outputs to see if more energy is coming out than going in.

  The second purpose of steady state is to allow the system to come to equilibrium. For example, if a rapid change in downstream pressure occurs, the difference temperatures of the oil across the cell will slowly change to reach equilibrium. The change is not instantaneous because the frame of the machine will still be the old temperature, and heat or cool the oil until it comes into thermal equilibrium too. Many physical equations are only valid in equilibrium, and can't be applied unless the system is in steady state.

- Thermocouple not touching enough circulating oil

The thermocouples that we used measure not only the temperature at the tip of the thermocouple, but also incorporate the temperatures close to the tip. If the thermocouple does not have sufficient contact with the oil, the measurement it gives will incorporate some of the temperature from the frame or ambient air. Based on experimentation with a calibration bath, 1 inch depth is more than adequate. In the later machine versions, the thermocouples were placed as deep into the stream as possible, given the 3/4 inch pipe diameter and a 3mm clearance from the other end of the pipe.

Additionally, contact must be with the moving oil in the stream. If the contact is only with a pocket of stagnant fluid off the stream, the temperature reading will be a poor estimate of the temperature in the stream due to insufficient mixing.

- Thermocouple is being hit by a rapid stream of fluid

  During run conditions, sometimes the fluid exiting the tip will form a jet which travels down the pipe surrounded by vapor, rather than filling the volume with liquid. When this occurred, the first thermocouple in the series of thermocouples on the exit side ($T_5$) would often disagree with the ones immediately after it $T_6$ and $T_{10}$. When $T_5$ disagreed it would almost always read a hotter temperature, sometimes as much as 1 C hotter.

  Based on experiments in the calibration bath, shaking a thermocouple will not effect its reading; however, tapping it with a metal object so that it creates a ringing sound does effect the reading. Stick on thermocouples along the length of the pipe exiting the cell also agreed with $T_6$. From this we concluded that $T_5$ was giving a noise offset due to fluid flow conditions and cavitation, and that its reading was not a real temperature effect.

  To handle this problem, we inserted a "clover leaf" structure into the stream after the exit chamber of the cell and before the thermocouples. It is a chamfered piece of metal shaped like $\bigoplus$, which breaks up the stream. After putting this into the stream, $T_5$ and $T_6$ agreed within .05 C.

- Thermocouples badly calibrated

  When the thermocouples were first calibrated, the reference temperature built into the bath was too far from the thermocouples themselves. The temperature near the thermocouples was affected by heat losses to the air, and so the calibration curve got farther from the actual temperature as the temperature rose. As a result, when taking difference between thermocouples, the error was much larger, especially for large differences in temperature. To avoid this, an independent reference temperature was placed right next to the thermocouples in later calibrations.

- DAQ reference temperature unstable

  The DAQ reference temperature changes as the DAQ warms up. The particular DAQ used in this experiment only warmed up while collecting data, and the temperature the reference stabilized to depended on the data acquisition rate. With a DAQ of this sort, temperature calibrations had to be done at each data acquisition rate used. Additionally, the temperature gradient inside the DAQ was not uniform. To account for this, this DAQ had multiple reference temperatures which could each handle four thermocouples. The different reference temperatures warmed up at different rates, so thermocouples which would likely be compared to each other (such at the thermocouples across the cell, or the ones around the heat exchanger) were placed on the same reference temperatures.

- RF Noise

  Under desirable working conditions, the motion of the oil against the acrylic produces Van de Graaff effects, including plasma, sparks, and electrical arcing. This electrical activity is associated with large amounts of RF noise, which can cause misreadings, increased noise, and equipment damage. Metallic shielding is recommended, particularly when adding a new measurement device. New measurement devices should also be tested with the machine both off and on,

to make sure that they are properly grounded and not affected by the three phase power to the pump.

- Other calibration errors

  Of course, a calibration error for any instrument used in final calculations will potentially result in misleading data.

From the raw data of the later versions of the machine, steady state points were chosen based on three criteria: how long the temperature had been within .2 C; the stability of the ratio between the temperature and the pressure; and the slope of the temperature.

We collected about 1.9 hundred thousand seconds worth of data, at a data rate of .1 $pt/sec$, over roughly 110 runs. Of these 19 thousand data points, 10 data points had to be thrown out because of a DAQ error, which resulted in all measurements reading max value. Each data point included at least nine temperature measurements, an electrical power measurement, an electrical current measurement, upstream and downstream pressure, oil flow, and water flow. Some contained an additional power measurement that was added later as a double check, and others contained an additional water flow measurement.

To see the raw data from two sample runs, see figures 8-1 and 8-2. In figure 8-1 the temperatures around the cell and upstream pressure are displayed for a run focused on experimenting with the light output of a tip. In figure 8-2 the same measurements are displayed. The focus of this run was taking several steady state points to compare the heat losses of one version of the machine to another version. In both runs, the two upstream temperature measurements ($T_3$ and $T_4$) are displayed on top of one another due to the scale of the y-axis. The same is true for the two downstream temperature measurements, $T_5$ and $T_6$.

From this body of raw data, 124910 seconds of raw data were used to create 158 steady state points. Every steady state point included averages of all of the measurements, their errors, the length of the steady state period, and some slopes of different measurements over time. Each of these points was placed into one experiment subset:

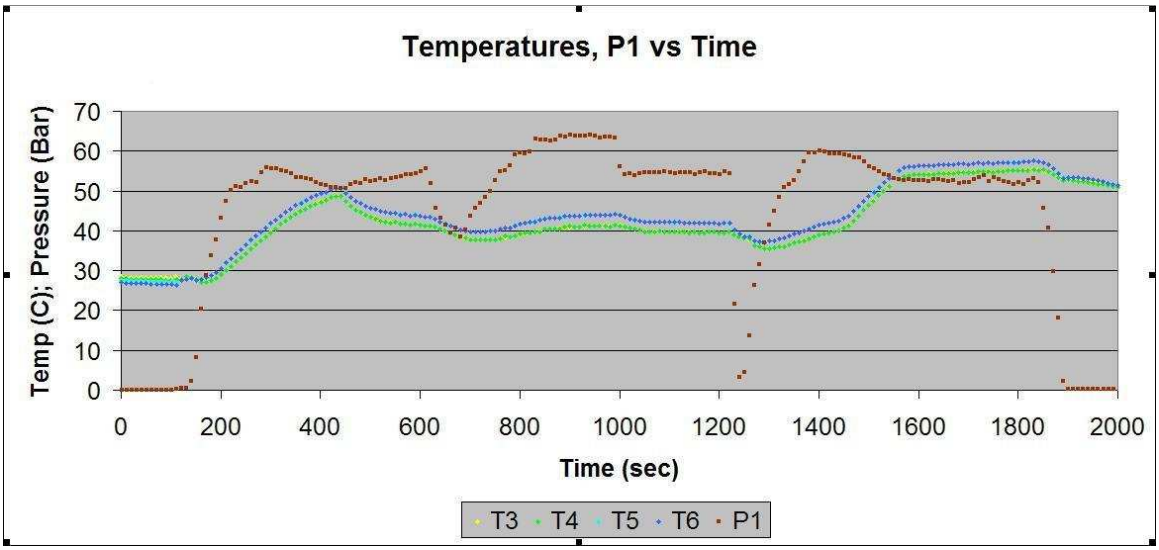


Figure 8-1: An example run without steady state data

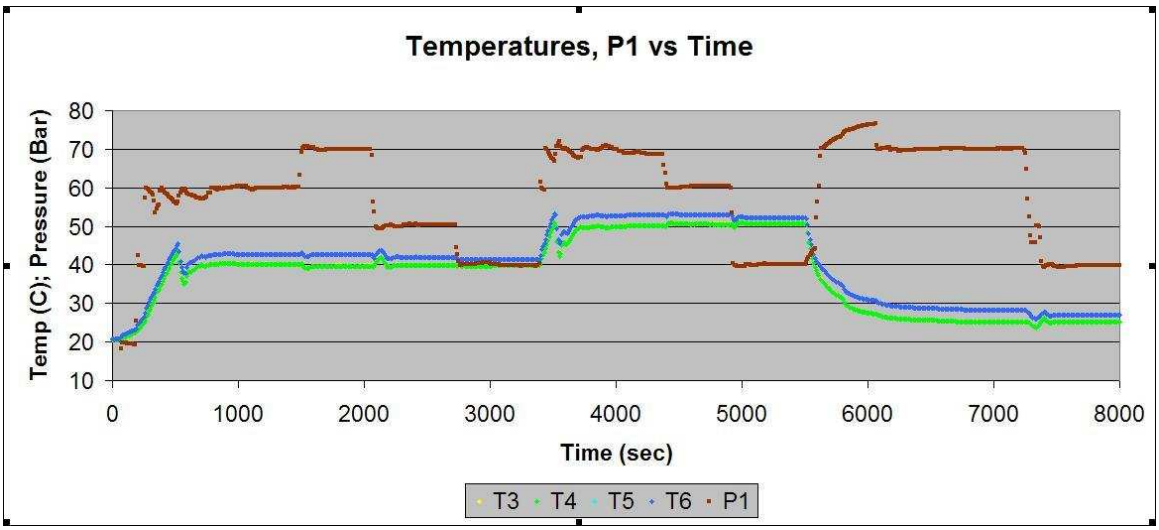


Figure 8-2: An example run with 9 steady state data points

heat loss fits; heater measurements; assorted tip designs; comparing tip material; $HD$ gas; $D_2$, $Xe$ and $He$ gas; $Xe$ and $He$ gas; $He$ gas; or trace gases. Plots comparing the energy input to output for these sets can be seen in the Analysis chapter (Chapter 10).

# Chapter 9

# Errors

When possible, an estimate of the systematic error was incorporated with the statistical error found repeatedly measuring a point $N$ times for a total error estimation,

$$\epsilon \approx \sqrt{\sigma^2_{statistic}/N + \sigma^2_{systematic}}$$

This section discusses the estimates for systematic errors.

Table 9.1 shows the error values for devices calibrated by outside companies. Three values used later are not in this table because the errors are not known for them: the specific heat of the oil $C_{oil}(T)$, the density of the oil $\rho$, and the specific heat of the city water $C_{water}$. These values were all treated as exact.

Because the DAQ had the capacity for many more voltage measurements than current measurements, all measurements which gave current loop outputs were changed from current to voltage signals through a $248.5 \pm .1\Omega$ resistor in parallel with the DAQ.

| Measurement | Error | Reference |
|---|---|---|
| $P_1$ | $\pm.5$ bar for $p > .25$ bar | [40] |
| $P_4$ | $\pm$ .015 bar | [41] |
| Water Flow | $\pm.25$ % at full flow | [43] |
| Oil Flow | $\pm.023$ % at 10% flow (22.7 kg/min) | [30] |
| Reference Thermistors | $\pm.014$ C | [22] |
| Fluke Process Calibrator | $\pm.05\Omega$ for $100\Omega < R < 11k\Omega$ | [11] |
| Fluke Process Calibrator | .5% V for sinusoidal signals | [11] |

Table 9.1: Estimates of statistical errors, based on outside calibrations

This source of error is in addition to the published sources of error for these devices, found in table 9.1, and effects all devices except for the fluke meter, thermistors, and thermocouples.

Two of the devices in the table were not used directly for measurements, but for the calibration of other devices. The fluke was used to calibrate the electrical input power measurement, and to measure the amount of power going into the heater when verifying that the system could measure heat. Two thermistors were used to calibrate the thermocouples. Table 9.2 shows the results of these calibrations.

| Meas. | Fit | Fit Error | Total Error |
|---|---|---|---|
| $T_1$ | $= t_1 - 3.38 \times 10^5 t_1^2 + 3.662 \times 10^3 t_1 + .383$ | $\pm .013$ | $\pm .019$ C |
| $T_3$ | $= t_3 - 5.80 \times 10^5 t_3^2 + 6.85 \times 10^3 t_3 + .144$ | $\pm$ .012 | $\pm .018$ C |
| $T_4$ | $= t_4 - 5.08 \times 10^5 t_4^2 + 4.92 \times 10^3 t_4 + .150$ | $\pm$ .012 | $\pm .018$ C |
| $T_5$ | $= t_5 - 5.66 \times 10^5 t_5^2 + 4.17 \times 10^3 t_5 + .145$ | $\pm$ .011 | $\pm .018$ C |
| $T_6$ | $= t_6 - 6.21 \times 10^5 t_6^2 + 4.47 \times 10^3 t_6 + .090$ | $\pm$ .012 | $\pm .018$ C |
| $T_7$ | $= t_7 - 6.44 \times 10^5 t_7^2 + 4.44 \times 10^3 t_7 + .0359$ | $\pm$ .011 | $\pm .018$ C |
| $T_8$ | $= t_8 - 6.81 \times 10^5 t_8^2 + 10.7 \times 10^3 t_8 - .115$ | $\pm$ .014 | $\pm .020$ C |
| $T_9$ | $= t_9 - 7.93 \times 10^5 t_9^2 + 5.97 \times 10^3 t_9 - .0718$ | $\pm$ .011 | $\pm .018$ C |
| $T_{10}$ | $= t_{10} - 6.73 \times 10^5 t_{10}^2 + 8.37 \times 10^3 t_{10} - .133$ | $\pm .011$ | $\pm .018$ C |
| $P_{electric}$ | $= 1.1543 p_{electric} + .0333$ | $\pm .019$ kW | $\pm .019$ kW |

Table 9.2: Estimates of statistical errors, based on calibration data

In table 9.2 the lowercase variable ($t_i$ or $p_{electric}$) represents the raw voltage signal of the measurement, and the uppercase variable ($T_i$ or $P_{electric}$) is the temperature based on the calibration. The fit error is the standard deviation of the residuals of the fit, and is only valid over the temperature range of the calibration, from 25 C to 65 C. The fit error and the error of the device calibrated to are used to obtain an estimate of the systematic errors through the equation $\sqrt{\sigma_{fit}^2 + \sigma_{reference}^2}$.

The error estimate is an underestimate – there was only time to take a calibration before runs began, so its uncertain how much drift occurred. It is also possible that the DAQ internal temperature references were not always consistent, due to changes in ambient temperature. The fit was done based on data after the DAQ had time to

warm up at the sampling rate used during normal data collection in an attempt to minimize this source of error.

The DAQ has several internal temperature references, each with their own characteristic response to the DAQ warming up. Each temperature reference could support four thermocouple measurements. Thermocouples $T_3$, $T_4$, $T_5$, and $T_6$ were all measured with the same reference temperature. $T_7$, $T_8$, $T_9$, and $T_{10}$ were also all on the same reference temperature. This set up was chosen because the analysis considers temperature differences across the cell and across the heat exchanger, but doesn't compare the two sets of temperatures. If one reference temperature changed unexpectedly during a run, the difference would be uneffected. Ideally, $T_1$ would have been able to share a temperature reference with one of these so that the machine temperature could be compared to the ambient temperature to calculate heat losses; however, the other temperature differences were deemed more important.

The errors in this chapter are used with the standard error on the mean found in experiment to create the error bars in Chapter 10. Systematic errors due to the difference in temperatures on the same reference temperature were considered negligible. This assumption reduced the error bars on the cell gain plot by around 30%. Error bars are not plotted along the x-axis of the following graphs because errors in temperature, pressure, and electric power were negligible compared to the scale of the axis.

# Chapter 10

# Analysis

This chapter covers the analysis of our data. Section 10.1 describes the derived measurements that are used to determine the energy balance of the system. Section 10.2 shows how the system responds to a heater inserted into the stream where the cell is. Section 10.3 describes a method for accounting for heat loss, and applies it to the three system versions that have been used during this experiment. The results of the fit are used to correct later data sets, and the correction is displayed alongside uncorrected derived measurements.

The rest of the sections are the graphical results of the experiments. Section 10.4 shows the results of the different tip designs which had steady state data. Section 10.5 compares three tips made of different materials, but with the same shape. Sections 10.6 and 10.7 cover the runs where gases were added to the reservoir. Finally, section 10.8 shows the data from the runs that were done after attempting to remove the gases added in section 10.7 with a vacuum pump. These runs are separate from the assorted tip runs because they contain trace elements of gases; however, they contain significantly smaller amounts of gas than the runs in section 10.7.

## 10.1 Analysis Method

From the measured quantities, three derived quantities are computed to shed light on the energy balance of the system: $C(T)\rho\Delta T/\Delta p$, Water Power $-$ Electric Power,

and Water Power / Electric Power.

$C(T)\rho\Delta T/\Delta p$ is the ratio of two powers across the cell, heat power ($C(T)\rho\Delta T\frac{dV}{dt}$) and mechanical power ($\Delta p\frac{dV}{dt}$). If an excess of heat was seen between the measurement devices on either side of the cell, in principle there should be an increase in this quantity. If an excess of heat was to occur before or after those measurement devices, this derived quantity should not change.

Based on tests conducted at Herguth Laboratories, we took the density of the oil $\rho = .81$ and the specific heat $C(T) = 1.798 + .0054T_6$, where $T_6$ is a temperature measurement downstream of the cell. Though density is a weak function of temperature, we treated density as a constant in this analysis.

Because there are two thermocouples on each side of the cell, the gain across the cell plotted below is an average of four different gains. Each gain calculates $\Delta T$ using two different thermocouples.

When in steady state, the power taken out of the system by the water from the heat exchanger is roughly equal to the power put in by the motor. Aside from losses from ambient heat loss, and trace amounts lost in light output and electrical arcing, water power can be considered the energy output of this system. The water power is

$$P_{water} = C_w\rho_w\Delta T_w dV_w/dt$$

where $C_w$ is the specific heat of water, $\rho_w$ is the density of water, and $\Delta T_w$ is $T_8 - T_7$, the temperature rise of the water over the heat exchanger. The electrical power is measured going into the motor. After the motor efficiency and any heat gain from running the system colder than ambient temperature, this is the energy input to the system. To compare output to input, we consider the difference of the two and their ratio.

Because the water measurement detects excess heat being produced anywhere in the system, if the cell gain measurement rises due to an excess heat over the cell, the water measurement should also respond.

For the analysis, these three derived quantities are plotted and compared to an expected result. $P_{water}/P_{electric}$ and $P_{water} - P_{electric}$ are plotted versus $P_{electric}$, and

$C(T)\rho\Delta T/\Delta p$ is plotted versus pressure, or both pressure and temperature.

## 10.2 Heater Measurements

To test if the instrumentation could measure a heat gain above unity, a heater was placed into the oil stream through a hole in the downstream portion of a modified cell.The cell contained a steel tip with a 2mm hole diameter. Heater power was measured with a fluke meter while keeping the heater slightly below room temperature with circulating oil.

At each pressure that the experiment was run, a steady state point of about 1000 seconds was taken with the heater off (but still in the stream), and with the heater on at either 24W or 69W. The experiment was kept slightly below room temperature ($T_{oil} = 17 \pm 1.5C$, $T_{room} = 18.9 \pm .5C$) during these runs to minimize radiative heat loss effects.

Based on this analysis, the gain across the cell compared to a known energy balance appears to be a more sensitive measurement than either water measurement. Additionally, discerning excess heat is harder at higher pressures. For the pressures in most runs, excess heat over 69W should be visible.

## 10.3 Fits for Heat Loss in the System

Two linear regression fits were used to model the heat loss in the system, one for losses over the cell and the other for losses over the entire machine. The fits were done for three versions of the machine: the initial version, a version after the cell had been slightly insulated by reducing its contact with metal, and a version where an additional reservoir was added to the system with the insulated cell.

To find out how the heat loss over the cell affected the $C(T)\rho\Delta T/\Delta p$ measurement,

$$Gain_{cell} = P_{heat}/P_{mechanical} = \frac{C(T)\rho\Delta T dV/dt + P_{heatloss}}{\Delta p dV/dt}$$

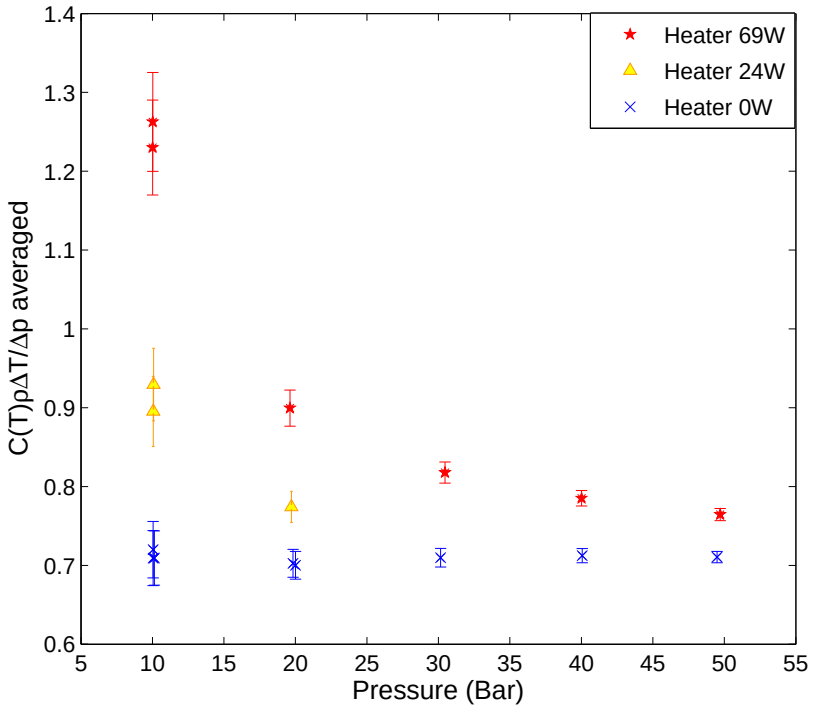


Figure 10-1: Gain across the cell with a heater

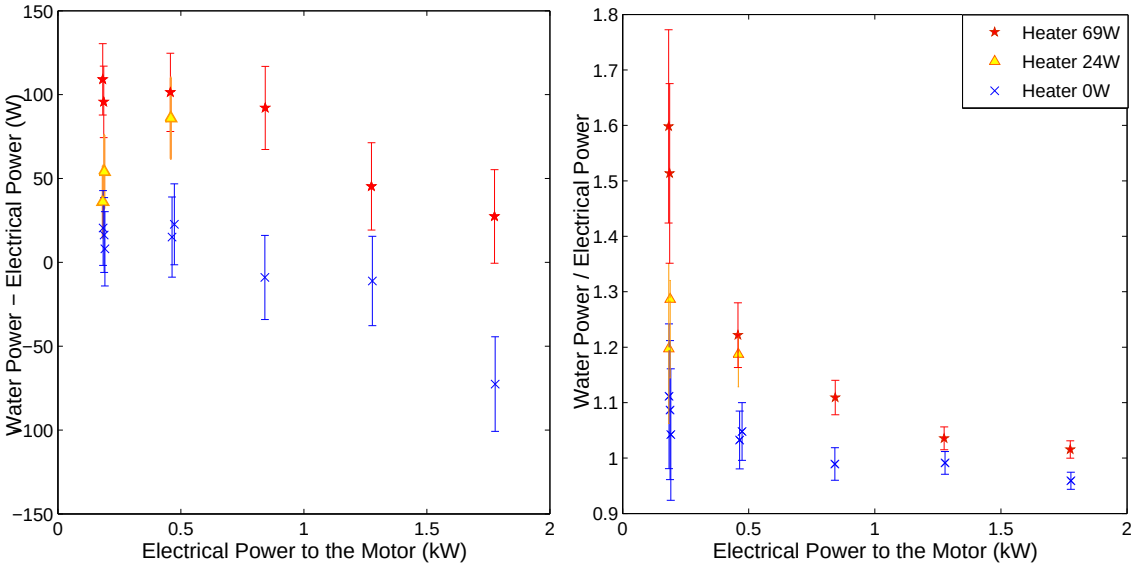


Figure 10-2: Water power versus electrical power with a heater

$$Gain_{cell} = \frac{C(T)\rho\Delta T}{\Delta p} + \frac{P_{heatloss}}{\Delta p dV/dt}$$

Assuming that the energy lost due to heat loss is convective, $E_{heatloss} = a(T_{body} -$

| system | $g_c$ | $a$ | $R^2$ | $\xi_{motor}$ | $b$ | $R^2$ |
|---|---|---|---|---|---|---|
| Initial Design | $.7154 \pm .0011$ | $1.0862 \pm .016$ | 1.000 | $.9187 \pm .013$ | $.0180 \pm .0014$ | .9991 |
| Cell Insulation | $.7148 \pm .0021$ | $.8435 \pm .056$ | 1.000 | $.9249 \pm .027$ | $.0194 \pm .0032$ | .9982 |
| Reservoir Add. | $.7132 \pm .0010$ | $.8409 \pm .027$ | 1.000 | $.9188 \pm .024$ | $.0217 \pm .0029$ | .9978 |

Table 10.1: Table of fit values

$T_{room}$), where $a$ is a constant based on many parameters such as the surface area of the machine. $T_{body}$ was taken to be $T_6$ since it is close to the cell, and $T_{room}$ was $T_1$, a thermocouple left open to air during the runs. Letting $g_c$ be an estimate of the gain across the cell, a fit to the equation

$$\frac{C(T)\rho\Delta T}{\Delta p} = g_c - a\frac{T_6 - T_1}{\Delta p dV/dt}$$

will give a value for the loss coefficient, $a$, and the expected gain, $g_c$. The results of the fit to this equation are in table 10.1.

To find the effect of heat loss over the entire machine, we calculated a fit to the water data. Assuming energy balance,

$$P_{in} = P_{out}$$
$$\text{MotorEfficiency} \times P_{electric} = P_{water} - P_{heatloss}$$

Energy lost due to motor efficiency is assumed not to go into heating the oil in this equation, even though it probably goes into heating the motor. The assumption is reasonable, since the ventilation fan intake is directly above the motor.

Letting $\xi_{motor}$ be an estimate of the motor efficiency, and again assuming that heat loss is convective, the fit equation is

$$P_{water} = \xi_{motor} P_{electric} - b(T_6 - T_1)$$

This equation was also fit to a linear regression fit, and the results can be seen in table 10.1. $R^2$ gives an estimate of the quality of the fit for each model and data set.

The runs in this sections were all executed with a steel tip with 2mm diameter hole for the purpose of comparing heat losses in the different machine versions. As these runs are used in the fit, they are not included in the later sections.

The following graphs show how these fits compare to the raw data sets they were built from. Because $C(T)\rho\Delta T/\Delta p$ is a function of both temperature and pressure, in the following graphs, $C(T)\rho\Delta T/\Delta p$ is plotted against pressure and temperature so that the functional relationship can be seen on raw data. Water power is compared to electrical power in two ways, the difference and the ratio.

Throughout the rest of this chapter, graphs have a dotted line at the expected energy balance. The line is at $g_c$ for the gain across the cell, 0 for the difference in water and electric power, and the manufacturer's reported motor efficiency ($\approx 91.7\%$) for the ratio of water and electric power.

□

### 10.3.1 The Initial Unit at FRC

This version of the machine was in use from September 29 through October 23, 2006. The fit parameters from this data set characterize the assortment of tips done during this time period (section 10.4.1), comparing different tip materials (section 10.5), and HD gas tests (section 10.6).

One data point taken at low power is not shown on the graph of $P_{water}/P_{electric}$ because the power is too low for this calculation to be reliable.

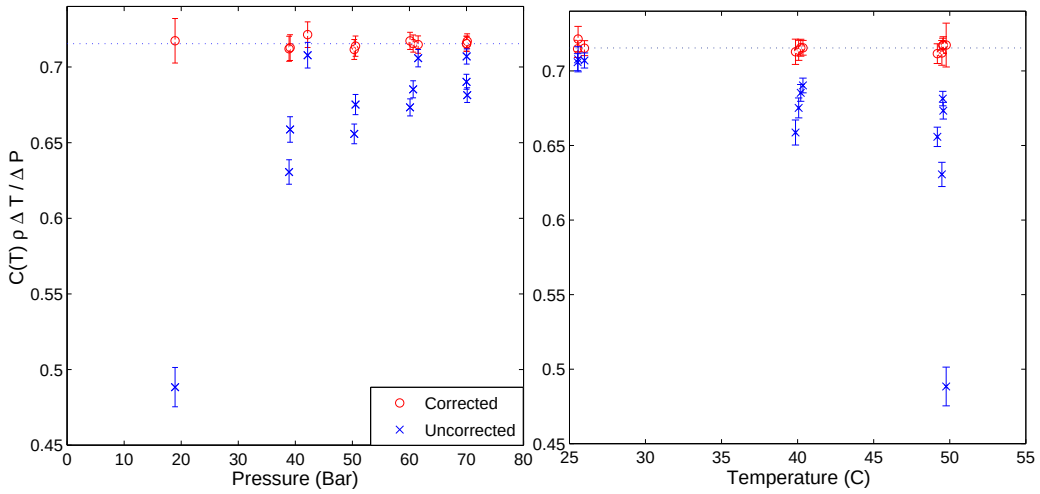


Figure 10-3: Gain across cell on initial unit at FRC

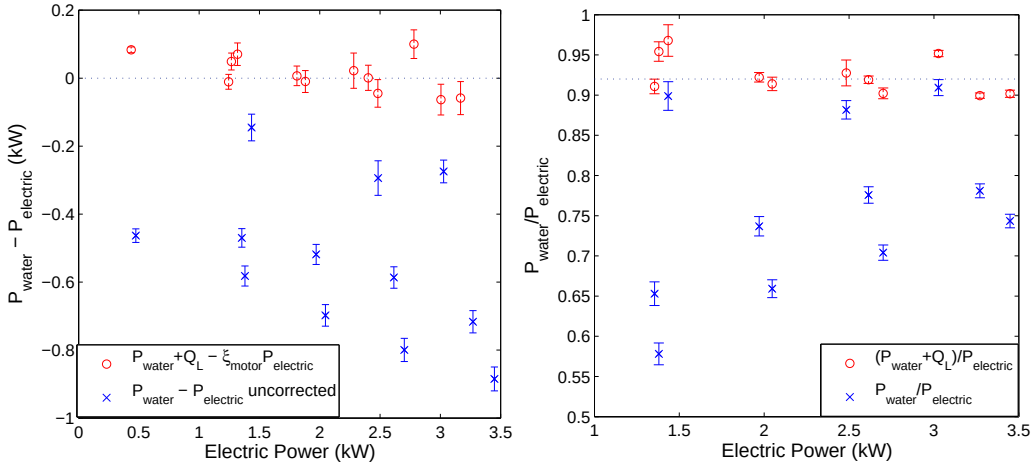


Figure 10-4: Water power on initial unit at FRC

### 10.3.2 Effect of Insulating the Cell

This version of the machine was in use on October 24, and from October 27th, 2006 onwards. The fit parameters from this data set characterize the assortment of tips done during this time period (section 10.4.2), gas tests (section 10.7), and degassed tests (section 10.8).

Before this change, the sides of the cell were in direct contact with two large plates of aluminum. Afterwards, the cell was insulated from the aluminum with Delrin. The fit on insulated data has a lower heat loss slope, $a$, than the fit without, as expected.

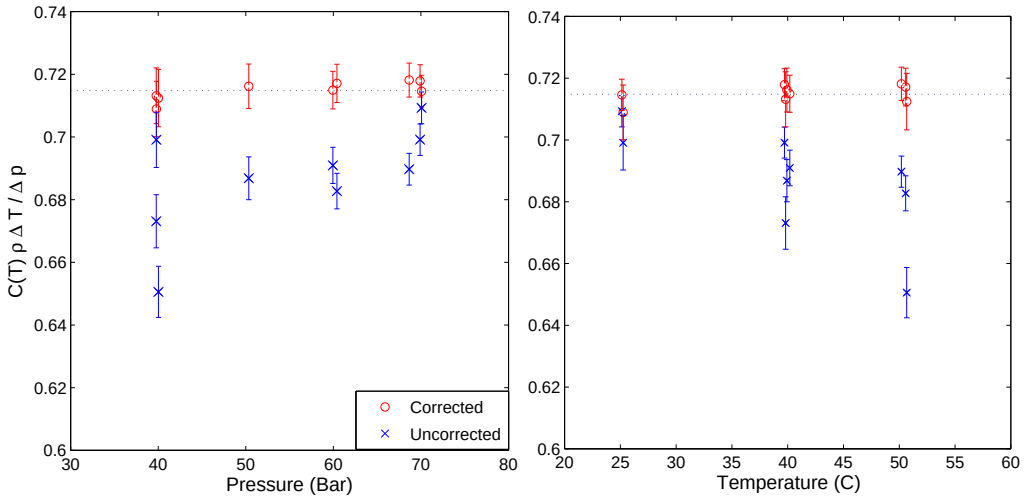


Figure 10-5: Gain across cell after cell insulation

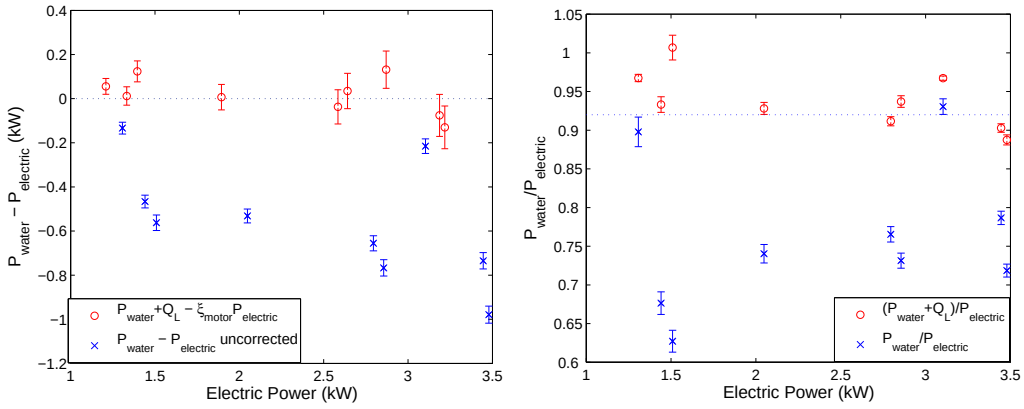


Figure 10-6: Water power after cell insulation

### 10.3.3 Effect of Adding a Reservoir

This version of the machine was in use from October 25th to October 27th, 2006. The fit parameters from this set of data are used to characterize the assortment of tips done during this time period (section 10.4.3). This version took the insulated cell version, and placed an additional cylindrical reservoir next to the first one, roughly doubling the reservoir surface area exposed to air.

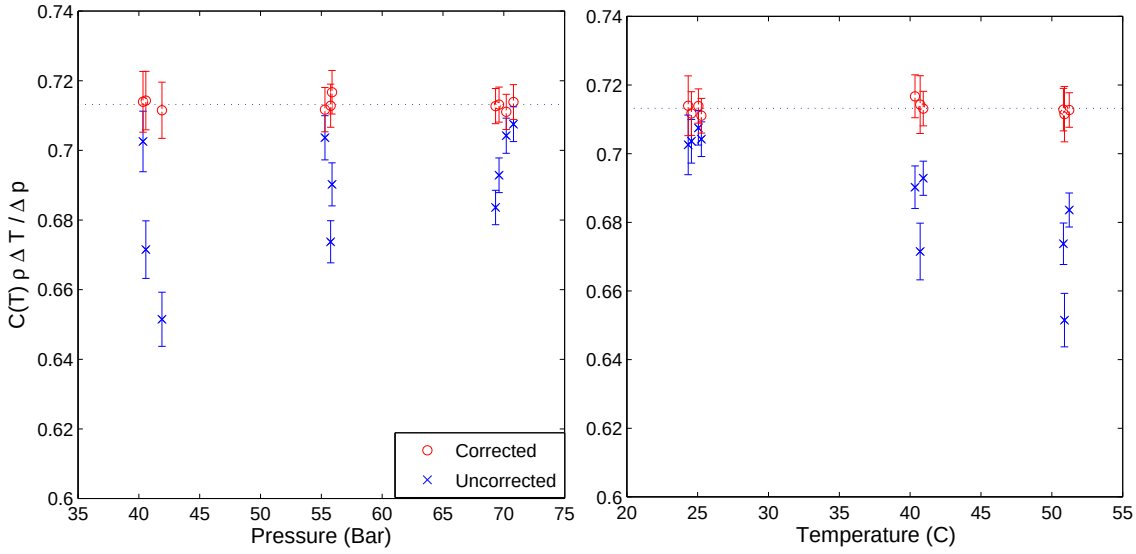


Figure 10-7: Gain across cell after reservoir addition

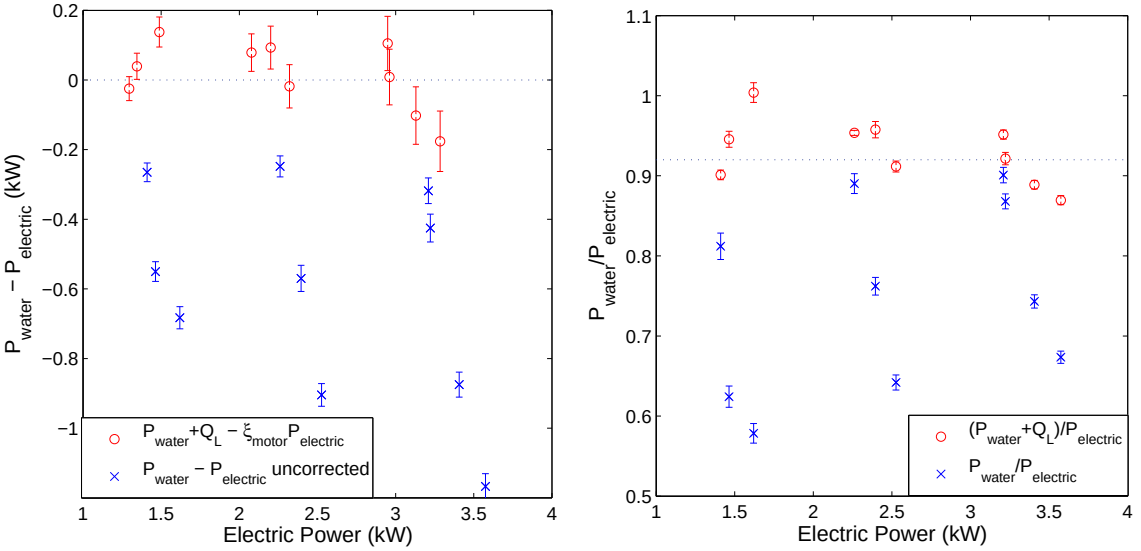


Figure 10-8: Water power after reservoir addition

## 10.4 Assorted Tip Designs

These data sets represent our best efforts to reproduce the experiment verbatim. An assortment of tips was run to maximize light output and electrical discharge. Some of these tips are not in the data and tip lists because electrical arcing through the tip material forced the run to be aborted before a steady state point could be acquired.

For each system version, $C(T)\rho\Delta T/\Delta p$ is plotted versus pressure, and water power is compared to electrical power in plots of their difference and ratio.

Because deoxygenating the reservoir leaves it at a vacuum, nitrogen overpressure was used in some of these runs.

### 10.4.1 Tips on the Initial Unit at FRC

Describing the tip designs upstream to the downstream, the tip designs plotted in these runs include:

- 2mm dia, 1 hole Acrylic (Acr) tip, with a 2.2 mm dia Acr disk.
- 1.5mm dia,1 hole Al tip, 1.5 mm dia Al disk
- 2mm dia, 1 hole Acr tip
- 1.8mm dia 1 hole Acr tip, Al disk, 2 mm dia Acr disk, Al disk, 2.4mm dia Acr disk, Acr spacer, 6 hole Acr swirler
- 1.9 mm dia 1 hole Acr tip, 2mm dia Al disk, 2.0mm dia Acr disk, 2mm dia Al plate, 2.2 mm dia Acr plate, 2mm dia Al plate, Acr spacer, 6 hole swirler
- 2mm dia 3 hole Acr tip, 2mm dia Silver
- same as above, but with Al rather than silver plate
- a tip with a longer shank than usual
- 2 tip designs created by Chansoo Kim for light output qualities

Three of these points show discrepancies between the two downstream thermocouples, $T_5$ and $T_6$. These points were run before the 'clover leaf' flow diffuser was installed just after the cell. The points with discrepancies are circled in figure 10.4.1. The top circle is the value of $C(T)\rho\Delta T/\Delta p$ when averaging over both $T_5$ and $T_6$ while the bottom circle only considers $T_6$. Since $T_6$ is only a few inches after $T_5$, a real heat effect at $T_5$ should still be present at $T_6$.

In the water plot, figure 10-10, two points were removed from late September because they lacked information on the water flow.

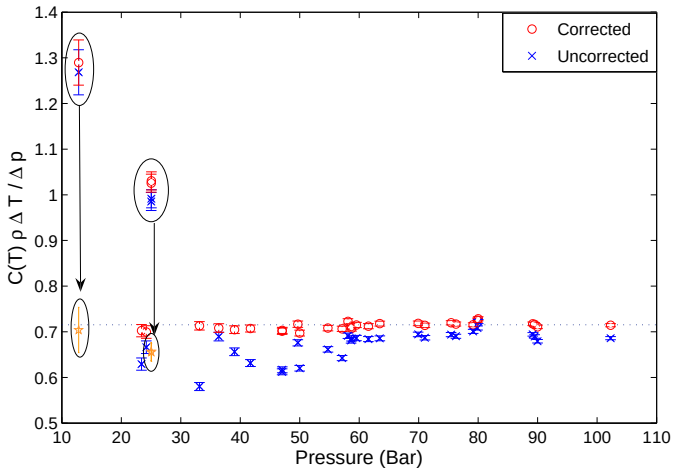


Figure 10-9: Gain across cell of assorted tips with initial system

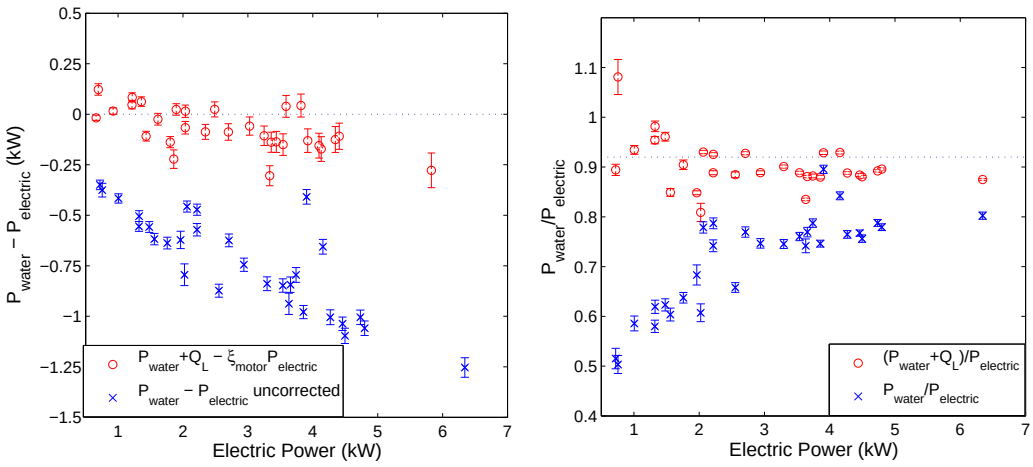


Figure 10-10: Water power versus electric power of assorted tips on initial system

### 10.4.2 Tips After Insulating the Cell

The tip design plotted in this run is the 2mm acrylic tip.

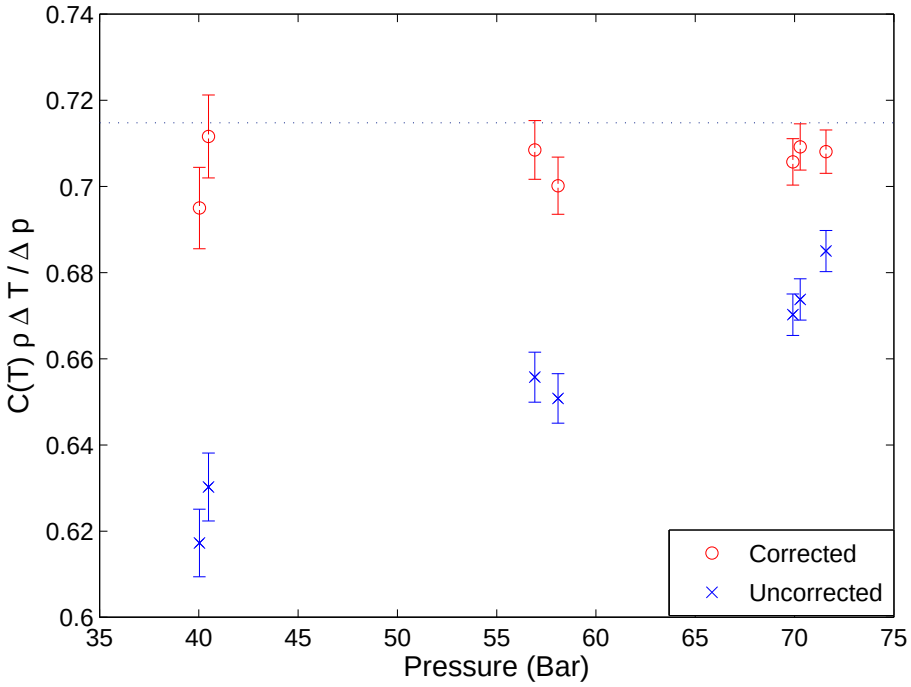


Figure 10-11: Gain across cell of assorted tips with insulated cell

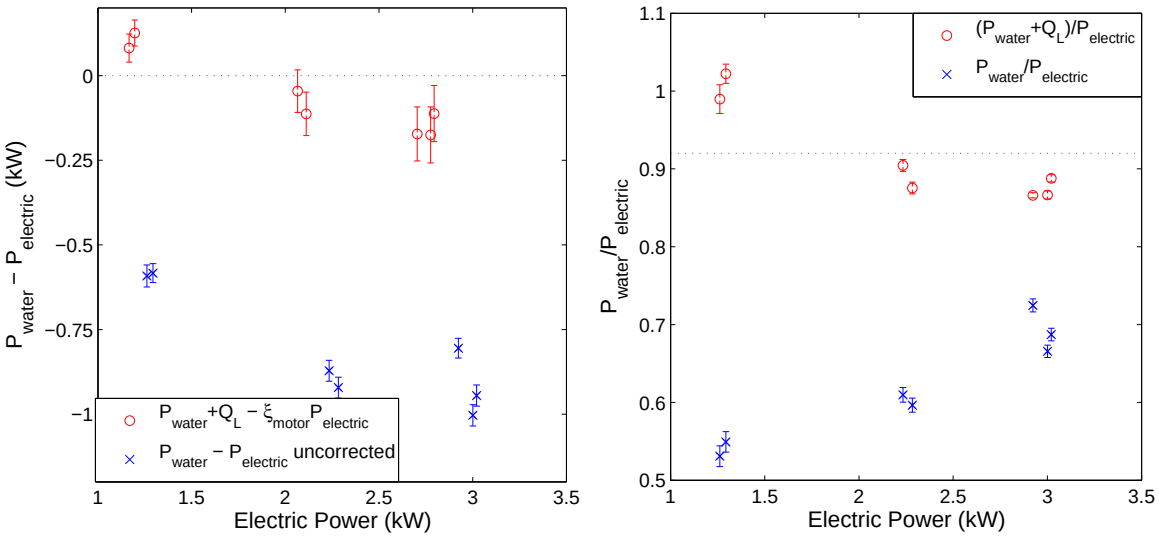


Figure 10-12: Water power versus electric power of assorted tips with insulated cell

### 10.4.3 Tips After Adding a Reservoir

The data here is only from 2mm acrylic tips.

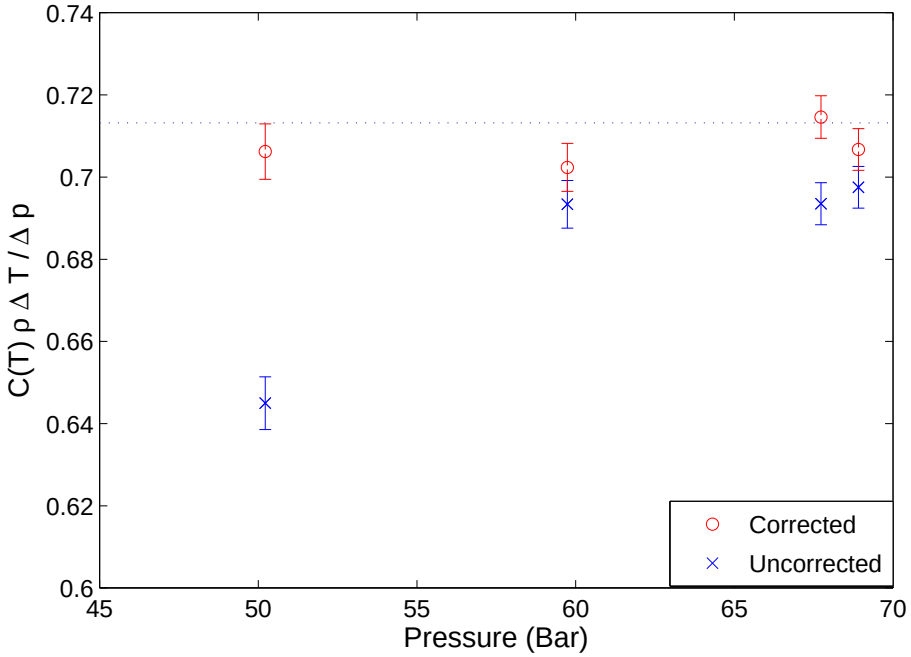


Figure 10-13: Gain across cell of assorted tips with reservoir addition

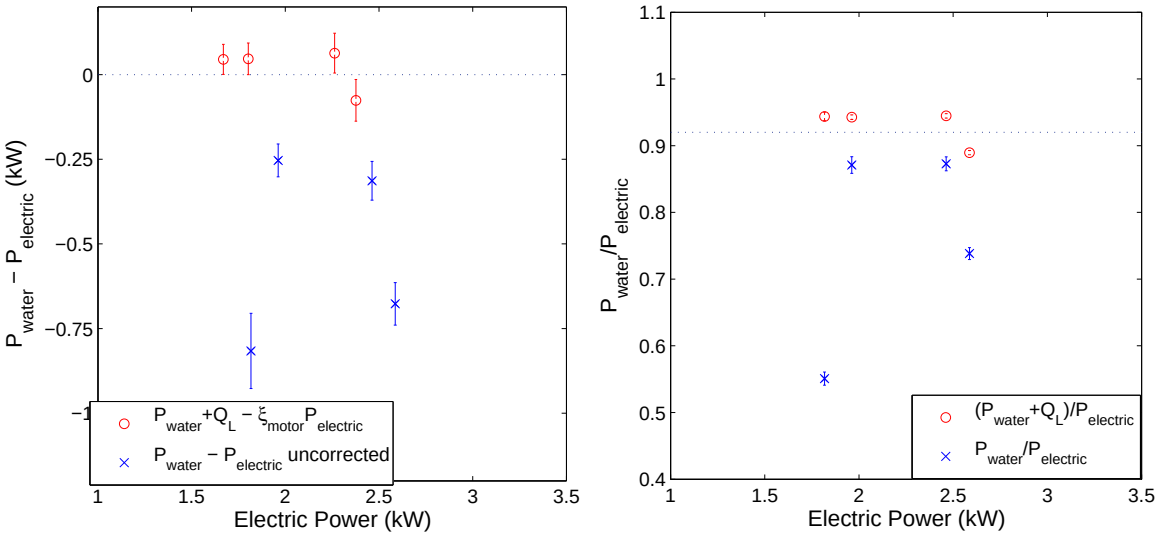


Figure 10-14: Water power versus electric power of assorted tips with reservoir addition

## 10.5 Comparing Tip Material

Because the graphs in this document are now comparing multiple data sets, the raw data and the data corrected with the fits is displayed on two separate graphs side by side.

These three data sets were run on the initial system design. They are all from 1 hole 2mm diameter tip designs, which vary only in the material. Though acrylic and steel 1 hole 2mm tips are mentioned in earlier runs, these data points were taken independently.

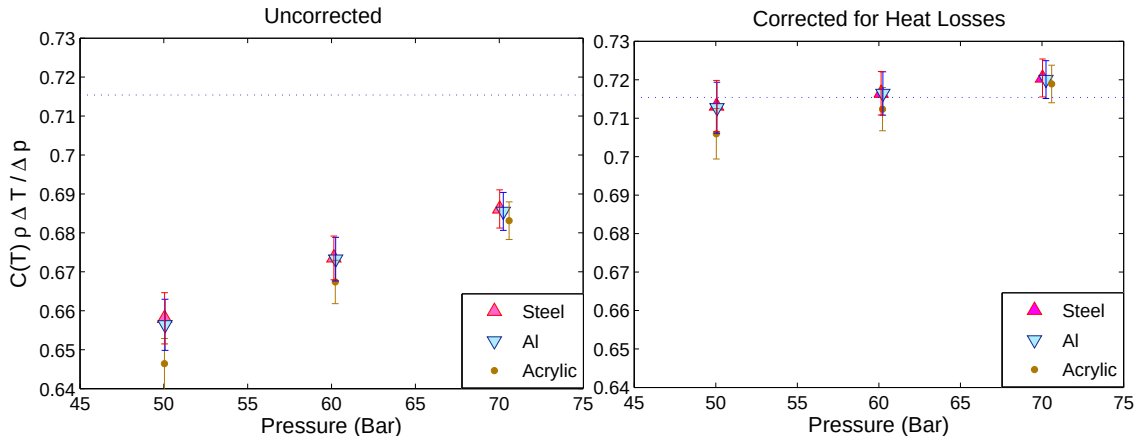


Figure 10-15: Gain across cell of three tip materials

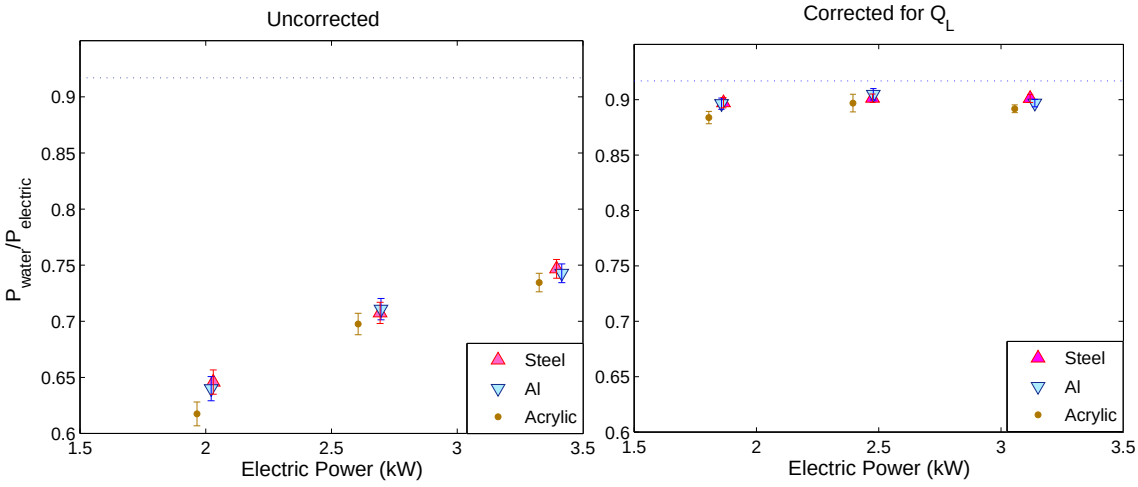


Figure 10-16: Water power/electrical power of three tip materials

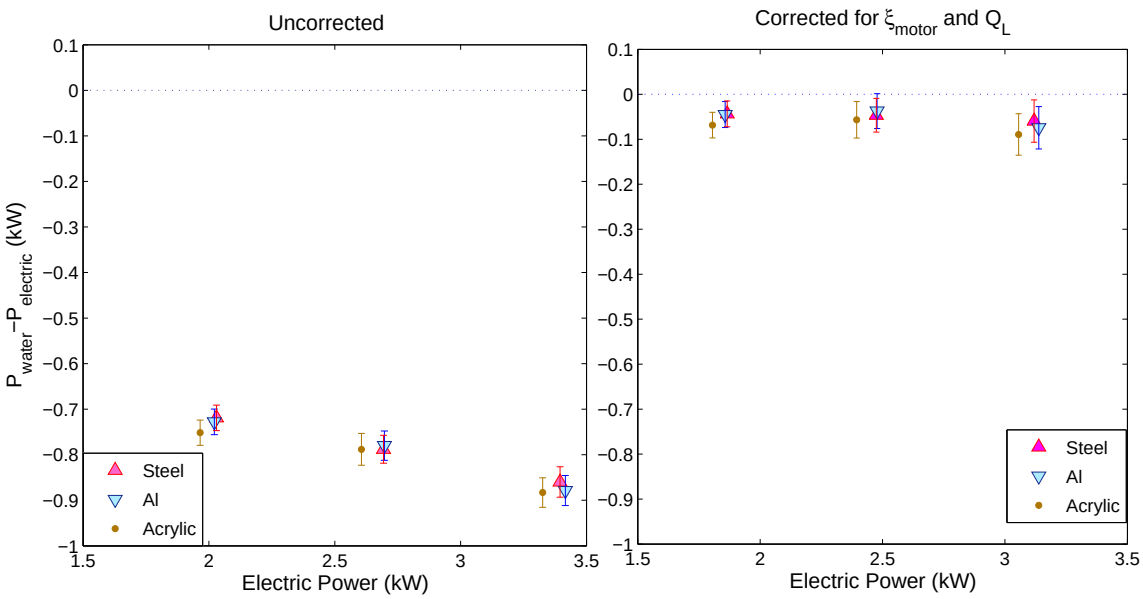


Figure 10-17: Water power - electrical power of three tip materials

## 10.6 HD Gas

These runs were conducted on the initial machine design; however, the experiment was modified and HD gas was put into the reservoir before the run began.

For the lower concentration of HD, about 0.001 mole of HD was added to the reservoir chamber and mixed by running the oil. About ten times as much as added for the higher concentration runs, and based on the drop in reservoir pressure, at least .002 mole was absorbed into the roughly 32 moles of oil.

One of the data points in this run shows a higher gain. This run has a discrepancy in the two downstream thermocouples, $T_5$ and $T_6$. Like before, the clover leaf was not installed at this time. The run with a discrepancy is circled, with an arrow pointing to the value for $C(T)\rho\Delta T/\Delta p$ obtained using only $T_6$. Fig. 10-20 has an arrow to this point so that the cell gain measurement can be compared to the water measurement.

Tips used with the smaller concentration of HD gas were based on a single hole acrylic tip, with a diameter of either 2.0mm, 2.2mm, or 2.4mm. The tip was preceded by zero, one, or two acrylic disks, and usually by an acrylic spacer and an Aluminum six hole 35/35 swirler. In one run, the tip additionally had a palladium disk. The goal

of this variation was to find a tip with bright light output under the run conditions that did not get destroyed by discharges.

One tip was chosen for the runs with a larger $HD$ concentration, a 2.4 mm diameter acrylic tip preceded by a 2.6 mm diameter acrylic disk, a 2.8 mm diameter 10 mm acrylic disk, an acrylic spacer, and an Aluminum six hole swirler.

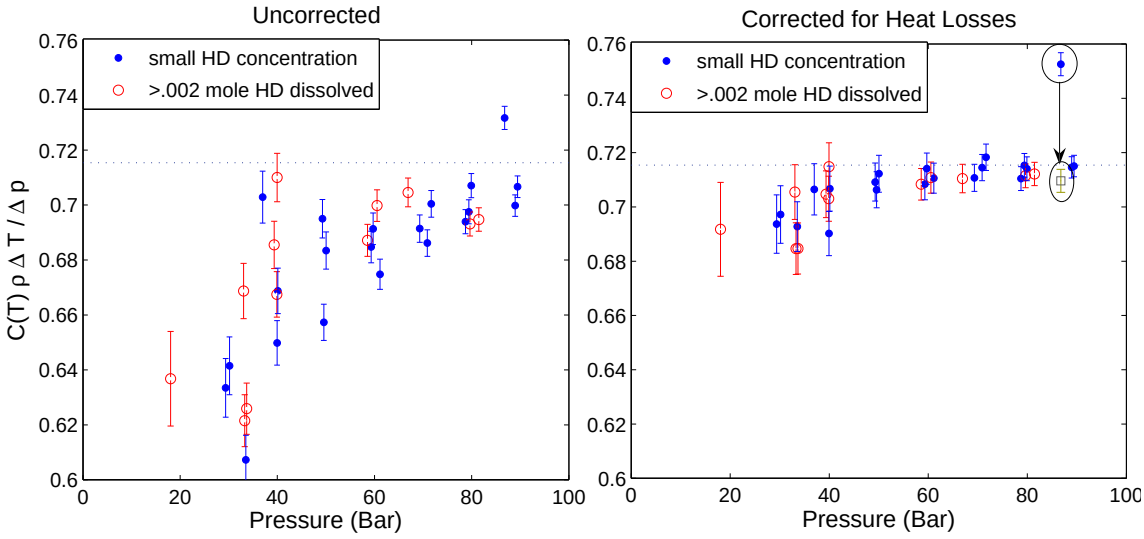


Figure 10-18: Gain across cell with HD gas

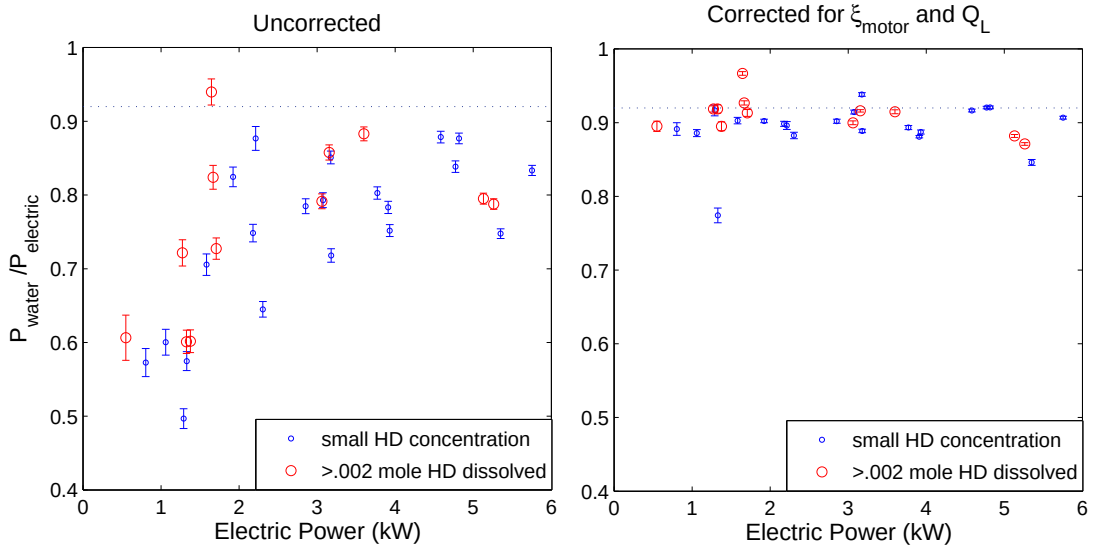


Figure 10-19: Water power/electrical power with HD gas

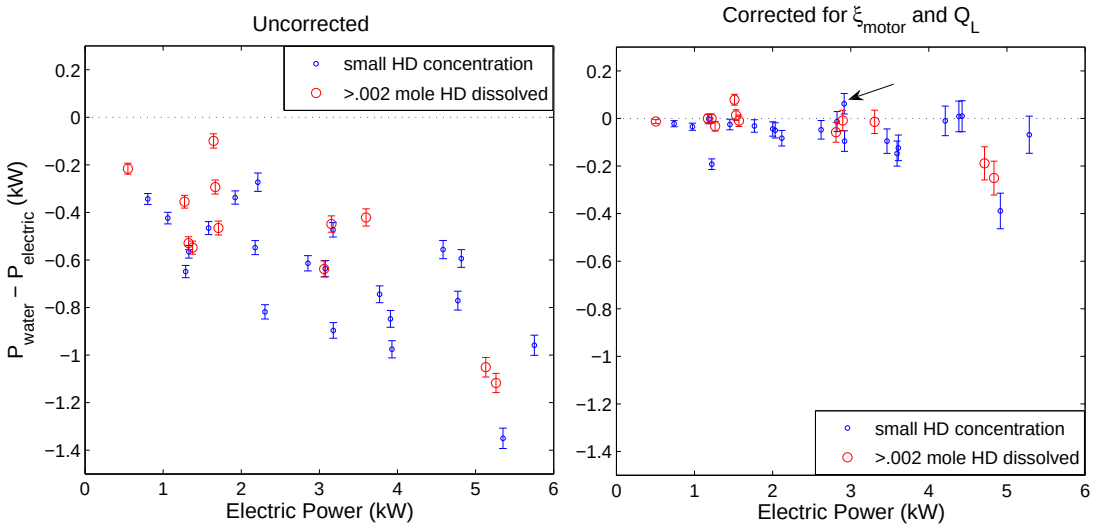


Figure 10-20: Water power - electrical power with HD gas

## 10.7 $D_2$, Xe, and/or He

When He gas is added, it is about .5 atm to a roughly half liter volume at the top of the reservoir. In the xenon runs, it is accompanied by at least 1 atm of Xe gas. In the $D_2$ run, about 1 atm of $D_2$ is added to that.

For one of these runs, the flow meters were not on. The oil flow was estimated by computing the pump efficiency from the same tip design but a different run, and dividing by the pressure from the run in question. The water flow could not be reconstructed well, so that data point does not appear on the water graphs.

Runs in this section and the next were done on the insulated cell system design with one of two different tip designs: a four acrylic tip preceded by two plates of palladium metal separated by acrylic disks, or a one hole acrylic tip preceded by an acrylic spacer and an aluminum six hole swirler.

Several runs at the beginning of November showed pressure buildup at the top of the reservoir during runs. An example is given in Fig. 10.7. Pressure built up above atmosphere, so the effect was not accounted for by a leak in the system. The effect began after palladium and helium had been introduced to the oil, and while it continued after degassing under vacuum, it is likely that not all the helium was removed. When the oil was changed, this effect went away.

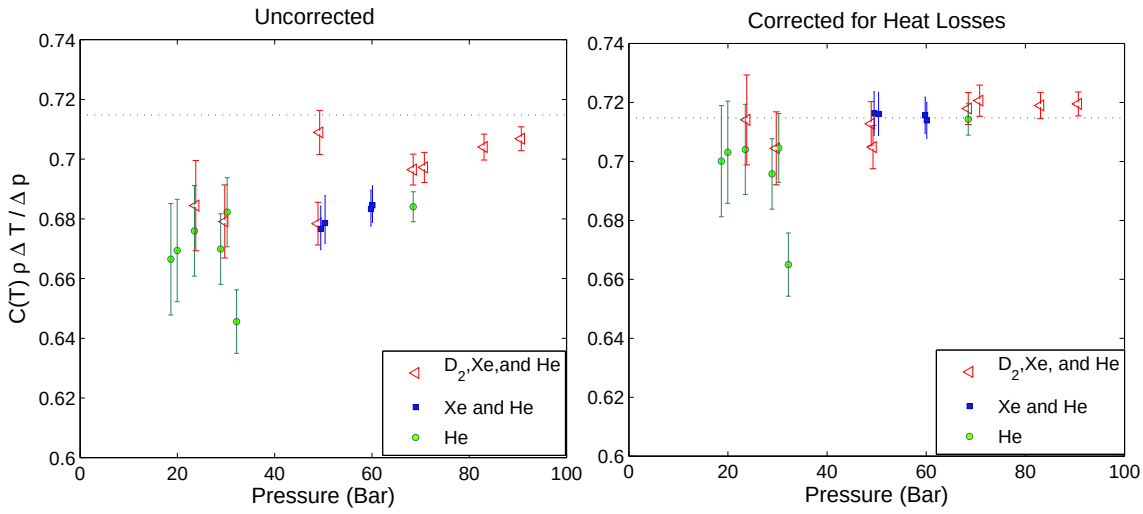


Figure 10-21: Gain across cell with $D_2$,Xe, and/or He gas

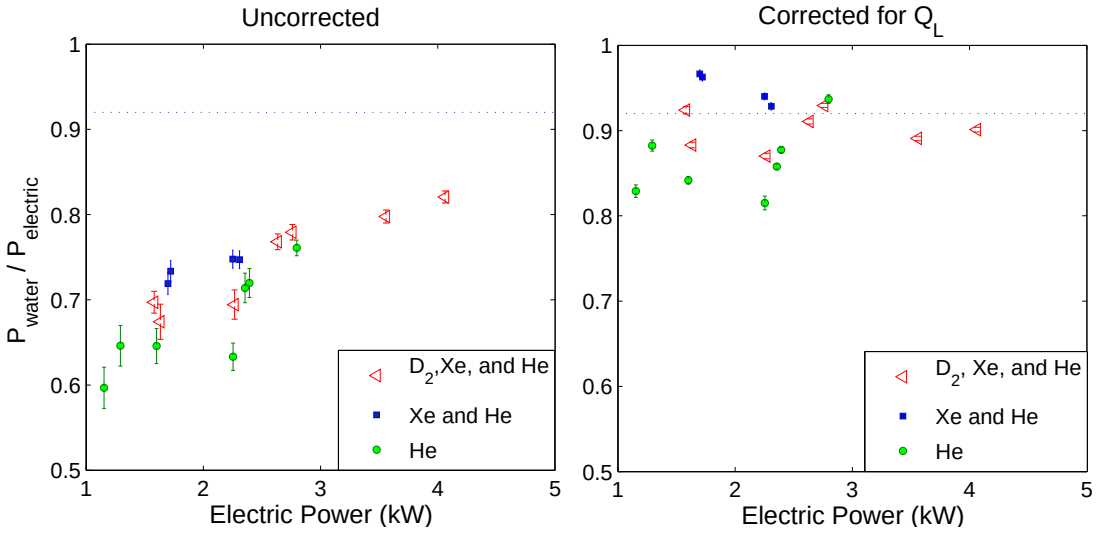


Figure 10-22: Water power/electrical power with $D_2$,Xe, and/or He gas

This gas produced a response in a hydrogen sensor. The response signal showed rapid rise and decay in a similar way to the sensor's response to propane, and unlike the long rise and decay response of the sensor to an $H_2$ calibration tank. Because of this, it is suspected that the gas is predominately short chain, volatile hydrocarbons.

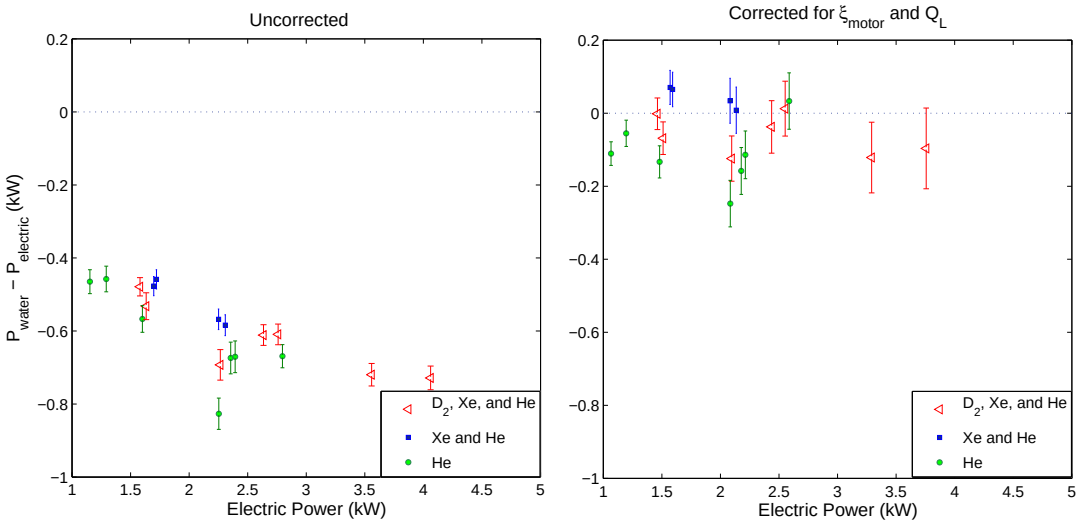


Figure 10-23: Water power - electrical power with $D_2$,Xe, and/or He gas

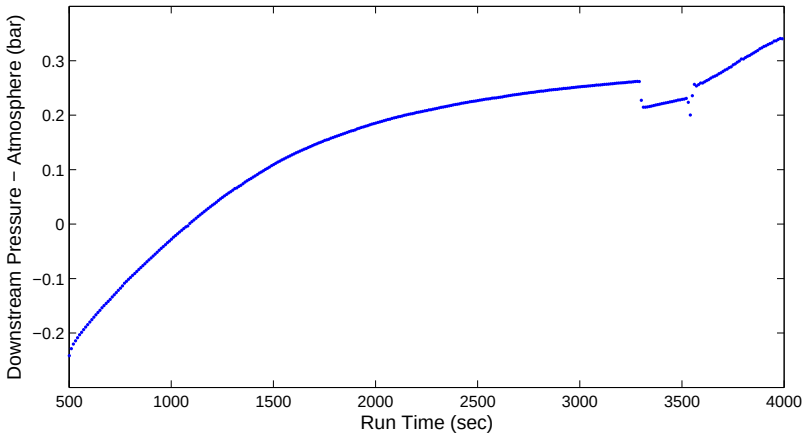


Figure 10-24: Downstream pressure buildup seen with palladium tip and helium

## 10.8 Runs After Removing Gases

These runs were done on the system with an insulated cell, after a run with some combination of $D_2$, $^4He$, and $Xe$. The reservoir was put under vacuum to remove the gases already in the system. Since trace amounts could still be present, these runs have been separated out from the other graphs.

Two points were run at too low a power to be interpreted on the water power/electrical power graph, and have been removed from that graph.

Some of these runs also showed downstream pressure buildup similar to that in section 10.7.

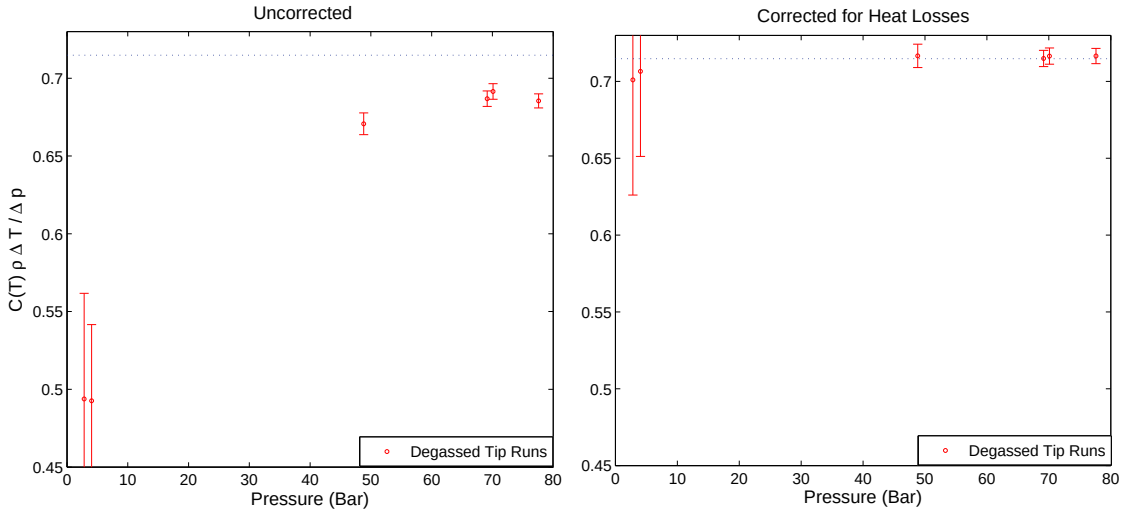


Figure 10-25: Gain across cell after gases removed from system

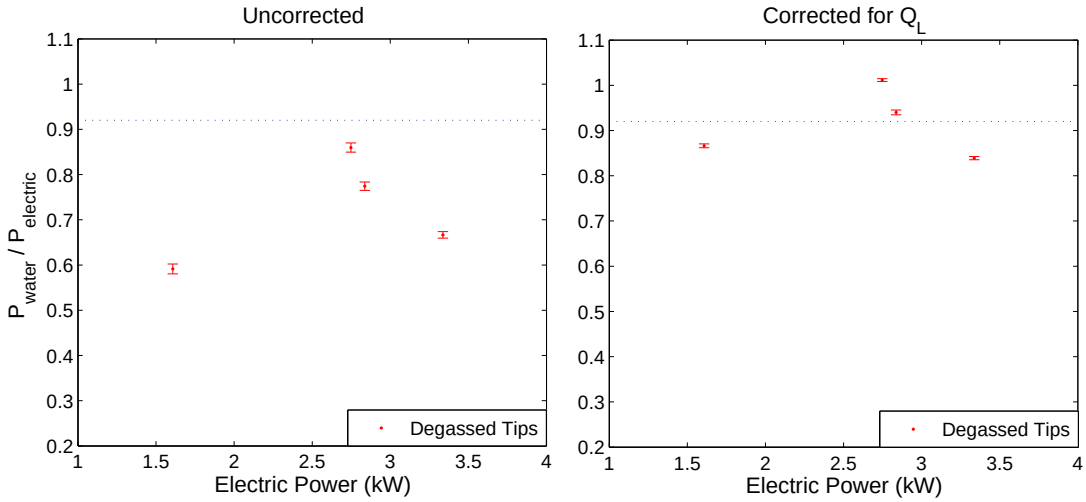


Figure 10-26: Water power/electrical power after gases removed from system

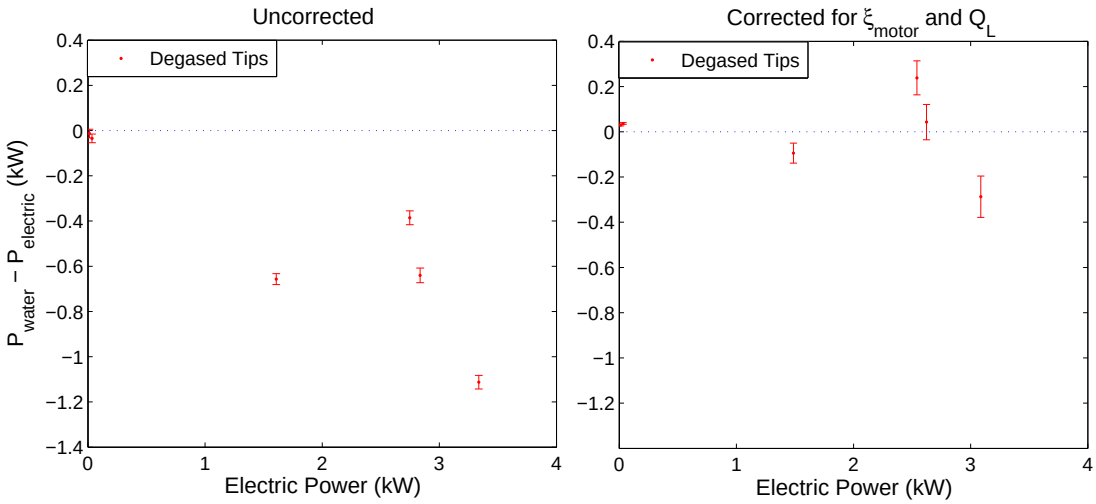


Figure 10-27: Water power - electrical power after gases removed from system

# Chapter 11

# Discussion

In this chapter, I will first discuss my interpretation of the data, in regards to excess heat production. Following that is a discussion of how the collected data impacts the theories presented in Chapter 4 and Chapter 5.

## 11.1 Results

Based on the data presented in Chapter 10, I do not think that the current machine produces excess heat. There are two measurements which looked for excess heat. I will discuss the measurement of the gain across the cell first, since the data from the heater experiment in section 10.2 suggests that it is more reliable. Next, I will discuss measurements of the gain over the entire system, since an effect which occurred after the thermocouples around the cell would not be detectable by the first measurement.

### 11.1.1 Gain Over the Cell

For this measurement, the gain is compared to $g_c \approx 0.7$ due to the result of the fits. In theory, if all the energy from the pressure went into heat, then this value should be unity. Thirty percent of the energy is not lost however; the energy ratio at the water measurement is close to unity. One explanation is that the energy is stored between $T_3$ and $T_6$ in something other than heat, but is transfered into heat by the time it

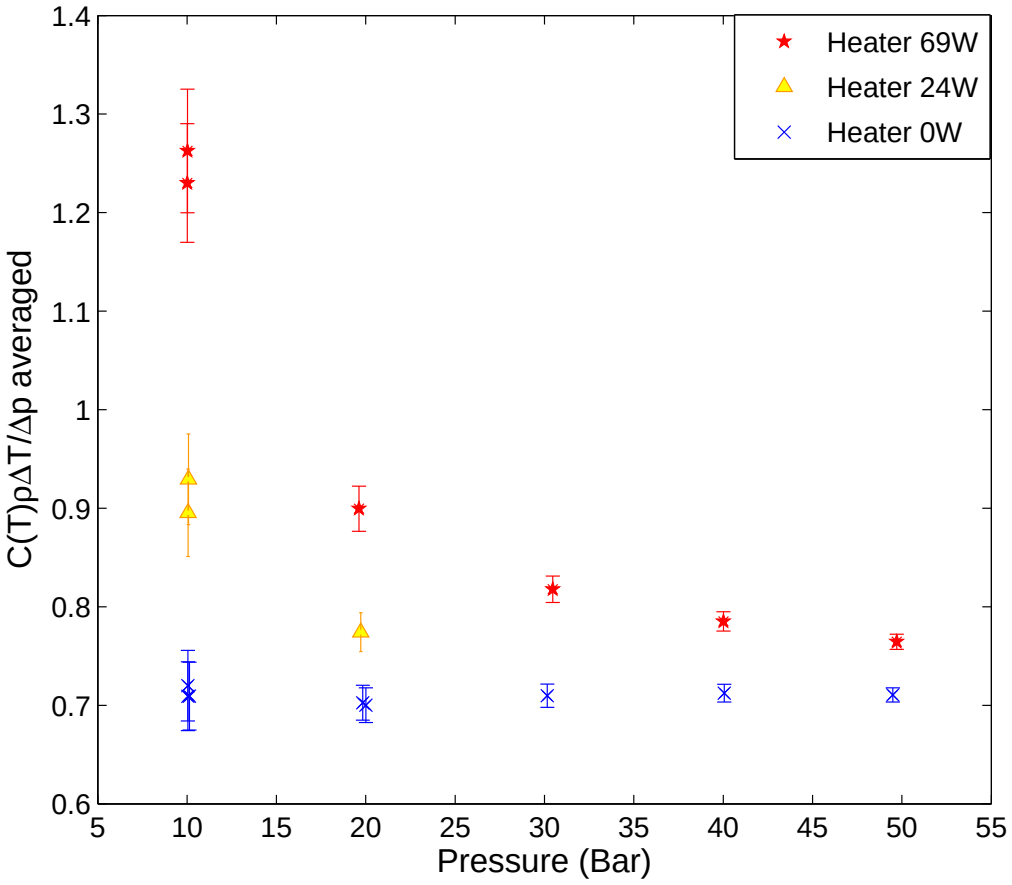


Figure 11-1: As a reminder of the calibration of the device to measuring heat, the graph of gain measured in the system when a heater is in the oil stream is reproduced here from the analysis section.

reaches the heat exchanger.

Some ways that energy might be stored include phase change to gas, kinetic energy in the motion of the fluid, or chemical changes. Since the energy put into the system via the pump is nearly completely seen as heat in the cooling water, it is very unlikely that the energy is stored chemically. Phase change from liquid into cavitation bubbles or an increase in kinetic energy are both storage mechanisms which persist past the thermocouples around the cell, but transform into heat by the time the oil reaches the heat exchanger.

After accounting for heat losses, the amount of energy not going into heat appears to always be 30% of the pressure energy. It is possible that the increase in pressure

results in more oil flowing through the nozzle such that the amount of energy due to phase change and kinetic energy is always 30%. It is also possible that the constant 0.7 is an artifact of the fit. The fit has a constant parameter for the expected gain across the cell over all pressure and temperature conditions. Even if the value varied, the construction of the fit would report a constant. Because the data appears to agree with the fit so well, the fit still provides a useful way to compare data taken at different temperatures and pressures. If extra heat was present, it should be easier to notice because the measurement only needs to be compared to a constant after the fit.

For four of the data points in Chapter 10, the temperature across the cell is up to some debate since the two thermocouples upstream of the cell ($T_5$ and $T_6$) disagree. These data points are all from a system design which did not protect $T_5$ from rapid fluid streams, and as a result, $T_5$ appears to have been occasionally faulty. There are several reasons to assume that the fault lies with $T_5$. First, if excess heat was produced at the cell, it should have been taken out of the water. Even after heat losses were accounted for, the water measurement of these points agrees with energy balance. Second, if the oil was hot at $T_5$, then $T_6$ should have also measured a hot temperature, since it was only a few inches away. Third, stick on thermocouples along the outside of the pipe from $T_5$ to $T_6$ agreed with $T_6$, so it is unlikely that the temperature effect was somehow a local hot area.

Assuming that when $T_5$ and $T_6$ disagree $T_6$ is correct, data points from the gain across the cell are uniformly below $g_c$ before the fit, and after the fit are below $g_c$ or within error of it.

### 11.1.2 Gain Over the Entire Machine: Water Measurements

Based on the heater tests, water measurements are expected to be less clear than the measurement over the cell. However, it is still important to consider this test, because if the heat effect was due to a reaction which was delayed in time , and so occurred after it had traveled down the stream past $T_5$ and $T_6$, then the cell measurement would not detect it.

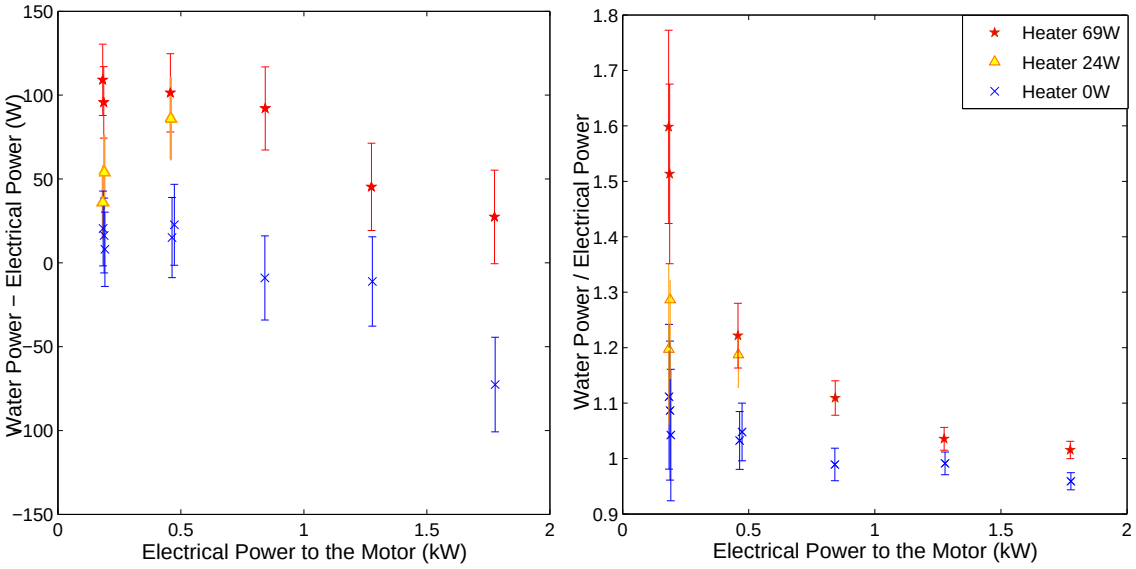


Figure 11-2: As a reminder of the calibration of the device to measuring heat, the graph of water power compared to electrical power measured in the system when a heater is in the oil stream is reproduced here from the analysis section.

After the fit, the water measurement appears to have more noise than is accounted for by the error bars. There are at least two explanations: variations in cooling rates, and additional error in the water flow measurement.

This fit is sensitive to the rate of cooling, due to the large surface area of the device, and the calculation does not take this into account. The noise in this section might be due in part to variations in airflow moving past the machine. During a few runs, the trailer that housed the unit had an open door, which would increase the air flow in the room and the rate of cooling. A record was not kept of when this was the case.

The error bars in the water flow measurement were based partly on the error of the mean, $\sigma/\sqrt{N}$, where $N$ is the number of sample points. This calculation assumes a Gaussian distribution of noise, which was not necessarily the case. Some steady state points had varying water flow to keep them in steady state. These adjustments may have contributed to a noisier water flow measurement.

There are two ways of comparing the heat taken out in the water to the electrical power put into the motor, through the difference and the ratio. I will discuss

the difference first, and then the ratio, with the assumption that the error bars are reasonable.

Before the fit, the difference between the water and electrical power is less than zero. After the fit, the data is usually less than zero, and always within three sigma. If a heat effect exists, it is less than the heat losses. In the cases where the fit data is above energy balance by more than the confidence bounds it is on the order of 100 W, and likely due to over adjustment from the fit.

Now considering the ratio between the water and electrical power, again the uncorrected points are below energy balance or within error of it. This observation agrees with the difference analysis. Corrected points are usually below energy balance or close to it, within the error on the pump efficiency measurement from the fit. The error on the fit to the motor efficiency is not included in the ratio correction, and so this error was not included in the error bars in those graphs. However, it is related to the ability of the fit to account for data in terms of the motor efficiency.

Even after accounting for this error, there are still a few points which are outside the confidence bounds of the error on the motor efficiency. All but one of these data points were run at temperatures hotter than those used in the fit. The fit is likely over compensating for heat losses at these temperatures.

Fig. 10-26 contains the point which is not explainable by these other arguments. It was run around 45 C, a fairly average temperature for this experiment, which was well accounted for in the fit data. This point is also interesting in that it was one of the few for which the downstream pressure was rising over the course of the run.

I am not claiming that this point is excess heat. However, I do not know why it is above unity after the fit. Regardless, it does not exhibit a large gain (around 10%), and was not repeatable.

From these three ways of looking at two independent measurements, an excess heat effect was not occurring on a magnitude large enough to overcome heat losses to the room. After correcting for heat losses, it appears unlikely that an effect above 70 W was occurring. If it was, it was not repeatable.

Despite the data from this experiment being negative, the theories discussed in

Chapter 5 are not greatly impacted. There are many possibilities as to why this particular instance of the machine didn't work. The impact of this data on the theories is explained in the next section.

## 11.2 Comparison to Theory

This section discusses the results in relationship to three of the theories presented in Chapter 5. The possibility of measurement error at iESi as an explanation will not be covered further, since the data from this experiment was on a different machine, and cannot support or deny such a claim.

### 11.2.1 Theory Presented in the Patent

While the setup of the machine met the requirements in the patent, the procedures done on the machine may not have been sufficient. The procedures required two things which may not have been obtained: powerful enough voltages to overcome the Coulomb barrier, and a resonance condition with the setup of the machine to encourage trapped ions to approach each other. This resonance condition is prescribed in the patent application, though I am unclear on the specific requirements for it. From this viewpoint, more experimentation with varying pump frequencies may be needed to find the required resonance, and experimentation with tip designs to sustain more powerful discharges.

### 11.2.2 Phonon Exchange with Two 2-State Systems

Two kinds of gas tests were run to test the model of phonon exchange with two state systems, one with HD and one with $D_2$, $^4$He, and Xe. At the time that these experiments were designed, the strong coupling model had not been formulated. The goal of these two experiments was to test the weak coupling model on the system.

The weak coupling model predicts the HD test should succeed, using either $^3$He $\rightarrow$ HD(compact state) as the two-state receiver system, or $^{13}$C$\rightarrow$ $^{13}$C$^*$. This was not

observed, implying that the weak coupling case does not apply in this system.

The strong coupling model predicts that the HD test will fail without a large electron screening, as is found in some metals. The oil does not provide this screening. Bits of metal chips are found in the oil after a long run time and provide surface area. Metal surfaces are also present in the pipes of the machine. However, a controlled doping test has not been conducted yet. Once metal had been doped with hydrogen isotopes, $^3$He should be the next limiting factor.

The predictions of both models are qualitatively similar for the experiment with $D_2$, $^4$He, and Xe. This experiment was also conducted before the strong coupling model was developed. Its goal was to explicitly have donor populations in both the excited and ground state at the beginning of the experiment. Xe was added as a possible receiver side two-state system. Palladium tips were also used to provide a possible receiver side two-state system. An additional receiver side two-state system is $^4\text{He} \rightarrow D_2(\text{compact})$.

Again, the weak coupling limit implies that this experiment should produce excess heat; though because D+D reactions are more difficult than H+D reactions, the weak coupling limit predicts a slower system response in this experiment than in the HD case. The strong coupling limit implies that this experiment will not produce excess heat unless there is large electron screening. As with the HD experiment, introducing $D_2$ into metals in a controlled fashion was not attempted, and will need to be done before the strong coupling model can be tested.

### 11.2.3 Combustion

Two of the components necessary for combustion are available, fuel and energy. It appears that the system can get into an operating regime in which combustibles are consistently produced for a time duration of at least several runs. Additionally, thin ash residues were seen on the backs of tips which had been run a long time with a lot of electrical discharge. This ash implies that incomplete combustion was occurring, despite degassing under vacuum to remove oxygen, and that the degassing did not completely remove all of the oxygen.

However, the problem remains of introducing enough oxygen into the system to create energetic effects of the size seen at iESi. Even though this experiment was run at a reduced level of oxygen, not degassing would not allow for enough oxygen to enter because the solubility of oxygen in oil is too low, as discussed in Chapter 4. Even though two of the components necessary for combustion are available, combustion is not an explanation for the events at iESi unless a method of introducing or storing more oxygen is found.

# Chapter 12

# Conclusions

We were interested in developing calorimetry to be able to reliably detect excess heat in a Yang-Koldamasov device. Two this end, we implemented two independent measurements of the power produced by the system: a differential calorimetry measurement, and a flow calorimetry measurement.

We upgraded the existing calorimetry on the device. Multiple thermocouples on either side of the cell, improved calibration, and steady state operating conditions were all important in improving the quality of this measurement. With this test we were able to observe heat at the 70 W level, based on calibrations of the device done with a heater in the oil stream.

We added flow calorimetry measurements to the device with an addition of a heat exchanger and flow meter on the water. Steady state and long measurement times are helpful in improving the accuracy of this measurement. On our system this test is not as accurate as the differential calorimetry measurement, and is trustworthy to around 100 W. However, it is important, because the differential calorimetry only measures gain over the cell. If interesting effects were to occur in another part of the device, they would only be detected by the flow calorimetry measurement.

The analysis of the flow calorimetry is presented both as a difference and as a ratio with the electric power. Both of these ways of looking at the problem are valid, and will have different weaknesses. At low power, the error on the ratio measurements grows very large, and the ratio provides little information. However, at high powers

the error on the ratio measurement becomes small, and is easier to interpret than the difference. Both ways of looking at the problem should be used side by side, so that if there are any anomalies, they will show up on at least one analysis. After an anomaly is found, the specific run can be looked at to see if anything unusual happened in the execution of the experiment, or if the run should be repeated.

On the experiments conducted, an effect was not seen within the error. Because the original machine was not available to test on, not seeing an effect in our experiment does not imply that an effect does not exist. However, the current knowledge of the effect is not yet sufficient to produce it on demand. Should FRC get the device back into a working regime, the calorimetry is ready to immediately signal that excess heat is occurring.

## 12.1 Contributions

The main contribution of this thesis to its field of research is a description of the experiment and an attempt at independent reproduction.

My contributions to this experiment were

- Helping to identify erroneous thermocouple signals and errors
- Calibrating thermocouple equipment
- Design and execution of the test with a heater with the assistance of FRC to verify that the machine could measure heat
- Participating in instrumentation discussions to increase the number of thermal measurements and improve the accuracy of the calorimetry
- Cataloging and analyzing collected data with Jim Gimlett
- Assisting in the running of the device

## 12.2 Recommendations for Future Work

I do not recommend that additional independent reproductions of this experiment be attempted until FRC has demonstrated that the device is working again. FRC is currently the best position to attempt to get the device back into a working regime. Because data collection is time costly, and many variables are involved, I recommend spending more time on theoretical developments to guide the experimental research. While it is possible to stumble across the effect, I am concerned that the associated probability may be low.

The calorimetry on this device can be improved in a few ways. In our analysis, the system was always run in steady state to avoid transient effects. An integral measurement of power over the run would allow for measurement of the transient effects. Additionally, the door to the trailer should always be left closed during any time period in which steady state measurements are desired. If the door is open, the air from the surrounding lab changes the rate of cooling of the device, reducing accuracy of the flow calorimetry measurements.

Should FRC claim to have a device which produces the effect, I do recommend that outside scientists visit to verify this with data collection. FRC has been very welcoming and open so far to scientists, and has made great improvements in their instrumentation. Once such verifications have been made, independent reproductions may be possible.

# Appendix A

# Notation

| | |
|---|---|
| $C(T)$ | Specific heat of the oil as a function of temperature |
| $\rho$ | density |
| $dV/dt$ | oil flow in volume per time |
| $T$ | Temperature |
| $p$ | pressure |
| $P$ | Power |
| $C_w$ | Specific heat of water |
| $dV_w/dt$ | Water flow in volume per time |
| $\xi_{motor}$ | an estimate of the motor efficiency |

Table A.1: List of Mathematical Symbols

| | |
|---|---|
| FRC | Fusion Research Corporation |
| iESi | Innovative Energy Solutions Inc. |
| EROEI | Energy Return on Energy Invested |
| ERAB | Energy Research and Advisory Board |
| ICCF | International Conference on Cold Fusion<br>later renamed the International Conference on Condensed Matter |

Table A.2: List of Abbreviations

| | |
|---|---|
| $T_1$ | Room Temperature |
| $T_2$ | Not used. |
| $T_3$ | First temperature sensor upstream of the cell |
| $T_4$ | Second temperature sensor upstream of the cell |
| $T_5$ | First temperature sensor downstream of the cell |
| $T_6$ | Second temperature sensor downstream of the cell |
| $T_7$ | Water temperature just after the heat exchanger |
| $T_8$ | Water temperature just before the heat exchanger |
| $T_9$ | Temperature at the bottom of the reservoir, just before the heat exchanger |
| $T_{10}$ | Temperature just after the heat exchanger, before the pump |
| $P_1$ | Upstream pressure |
| $P_4$ | Downstream pressure |

Table A.3: List of Instrumentation Symbols

# Bibliography


[1] Apparatus for Generating Energy and Method Therefor. Patent Application for a Yang-Koldamassov Device.

[2] 2004 US Department of Energy Cold Fusion Review Reviewer Comments.

[3] M. Aliotta, C. Spitaleri, and M. et al Lattuada. Improved Information on Electron Screening in $^7Li(p,\alpha)\alpha$ using the Trojan-horse Method. *The European Physical Journal A*, 9:435–437, Nov 2000.

[4] Stefano Atzeni and Jürgen Myer-ter Vehn. *The Physics of Inertial Fusion, Beam-Plasma Interaction, Hydrodynamics, Hot Dense Matter*. Clarendon Press, June 2004.

[5] K. Czerski, A. Huke, and A. et al Biller. Enhancement of the Electron Screening Effect for d+d Fusion Reactions in Metallic environments. *Europhysics Letters*, 54(4):449–455, May 2001.

[6] Kenneth S. Deffeyes. *Hubbert's Peak: The Impending World Oil Shortage*. Princeton University Press, Princeton NJ USA, Oxford UK, 2001.

[7] Patricia Dehmer and Denis Kovar. Mail Review Charge Letter, 2004.

[8] A. M. A. Dias, R. P. Bonifácio, I. M. Marrucho, A. A. H. Pádua, and M. F. Costa Gomes. Solubility of oxygen in n-hexane and in n-perfluorohexane. Experimental Determination and prediction by molecular simulation. *Phys. Chem. Chem. Phys.*, 5:543–549, 2003.

[9] Elizabeth Douglass. U.S. motorists cutting back a bit. *Los Angeles Times*, Jan 2007.

[10] Richard B. Firestone. The Berkeley Laboratory Isotopes Project's Exploring the Table of Isotopes, 2000. Online database of nuclear isotopes.

[11] Fluke Corporation, USA. *Fluke Documenting Process Calibrator 744, Users Manual*, rev. 1 edition, Sept 1998.

[12] Jim Gimlett. Private email communication, Feb 2007.

[13] Peter Hagelstein. Personal Interview, Jan 2007.

[14] Peter L. Hagelstein and Irfan U. Chaudhary. Two-level systems coupled to an oscillator: Excitation transfer and energy exchange. *ArXiv.org*, 0612306, Dec 2006.

[15] Peter L. Hagelstein and Scott R. Chubb, editors. *Condensed Matter Nuclear Science: Proceedings of the 10th International Confrence on Cold Fusion*. World Scientific Publishing Co., Toh Tuck Link, Singapore, 2006.

[16] Richard Heinberg. *The Party's Over: Oil, War and the Fate of Industrial Societies*. New Society Publishers, Gabriola Island, Canada, Mar 2004.

[17] Toby Hemenway. Apocalypse Not - A Critical Look at Peak Oil. *Permaculture Activist*, 59, Feb 2006.

[18] Herguth Laboratories Inc. *Certificate of Analysis*, Sept 2006. Analysis of Petro-Canada Turboflo R&O 10.

[19] M. King Hubbert. Energy from Fossil Fuels. *Science*, 109:103–108, 1949.

[20] M. King Hubbert. Nuclear Energy and the Fossil Fuels. In *Presented before the spring meeting of the Southern District Division of Production, Americal Petroleum Institute*, Houston, Texas, 1956. Shell Development Co.

[21] M. King Hubbert. Oil, the Dwindling Treasure. *National Geographic*, June 1974.

[22] Instrulab, Inc. *Report of Calibration for model 3312A-14-24 S.N. 31120*, Oct 2005. Thermistor calibration data sheet.

[23] A. I. Koldamasov, Hyun Ik Yang, Hyun Suk Chai, A. A. Kornilova, V. I. Vystoki, and A. V. Desyatov. Observation and Investigation of $He^4$ Fusion and Self-Induced Electric Discharges in Turbulent Distilled Light Water. In *ICCF12 Abstracts*, Dec 2005.

[24] A.I. Koldamasov, Hyun Ik Yang, Hyun Suk Chai, A. A. Kornilova, V. I. Vysotskii, and A. V. Desyatov. Observation and Investigation of $^4$He Fusion and Self-Induced Electric Discharges in Turbulent Distilled Light Water.

[25] Ludwik Kolwalski. Blog entry 237: A very importiant report. Web blog reporduction of a due-diligence report on Peter Hagelstein's visit to iESi to observe demonstrations, June 2005.

[26] S. E. Koonin and M. Nauenberg. Calculated fusion rates in isotopic hydrogen molecules. *Nature*, 1989.

[27] Steven B. Krivit. Introduction to a New Method to Initiate Cold Fusion/Condensed Matter Nuclear Reactions. In *Proceedings of the 12th International Conference on Condensed Matter (ICCF12)*, Japan, Dec 2005.

[28] Steven B. Krivit. Introduction to the Hydraulic-Electrostatic Cold Fusion Method. Presentation slides from ICCF12, Dec 2005.

[29] Denis McConnell. Personal interview, Nov 2006.

[30] MicroMotion Inc. *Mass Flowmeter Calibration Certificate*, Nov 2005.

[31] US Department of Energy's Office of Science. Report of the Review of Low Energy Nuclear Reactions.

[32] F. Raiola, B. Burchard, and Z. et al Fülöp. Electron Screening in d(d,p)t for Deuterated Metals: Temperature Effects. *Journal of Physics G: Nuclear and Particle Physics*, 31:1141–1149, 2005.

[33] F. Raiola, J. Cruz, and G. et al Gyürky. Electron Screening: A Review. *Frontiers in Nuclear Structure, Astrophysics, and Reactions*, pages 296–303, 2006.

[34] F. Raiola, L. Gang, and C. et al Bonomo. Enchanced Electron Screening in d(d,p)t for Deuterated Metals. *The European Physical Journal A*, 19:283–287, 2004.

[35] Paul Roberts. *The End of Oil: on the Edge of a Perilous New World*. Houghton Mifflin Company, Boston, New York, 2004.

[36] Deodatta Shenai-Khatkhate, Randall Goyette, Ronald DiCarlo Jr, and Gregory Dripps. Environment, Health and Safety Issues for Sources Used in MOVPE growth of Compound Semiconductors. *Journal of Crystal Growth*, 272:816–821, Dec 2004.

[37] J. C. Sprott. Plasma Physics and Nuclear Fusion, Oct 1998. Lecture Slides Presented to Physics 208.

[38] E. S. Thomsen and J. C. Gjaldæk. *Acta Chem. Scand.*, 17:127, 1963.

[39] Wladek Walukiewicz. Full Solar Spectrum Photovoltaic Materials Identified. Ernest Orlando Lawrence Berkley National Laboratory Materials Sciences Division Research Highlights, Oct 2002.

[40] WIKA Alexander Wiegand GmbH & Co. KG. *Operating instructions, Pressure Transmitter*, Oct 2004.

[41] Winters Co., 121 Railside Road, Toronto, ON. *Liquid Filled (LF) Series Quality*. Data Sheet of part numbers, ranges, and errors.

[42] John Wood, Gary Long, and David Morehouse. Long-Term World Oil Supply Scenarios. Aug 2004.

[43] Yokogawa Electronic Corporation, Tokyo, Japan. *General Specifications: AXF Magnetic Flowmeter, Integral Flowmeter, /Remote Flowtube*, 7th edition, May 2006.

[44] Walter Youngquist and Eugene Oregon. Alternative Energy Sources - Myths and Realities. *Electronic Green Journal*, 9, Dec 1998.